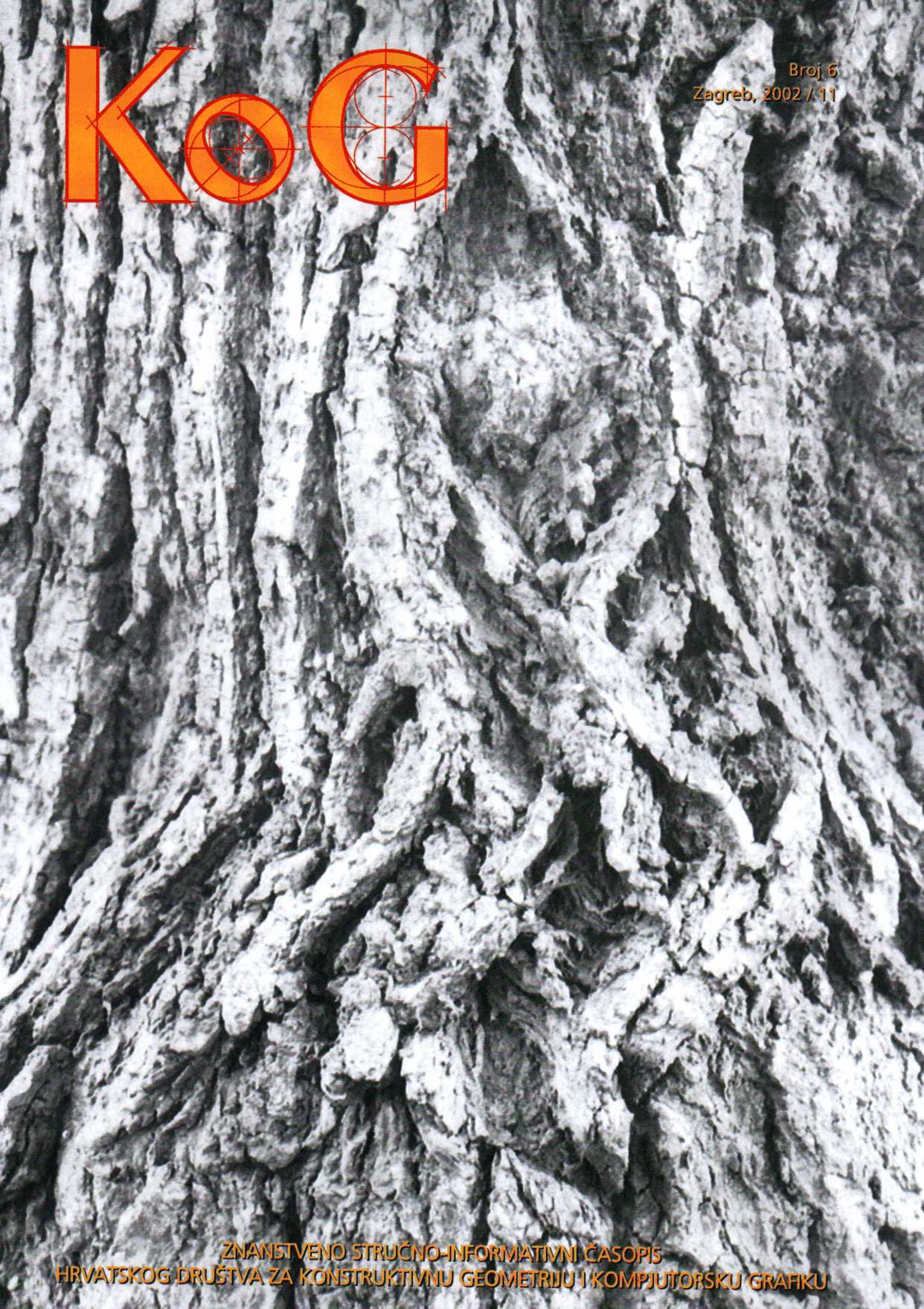

KoG

Broj 6
Zagreb, 2002 / 11

ZNANSTVENO STRUČNO-INFORMATIVNI ČASOPIS
HRVATSKOG DRUŠTVA ZA KONSTRUKTIVNU GEOMETRIJU I KOMPJUTORSKU GRAFIKU

ISSN 1331–1611

KoG

BROJ 6
Zagreb, 2002

ZNANSTVENO-STRUČNO-INFORMATIVNI ČASOPIS
HRVATSKOG DRUŠTVA ZA KONSTRUKTIVNU GEOMETRIJU I KOMPJUTORSKU GRAFIKU

SADRŽAJ

OBLJETNICE

IZVORNI ZNANSTVENI RADOVI

STRUČNI RADOVI

GEOMETRIJA I GRAFIKA

ISSN 1331–1611

KoG

No. 6
Zagreb, 2002

SCIENTIFIC AND PROFESSIONAL INFORMATION JOURNAL OF
CROATIAN SOCIETY FOR CONSTRUCTIVE GEOMETRY AND COMPUTER GRAPHICS

CONTENTS

ANNIVERSARIES

ORIGINAL SCIENTIFIC PAPERS

PROFESSIONAL PAPERS

GEOMETRY AND GRAPHICS

UPUTE SURADNICIMA

"KoG" je časopis koji objavljuje znanstvene i stručne radove te ostale priloge iz područja konstruktivne geometrije i računalne grafike

ZNANSTVENI I STRUČNI ČLANCI

1. Izvorni znanstveni rad sadrži neobjavljene rezultate izvornih znanstvenih istraživanja, a znanstvene su informacije izložene tako da se točnost analiza i izvoda, na kojima se rezultati temelje, može provjeriti.

2. Prethodno priopćenje znanstveni je rad što sadrži jedan ili više novih znanstvenih podataka priroda kojih zahtijeva hitno objavljivanje. Ne mora nužno imati dovoljno pojedinosti za ponavljanje i provjeru rezultata.

3. Pregledni rad znanstveni je rad što sadrži izvoran, sažet i kritički prikaz jednog područja ili njegova dijela u kojemu autor aktivno djeluje. Mora biti istaknuta uloga autorova izvornog doprinosa u tom području s obzirom na već publicirane radove te pregled tih radova.

4. Stručni rad sadrži korisne priloge iz područja struke koji nisu vezani uz izvorna autorova istraživanja, a iznesena zapažanja ne moraju biti novost u struci.

Rad mora biti neobjavljen i ne smije se istodobno ponuditi drugom časopisu. Autor za svoj rad predlaže kategoriju, a konačnu odluku o svrstavanju donosi Izdavački savjet na temelju zaključaka recenzenata. Znanstveni radovi mogu biti napisani na engleskom ili njemačkom jeziku, stručni na hrvatskom, engleskom ili njemačkom. Autor predaje tekst na jeziku koji odabere, te sažetak na hrvatskom i engleskom jeziku. Članci trebaju biti dopunjeni kontaktnim podacima o autorua, a dostavljaju se na adresu Uredništva KoG-a (vidi posljednju stranicu) ili elektronskom poštom na adrese urednica (sgorjanc@grad.hr, jbeban@geof.hr).
O prihvaćanju ili odbijanju rada autor će biti obaviješten. Prihvaćene radove autori dostavljaju elektronskom poštom kao ASCII datoteke. Preporučuje se LaTeX format.

OSTALI PRILOZI

To su stručni osvrti i prikazi različitih sadržaja iz širokog područja geometrije i grafike, vijesti i izvješća o znanstveno-stručnim skupovima, prikazi knjiga, časopisa, studentskih radova, softvera i hardvera, koji se objavljuju u rubrikama "Geometrija i grafika" i "Vijesti, izvješća, prikazi".

GUIDE TO THE COLLABORATORS

"KoG" is the journal publishing scientific and professional papers and other contributions from the field of constructive geometry and computer graphics.

SCIENTIFIC AND PROFESSIONAL PAPERS

1. Original scientific paper contains unpublished results of the original scientific research, and the scientific information is presented in such a way that it permits the exactness of analysis and derivations the results are based upon to be checked.

2. Preliminary communication is a scientific work containing one or more new scientific data, the nature of which requests urgent publishing. It need not necessarily convey sufficient number of details for repetition or checking of results.

3. Review is a scientific paper containing original, condensed and critical presentation of a field or its segment in which the author participates actively. The role of the author's original contribution in this field must be pointed out as related to already published works, accompanied by the survey of these works.

4. Professional paper contains useful contributions from the professional field which are not bound to the original research of the author, and the observations presented need not be a novelty in the profession.

The paper should be unpublished and it mustn't be offered to some other journal at the same time. The author suggests for his/her paper the category, and the final decision about how it is going to be classified is reached by the Publishing Council on the basis of the conclusions made by reviewers. The scientific paper can be written in English or German. The professional paper can be written in Croatian, English or German. Author hands in the text in the language he/she has chosen, and the abstract in Croatian and English. The articles should be supplemented by the notes to authors. The papers should be supplied to the Editorial Office of KoG (the address is at the last page) or by e-mail to editors (sgorjanc@grad.hr, jbeban@geof.hr).
Author will be notified about his paper being either accepted or rejected. Accepted papers are to be sent by authors by electronic mail as ASCII files. LaTeX format is recommanded.

OTHER ATTACHMENTS

These are professional reviews and presentations of various contents from the wider area of geometry and graphics, news and reports about scientific and professional gatherings, presentations of books, journals, student papers, softwares and hardwares published in the departments on "Geometry and Graphics" and "News, reports and presentations".

priredila: SONJA GORJANC

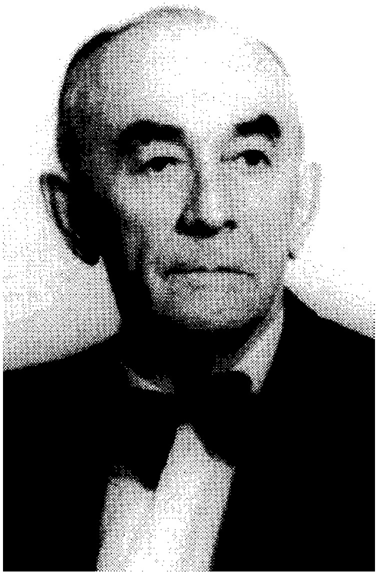

Stogodišnjica rođenja

Vilka Ničea

(1902. - 1987.)

Za ovaj su broj KoG-a naše mlade kolegice **Marija Šimić** i **Ema Jurkin**, koje predaju geometriju na tehničkim fakultetima, za našu rubriku "Vijesti, izvješća, najave" poslale kratko izvješće o zimskom sastanku našega društva, u kojem piše:
"... Prvi dio sastanka posvećen je stogodišnjici rođenja Vilka Ničea. Spomenuli smo ga se kao velikog znanstvenika i još većeg čovjeka, o čemu su nam svjedočile ...
Svoje uspomene i razmišljanja o njemu podijelili su s ostalima ..."
Zašto ovaj citat smatram toliko važnim da ga u priređivanju teksta povodom stogodišnjice rođenja Vilka Ničea, našeg učitelja, dopuštam sebi staviti na prvo mjesto. Zato što se u tom izvatku iz zapisnika vidi da su i naše mlade kolegice imale kada je o Vilku Ničeu riječ nešto čega su se mogle sjetiti te da su sudionici sastanka nešto međusobno podijelili. Prepoznala sam to kao ponovni živi dodir s utjecajem Vilka Ničea na našu sredinu.
Da se prije stotinu godina u našoj sredini nije rodio Vilko Niče sigurno je da ne bi postojao ovaj broj časopisa "KoG". Naš je časopis samo jedan od projekata inspiriranih njegovim djelom. Njega je pokrenulo i na njemu radi više generacija onih koji su u svom znanstvenom radu koristili njegovu metodologiju te istraživali dalje u nekoj od mnogih tema koje je u svojim radovima naznačio.

U prvom broju "KoG"-a, u tekstu *200 godina sustavnog grafičkog komuniciranja* **Branko Kučinić** piše:

"... Vilko Niče (1902.-1987.) svakako je bard hrvatske geometrije. Taj akademik, okorjeli sintetičar i pedagog, ostavio je iza sebe opus od 71 znanstvenog rada i 6 knjiga, čemu treba pridodati veći broj mentorstva, dakle 'njegovih' doktora i magistara znanosti. Golem je broj matematičara i inženjera kojima je Niče u živom sjećanju.

Osim što je gostovao na Prirodoslovno-matematičkom fakultetu u Zagrebu (Nacrtna geometrija II i III, Sintetička geometrija, Poslijediplomski studij) i drugdje, radio je stalno najprije na Tehničkom fakultetu, zatim na AGG fakultetu te najzad na Arhitektonskom fakultetu. Kraj rata 1945. zatekao ga je na dužnosti dekana Tehničkog fakulteta, gdje je od razaranja spasio biblioteku AGG fakulteta te laboratorije Zavoda za mehaniku. Nakon rata bio je u zvanju degradiran te je iz početka, po drugi put gradio sveučilišnu karijeru. Za razliku od drugih profesora slične sudbine, valjda greškom nije rehabilitiran.

Niče je bio prototip pravog gospodina i veliki čovjek. Njega bi čak i Diogen pronašao. Gotovo uvijek s leptir-kravatom i u lovačkom hubertusu, okupljao je velik broj prijatelja, među kojima su se isticali matematičar Blanuša, arhitekti Deuzler i Vrkljan te geodet Macarol. Područje njegova znanstvenog djelovanja neobično je široko - od istraživanja krivulja i općih i pravičastih ploha, preko specifičnih izvođenja: cisoidalnog, nožišnog, preko sustavno izvedenih kvadratnih transformacija, pa do krune njegova djelovanja: četiri kompleksa vezana uz pramenove polarnih prostora kvadrika. Jedan od ta četiri kompleksa ušao je u svjetsku literaturu kao Ničeov kompleks.

Mnogo je matematičara koji su surađivali s Ničeom ili nastavili njegovo djelo. Spomenimo svjetske: Decuyper (Francuska), Bothema (Nizozemska), Hohenberg (Austrija), Wunderlich (Austrija), Brauner (Austrija), Mateski (Makedonija), Vujaković (Bosna i Hercegovina), ...

Valja spomenuti i domaće (tzv. Ničeovu školu): Palman, Dočkal, Šćurić, Kučinić, Horvatić, Sliepčević, Gorjanc, Saler ...”

Predsjednica našega društva **Ana Sliepčević**, na ovogodišnjem skupu geometričara “Geometrie-Tagung” u Vorau, povodom stogodišnjice rođenja evocirala je u svom izlaganju *So hat Vilko Niče nachgedacht* uspomene na Vilka Ničea. I sama je bila iznenađena koliko je topline i interesa njezino izlaganje pobudilo. Na tom se skupu svojim sjećanjima na Vilka Ničea nadovezao i Hellmut Stachel.
Svi koji su imali priliku slušati profesora Ničea kao predavača govore o izuzetnom geometrijskom doživljaju. Njega opisuje Ana Sliepčević u tekstu *U spomen Vilku Ničeu*, “Matematika i škola”,15/2002, gdje između ostalog kaže:

“... Imaginarni su mu elementi bili jednako bliski kao i realni, prostorni odnosi među najsloženijim geometrijskim tvorevinama zorni i dohvatljivi, a znao je o svemu tako predavati, da su vam se ispred očiju jednostavno redali kompleksi, kongruencije, plohe, ... Osjećali ste se kao da ste u jednoj višoj dimenziji. Pomoću realnih i imaginarnih, beskonačno dalekih točaka i pravaca uspio je doći do nevjerojatnih zaključaka i učiniti ‘vidljivim’ i ono što inače nije moguće vidjeti. Znao je tako dobro zamišljati u prostoru, a zatim o tome što je zamislio, tako dobro glasno razmišljati i raspravljati, da je pažljivom slušatelju uspijevalo stvoriti realnu predodžbu onoga što je bilo predmetom razgovora. ...”

Na godišnjicu smrti Vilka Ničea izdala je tadašnja JAZU *Spomenicu* preminulom članu. Ovdje prenosimo gotovo u cijelosti kratku biografiju što ju je za in memoriam preminulom kolegi nadahnuto napisao sada pokojni akademik **Stanko Bilinski**.

“... Vilko Niče rođen je 1902. godine u Podravini u Grubišnom Polju. Škole je polazio u rodnom mjestu, a zatim u Karlovcu, Zagrebu i Bjelovaru, gdje je i maturirao. Na Filozofskom fakultetu u Zagrebu studirao je matematiku, a tu je i diplomirao. Tu je još kao student prve godine studija 1923. godine bio demonstrator na katedri geometrije kod prof. Jurja Majcena, koji je bio znanstveni radnik na području geometrije i nacrtne geometrije, istaknut i poznat i u svjetskim razmjerima, a s kojim je bio u uskoj i znanstvenoj i prijateljskoj vezi. Ova njihova iako nažalost kratka suradnja, koja je potrajala jedva neka 3 semestra, bila je presudna za cijeli daljnji razvoj Vilka Ničea kao znanstvenog radnika. Po završetku studija matematike Vilko Niče je bio izabran za asistenta na Katedri nacrtne geometrije na tadašnjem jedinom Tehničkom fakultetu u Zagrebu. Nažalost, nakon što je Majcen - tada još vrlo mladi profesor - nenadano preminuo, Vilko Niče se dalje razvijao zapravo kao samouk bez pravog kontakta s ostalim znanstvenim svijetom, jer u Zagrebu je tada bilo malo znanstvenih knjiga iz područja geometrije, a o periodičnim znanstvenim publikacijama iz područja matematičkih nauka da se i ne govori. Poticaji za znanstveni rad u području geometrije jedva da su do Vilka Ničea i mogli doći. O nekim specijalizacijama, inozemnim stipendijama i studijskim boravcima u svjetskim znanstvenim centrima, što je danas gotovo samo po sebi evidentno i vrlo uobičajeno, tada nije moglo biti ni govora. Zato njegov znanstveni rad, silom prilika, možda izgleda malo nesuvremen, ali zato nosi obilježja znatne originalnosti i samostalnosti.

Vilko Niče je nastavio svoj rad na Katedri nacrtne geometrije, koja je nakon diobe Tehničkog fakulteta pripala Arhitektonskom fakultetu, ali je poslije rata pa sve do prije desetak godina, bio aktivan kao nastavnik i na Prirodoslovno-matematičkom, Građevinskom i Geodetskom fakultetu, a osim toga i na Umjetničkoj akademiji, pa i na Višoj pedagoškoj školi u Zagrebu. On je držao predavanja i na postdiplomskim studijima u Zagrebu i Beogradu. Pod njegovim vodstvom završilo je taj studij i dobilo zvanje magistra matematičkih nauka više desetaka kandidata iz Zagreba, Beograda, Skoplja, Ljubljane, Sarajeva, Maribora, Novog Sada, Niša, Rijeke i Splita, a desetak doktora matematičkih nauka, koji su bili njegovi doktorandi, danas su docenti i profesori na mnogim fakultetima u gotovo svim republičkim centrima i većim gradovima Jugoslavije. Iz tih činjenica se razabire da je rad Vilka Ničea na izgradnji mladih nastavnika i znanstvenih radnika na području nacrtne i sintetičke geometrije bio intenzivan i vrlo uspješan. On je vrlo dobro znao oko sebe okupiti mlade i sposobne ljude i na njih prenijeti svoju ljubav i oduševljenje za znanstveni rad, a njegov prijeteljski i očinski odnos prema tim mladim ljudima bio je i više nego uzoran. Od milja zvali su ga međusobno ‘gazda’.

Znanstveni rad Vilka Ničea bio je usmjeren gotovo isključivo na područje sintetičke i posebno sintetičke projektivne geomtrije, a u tom je području bio pravi majstor, sigurno svjetski kapacitet. Njegov nevjerojatno razvijen prostorni zor pronikao je u mnoge zanimljive odnose prostornih figura i tvorevina, i tamo otkrivao neke vrlo lijepe zakonitosti i teoreme. Taj se njegov rad kretao ponajviše u području teorije konfiguracija i kompleksa, koji su vezani uz neke druge geometrijske tvorevine, no teško bi bilo i nabrojati makar i najvažnije rezultate do kojih je on tu došao.

Njegovi radovi čine izvanrednu cjelinu, koja se odlikuje jedinstvenošću metode što je autor dosljedno primjenjuje u svim svojim radovima, a postignuti su bili na taj način i mnogi vrlo lijepi i neslućeni rezultati. Prenoseći svoje oduševljenje za znanstveni rad na svoje mnogobrojne suradnike, profesor Niče nije nikada štedio u davanju pobuda na osnovi vlastitih originalnih ideja. Njegovi znanstveni radovi, svaki za sebe vrijedan, toliko su međusobno povezani da čitalac tih radova stječe dojam kako se tu radi o dijelovima jedne dobro zamišljene originalne monografije, koja osim svega daje i mogućnost za još dalje i dublje ulaženje u bit tih problema, pa tako otvara vidike na još mnoge neslućene mogućnosti.

U vezi s nastavnim radom Vilka Ničea treba još spomenuti da je on i autor triju odličnih udžbenika za visoke škole iz područja sintetičke i nacrtne geometrije. Svi su ti udžbenici pisani lijepim i lakim stilom, pa je za njima potražnja još i danas velika.

Vilko Niče je za svoj znanstveni i nastavni rad primio i mnoga priznanja. Godine 1960. izabran je za dopisnog člana JAZU, a 1973. godine za redovnog člana. Od 1978. do 1984. godine, dakle kroz 3 izborna perioda, bio je tajnik razreda za matematičke, fizičke i tehničke znanosti, i za sve to vrijeme nije se u tom razredu pojavio nikakav nesporazum, jer je svojim mirnim i taktičnim načinom svaki eventualni mogući nesporazum već unaprijed znao isključiti.

Za svoj rad Vilko Niče je primio i mnoga priznanja. Tako posebno:

1965. Orden rada sa crvenom zastavom,

1966. Nagrada 'Ruđer Bošković',

1969. Nagradu grada Zagreba,

1972. Nagradu za životno djelo.

Na to 'životno djelo' - kao što se kasnije pokazalo - još ni tada nije bilo završeno, iako mu je tada bilo prošlo već 70 godina.

Još godine 1956. Vilko Niče je primio ponudu za redovnu profesuru iz nacrtne geometrije na Tehničkoj visokoj školi u Hannoveru, no nije ju prihvatio. Ta njegova patriotska gesta došla je do izražaja i u publiciranju znanstvenih radova. Od svih njegovih znanstvenih radova, od kojih je zadnji - tj. 72. po redu - bio publiciran 1982. godine - dakle kada je već navršio 80 godina života - bilo je 29 radova publicirano u 'Radu' JAZU, a 25 u Glasniku matematičkom, dok su preostali radovi objavljeni u drugim zagrebačkim, odnosno drugim jugoslavenskim znanstvenim časopisima. Ipak su novi rezultati, koji su u tim radovima sadržani - ponajviše preko svjetskih referativnih žurnala - bili uskoro poznati i u svijetu stranih geometričara. Tako su na njegove ideje i postignute rezultate svoja istraživanja i radove nadovezali i mnogi strani geometričari, među ostalima Hohenberg i Tschupik iz Graza, Wunderlich i Brauner iz Beča, Decuyper iz Lillea i Giering iz Münchena.

Odlazak Vilka Ničea iz naše sredine bio je za tu sredinu vrlo bolan i veliki gubitak, koji ćemo još dugo i teško osjećati, a njega se uvijek s poštovanjem i ljubavi rado sjećati. ..."

Također u *Spomenici Vilku Ničeu* nalazimo i *Sjećanje na akademika prof. Vilka Ničea* koje je napisala **Vlasta Ščurić**, jedna od njegovih najbližih suradnica i prva predsjednica našega društva. Ovdje ga u cijelosti prenosimo.

"Prošlo je već 13 mjeseci od smrti našeg profesora i prijatelja, akademika Vilka Ničea. Zapao me je častan ali i vrlo odgovoran zadatak da pomognem evociranju sjećanja sviju nas na njegov život, znanstveni i nastavni rad, a posebno na njega kao čovjeka.

Oprostite mi što ću u tome pokatkad biti subjektivna. Za to postoje mnogi razlozi, a osnovni je taj što je profesor Niče neposredno utjecao na tok čitavog mog života: od diplomskog rada pod njegovim vodstvom, poziva na rad na fakultetu, uvođenja u znanstveni rad, mentorstva magistarskog rada i doktorske disertacije do daljnjeg poticanja na znanstveni rad. To šturo nabrajanje krije u sebi mnogo, mnogo više. U prvom redu beskrajnu zahvalnost i poštovanje prema dr. Vilku Ničeu kao čovjeku i učitelju.

Bilo bi prelijepo kad bi svatko imao sreće da ima svog voditelja u svim bitnim momentima života, posebno znanstvenog rada.

Vilko Niče nije bio te sreće. Bio je u trećem semestru studija kad je umro njegov profesor akademik Juraj Majcen. Ali i to kratko vrijeme od nepuna tri semestra bilo je dovoljno da usmjeri interes budućeg znanstvenika prema geometriji, a posebno projektivnoj geometriji obrađenoj sintetičkom metodom.

Mnogo godina kasnije prihvatio se Vilko Niče zadatka da dade 'prikaz života, rada i naučnog razvoja istaknutog naučnog i kulturnog radnika' Jurja Majcena, pa je u 'Radu' JAZU tiskan 1961. godine i rad *Juraj Majcen*. Dirljivo je čitati s kolikim poštovanjem piše Vilko Niče o Jurju Majcenu. Dozvolite mi da citiram nekoliko karakterističnih odlomaka iz tog rada. Iz njih je vidljiv i stav akademika Ničea prema svom profesoru akademiku Jurju Majcenu kao čovjeku i znanstvenom radniku, ali i razmišljanja Vilka Ničea o geometriji, posebno sintetičkoj geometriji.

'Kao posljednji demonstrator Jurja Majcena, a zvao me je asistentom, što, naravno, nisam bio, bio sam u prisnom dodiru s njim do posljednjeg dana. Asistenta u to doba nije imao.

U četrdeset devetoj godini prekinuta je nit života čovjeka u naponu snage, kojemu su neobična nadarenost izvanredna energija i marljivost omogućili da se duboko zadubi u ogromno carstvo apstraktnih geometrijskih istina. Pomoću svog znanja, svoje upravo zapanjujuće moći prostornog predočivanja i savršeno izgrađene matematičke logike, postavio je on običnom ljudskom umu na dohvat cio niz apstraktnih, ali prirodnih matematičkih istina.

Upravo se Majcenu može zahvaliti da je gajenje geometrije u Zagrebu postala tradicija. Broj njegovih učenika, a kasnije zapaženih geometričara, govori o ispravnosti postojanja zagrebačke geometrijske škole.'

U nastavku govori Niče o Jurju Majcenu kao nastavniku, ali je za nas mnogo interesantnije sagledati u tome Ničeov stav i razmišljanje o geometriji.

’U svojim predavanjima, kako sveučilišnim tako i popularnim, uvodio je Majcen svoje slušače u cio jedan svijet, u svijet za njih novih geometrijskih tvorevina i njihovih međusobnih odnosa, koje su oni prihvaćali i razumijevali u prvom redu pomoću psihološke sposobnosti prostornog predočivanja. Svaki geometričar mora priznati da je upravo sposobnost prostornog gledanja prva temeljna osobina onoga koji želi postati i biti dobar geometričar.’

U daljnjem tekstu: ’Vrijednost originalnih rezultata, dobivenih na novom području na svoj način, ne može se i ne treba uvijek mjeriti samo nekim matematičkim mjerilom. Vrijednost tim rezultatima daje osobit čar i užitak kod uspješnog njihova postizavanja kad se prodire pomoću precizne matematičke logike i prirođene moći prostornog gledanja u divan sklad začaranog geometrijskog svijeta. Matematička logika i moć prostornog gledanja omogućuju ljudskom umu da se nekim, moglo bi se reći, gotovo psihološko-kinematičkim putem kreće u ogromnom bogatstvu geometrijskog svijeta i njegovih tvorevina i da na tom putu otkriva sve novije i sve ljepše takve tvorevine i sve dalji i dublji sklad u njihovoj međusobnoj povezanosti.’

Nakon konkretnog prikaza jednog rada Jurja Majcena razmišlja Vilko Niče dalje: ’Vidimo dakle, da se u svakom, nazovimo to, *prodoru* u neki novi dio geometrijskog svijeta pojavljuje cio niz novih širokih vidika, na kojih tajanstvene putove ljudski um vodi katkad upravo nerazumljiva težnja. Juraj Majcen je majstorski izvodio takve *prodore*, ostavivši kasnijim generacijama otvoren put prema tim širim vidicima iza kojih se krije sve to veće bogatstvo matematičkih istina, što se dalje njihovim putem krećemo. Upravo Mjacenov rad *O posebnoj vrsti kubičnog kompleksa* izvršio je ovakvu markantnu pionirsku ulogu.’

Vilko Niče nije imao životnog voditelja u znanstvenom i nastavnom radu. Time mu se ukazala veća mogućnost vlastitog izbora životnog puta. Veliki autoritet Jurja Majcena pomogao mu je ipak da se u nastavnom i znanstvenom radu bavi onim za što je imao najviše afiniteta i ljubavi: u nastavi nacrtnom geometrijom, a u znanstvenom radu uglavnom projektivnom geometrijom obrađenom sintetičkom metodom. I to je činio s tolikim žarom, otkrivao je sebi, ali i svima koji smo bili uz njega, odnosno čitali njegove radove, tolike ljepote u samom radu i rezultatima koje je postizao, da je bilo gotovo nemoguće ne pokušati poći njegovim stopama. Sretni smo i ponosni što je vlastitim zalaganjem i prirodnim sposobnostima postao najveći stručnjak svog vremena iz područja sintetičke projektivne geometrije i zahvalni smo mu što je dokazao, zajedno sa svojim brojnim učenicima, da se tom matematičkom disciplinom mogu još uvijek elegantno i relativno jednostavno istražiti mnogi, drugim metodama jedva rješivi geometrijski odnosi.

Prva tri znanstvena rada Vilka Ničea tiskana su 1928.-29. godine. Nakon toga slijedi pauza od jedanaest godina, da bi od 1940. do 1982. god. bilo objavljeno još 68 radova.

Praktički je nemoguće u nekoliko minuta sačiniti dublju analizu svih tih radova. Zajednička im je osobina sintetička metoda istraživanja, koja omogućava čitaocu da ‘vidi’ problem, a isto tako i zorno prati njegovo rješavanje. Osim toga, mnogi radovi završavaju s primjedbom o još neriješenim problemima vezanim uz problematiku koja se obrađuje u dotičnom radu. Na taj je način Vilko Niče nesebično omogućavao svima da neposredno nastave njegov rad, što je nama, njegovim učenicima, bilo posebno dragocjeno i plodonosno.

Među prvim su radovima razmatrane pravčaste plohe 3. i 4. stupnja s jednim ili dva para izotropnih izvodnica, kojih su sjecišta ‘izolirane kružne točke’ tih ploha. Pokazano je da se kod njihove konstruktivne obrade pomoću kružnih točaka veoma pojednostavljuju grafički postupci. U mnogim se radovima istražuju pramenovi polarnih prostora kvadrika, te tim pramenovima određeni kompleksi zraka. Vilko Niče je ustanovio da su svakim pramenom kvadrika određena četiri takva kompleksa. Jedan od njih, i to Reyeev tetraedarski kompleks, bio je od ranije poznat i istražen, no Niče je ukazao na još mnoga njegova nepoznata svojstva. Uočio je, nadalje, da je uz pramen kvadrika vezan i kompleks koji je na drugi način definirao i istraživao Juraj Majcen. U čast svom profesoru nazvao je taj kompleks Majcenovim i odredio još niz njegovih svojstava, odnosno svojstava što ih čine razne tvorevine definirane zrakama tog komlepksa. Definirao je i kompleks normala incidentnih ploha pramena kvadrika, te odredio njegova svojstva. Kao najinteresantniji pokazao se ‘kompleks najkraćih dirnih putova’ među plohama pramena kvadrika. Uz niz svojstava tog kompleksa koje je odredio Vilko Niče, daljnja su istraživanja pokazala neočekivano bogatstvo osobina što ih određuju razne tvorevine određene zrakama tog kompleksa. Sretna sam što sam ta istraživanja nastavila ja, jer mi je to omogućilo da taj nadasve interesantan i u znatnijem broju radova istraživani kompleks nazovem, uz privolu prof. Ničea, ‘Ničeovim kompleksom’, koji je pod tim nazivom ušao u matematičku literaturu.

Najjednostavnija i najinteresantnija pravčasta ploha stupnja većeg od dva jest Plückerov konoid. U nekoliko radova pronašao je Niče niz njegovih svojstava, koja su u referalnim časopisima bila posebno istaknuta.

Istražen je nadalje pramen koaksijalnih linearnih ništičnih prostora, te pronađeni novi jednoparametarski sistemi kvadratnih i kubičnih ništičnih prostora, kao i njihovi nožišni kompleksi. U više radova obrađene su krivulje i plohe dobivene poopćenom kvadratnom inverzijom i cisoidalnim postupkom. Tu se prvenstveno istražuju plohe koje prolaze apsolutom, a napose one koje duž te apsolute dira izotropni stožac. - U nekoliko radova istražen je skup svih valjaka jedne kružnice u prostoru. Kod toga je istraživana npr. kongruencija fokalnih osi hiperoskulacionih valjaka odnosno kompleks osiju oskulacionih valjaka i sl. - Istraživani su i svežnjevi kvadrika, pa i kompleks zraka određen pramenovima kvadrika unutar svežnja.

I iz tog kratkog i nepotpunog prikaza tema koje je obrađivao dr. Vilko Niče vidljivo je koliko je bilo široko područje kojim se znanstveno bavio. Znao je za još mnogo problema koji tek traže rješenja. Nije ih zadržao za sebe, već ih je stavio kao ideje na papir. Upoznavao nas je s time riječima: 'Djeco, ako će nekome ustrebati,...'

Vilko Niče je u svom radu bio izuzetno sistematičan i marljiv. Radio je svakodnevno i prije i poslije podne, često i nedjeljom.

Iako je u stručnim krugovima najviše poznat kao geometričar-znanstveni radnik, mnogo je više onih koji se sjećaju profesora Ničea kao nastavnika i s ponosom još danas ističu da su bili njegovi studenti.

I u predavanjima za studente osjećalo se da prof. Niče radi posao koji voli. Bio je poznat kao izvrstan crtač, a sa svojim nenadmašnim prostornim zorom uspio je i komplicirane probleme tako zorno približiti studentima da su oni od pasivnih slušača postali aktivni sudionici nastavnog procesa. Mnogi inženjeri zahvaljuju upravo profesoru Ničeu što je u njih uspio razviti moć prostornog predočivanja, bez koje ne bi uspješno mogli obavljati svoju svakodnevnu praksu.

Uz brojna predavanja na Tehničkom fakultetu, gdje je u poslijeratnom razdoblju bilo upisano i preko tisuću studenata, predavao je prof. Niče i na Prirodoslovno-matematičkom fakultetu i Akademiji likovnih umjetnosti u Zagrebu. Za današnje pojmove praktički je neshvatljivo kako je uza sav nabrojeni posao imao vremena i snage održati i preko tisuću ispita godišnje, i to s krajnjom strpljivošću. Nastojeći zadržati svoj čvrsti kriterij, nikada nije na ispitu povisio glas niti pokazao nervozu.

Kad je 1962. god. započela postdiplomska nastava za geometriju na Prirodoslovno-matematičkom fakultetu u Zagrebu, predavao je prof. Vilko Niče nekoliko godina i na tom studiju. Većina sadašnjih sveučilišnih nastavnika iz kolegija nacrtna geometrija u SRH tadašnji su njegovi studenti. Koju godinu kasnije osnovana je postdiplomska nastava za nactnu geometriju pri Arhitektonskom fakultetu u Beogradu. Prof. Niče bio je ne samo predavač nego i sutvorac tog studija, a slušači su bili gotovo iz svih krajeva Jugoslavije. Možemo kazati da je veoma malen broj sveučilišnih nastavnika nacrtne geometrije u Jugoslaviji koji nisu magistrirali ili doktorirali kod akademika Ničea.

Pogledamo li kroz prozor prema Zrinjevcu, vidjet ćemo grb grada Zagreba sačinjen od cvijeća. Na njemu su najpoznatija otvorena gradska vrata koja simboliziraju i otvoreno srce njegovih stanovnika.

Svi oni koji su dolazili u sobu akademika prof. dr. Vilka Ničeu Kačićevoj 26 mogli su uočiti da su vrata njegove sobe uvijek bila otvorena. Tri sobe nas nacrtnaša su naime s unutrašnje strane povezane vratima, koja se nisu zatvarala. To nije bio samo simbolički znak, nego mnogo više. Ta otvorena vrata govorila su rječitije od ičega da smo uvijek dobrodošli. Mogli smo bez ikakvog straha doći k profesoru da s njim podijelimo radost, sreću, ali i probleme i žalost. Za svakoga od nas imao je razumijevanja i vremena. Volio je ljude, želio je s njima komunicirati, razgovarati, imati ih oko sebe. To se pogotovo odnosilo na nas, njegove učenike i suradnike. Često smo ga prekinuli u radu. Nikad nam nije prigovorio.

Šezdesetih godina, kad je većina nas upisala postdiplomsku nastavu iz područja geometrije, sastajali smo se u 11 sati u njegovoj sobi da popijemo kavu. Kava je bila formalni razlog sastanka. Svaki takav skup pretvorio se i mini-seminar iz geometrije. Razgovarali smo o svakodnevnim rezultatima naših istraživanja, traženja načina rješenja, izmjenjivali smo iskustva i sugestije. Teško bi se moglo naći bolju, plodonosniju, poticajniju, prijatniju atmosferu od one koja je tih godina vladala u sobi profesora Ničea. Uvjerana sam da je bila jedinstvena. Rad u takvim uvjetima morao je uroditi plodom.

Dr. Niče je, kao što je spomenuto, predavao i na postdiplomskom studiju za nacrtnu geometriju u Beogradu. Polaznici tog studija češće su navraćali u Zagreb zbog konzultacija odnosno polaganja ispita. I njih je prof. Niče priglio kao i nas. Svi koji ga spominju govore u prvom redu o njegovom velikom srcu.

Svima nama koji smo ga bolje poznavali usadio je osim ljubavi za svakodnevni nastavnički rad, interes, stvaralački poticaj, samopouzdanje i ponovno ljubav za znanstveni rad, ali i ono najvrednije, spoznaju da je postojao čovjek u punom i pravom smislu te riječi. Bio je to akademik Vilko Niče."

Popis radova Vilka Ničea dajemo također prema *Spomenici*.

Znanstveni radovi

[1] Konstrukcija pravilnog peterokuta i deseterokuta, ako im je zadana stranica. Nastavni vjesnik, 36(1928), 48-51.

[2] Neki izvodi za konoide trećeg i četvrtog reda. Nastavni vjesnik, 37, (1929.), 1-23.

[3] Harmonijski dvoomjer na krivuljama 3. reda roda nultog te njegova primjena na neke pravčaste plohe 4. reda. Sveučilišni godišnjak 1929/30-1932/33, 3-9.

[4] Prilog zakrivljenosti prostorne krivulje. Nastav. vjesnik, 49, (1940), 30-33.

[5] O polarnim trokutima kružnice i polarnim tetraedrima kugle, Nastav. vjesnik, 49, (1941), 346-351.

[6] Geometrijsko mjesto dirališta pramena ravnina i pramena površina drugog reda. RAD JAZU, 271 (84), (1941), 65-68.

[7] Površine 4. reda kao geometrijsko mjesto dirališta pramena ravnina i svežnja površina 2. reda. RAD JAZU, 271 (84), (1941), 69-76.

[8] O čunjosječnicama na pravčastim plohama 3. i 4. reda. Disertacija. (1941).

[9] Vanjska oznaka unikurzalne cirkularne krivulje 3. reda. Nastav. vjesnik, 50, (1942), 360-362.

[10] O svežnju ploha 2. reda. RAD JAZU, 274 (85), (1942), 163-169.

[11] Prilog konstruktivnoj obradi pravčastih ploha 3. reda. RAD JAZU, 274 (85), (1942), 286-298.

[12] Konstrukcija četverostrukog fokusa cirkularnih krivulja 3. i nekih 4. reda roda nultoga. Nastavni vjesnik 51, (1943), 271-280.

[13] Doprinos zajedničkim svojstvima ravninskih krivulja 3. i 4. reda roda nultoga. RAD JAZU, 278 (86), (1945), 55-61.

[14] Krivulje i plohe 3. i 4. reda nastale pomoću kvadratne inverzije. RAD JAZU, 278 (86), (1945), 153-194.

[15] O imaginarnim elementima u geometriji, GLASNIK mat. fiz. i astr. 1, (1946), 193-208.

[16] Četverostruki fokus unikurzalnih cirkularnih krivulja 3. reda i neki osobiti pramenovi tih krivulja. RAD JAZU, 271, (1947), 3-12.

[17] O cirkularnim krivuljama 4. reda roda nultog s neizmjerno dalekom dvostrukom točkom. RAD JAZU, 271, (1947), 23-31.

[18] O hiperoskulacionim kružnim valjcima jedne kružnice. GLASNIK mat. fiz. i astr. 4, (1949), 1-10.

[19] O Plückerovu i nekim drugim konoidima 3. i 4. reda. RAD JAZU, 276, (1949), 3-12.

[20] O strofoidali i prostornoj krivulji 4. reda na kugli. RAD JAZU, 276, (1949), 27-36.

[21] Jedan dokaz i nadopuna P. Appelova stavka o Plückerovu konoidu. GLASNIK mat.fiz. i astr. 4, (1949), 173-175.

[22] Kratki pregled sintetičke geometrije. VESNIK mat. fiz. NRS, 24, (1950), 73-82.

[23] Konstrukcija kubne čunjosječnice iz konjugirano imaginarnih točaka. VESNIK mat. fiz. NRS 4, (1950), 35-38.

[24] O nožišnim plohama rotacionog paraboloida, GLASNIK mat. fiz. i astr. 5, (1950), 3-11.

[25] Plohe izotropnih izvodnica u kongruencijama 3. 2. i 1. razreda. GLASNIK mat. fiz. i astr. 6, (1950), 97-105.

[26] O nekim novim rezultatima i još otvorenim problemima na području sintetičke geometrije u okviru ploha 3. i 4. reda. Referat na kongresu matematičara, Bled (1950), 1-6.

[27] Strofoidalne plohe 3. reda. ZBORNIK mat. instituta SAN, Beograd, 2, (1952), 97-112.

[28] Les surfaces strophoidales du 3e ordre. PUBLICATION de L'institute mathem. de l'Academie serbe, IV. (1952), 113-120.

[29] Prilog geometriji tetraedra. GLASNIK mat. fiz. i astr. 7, (1952), 228-243.

[30] Bošković i geometrija, Almanah Bošković (1952), 32-60.

[31] Über die isotropen Strahlpaare 2. Art. der Strahlkongruenzen 1. Ord. 3., 2. und 1. Klasse. GLASNIK mat. fiz. i astr. 7, (1952), 293-296.

[32] Izolirane kružne točke na pravčastim plohama 3. i 4. reda. RAD JAZU, 292, (1953), 193-222.

[33] Prilog načinima izvođenja ploha 3. reda. RAD JAZU, 292, (1953), 170-191.

[34] O fokalnim osobinama bicirkularnih krivulja i nekih ciklida 4. reda. RAD JAZU, 296, (1953), 184-197.

[35] O pregršti ploha 2. reda određenoj sa šest točaka u prostoru. RAD JAZU, 302, (1955),. 4-13.

[36] O geometrijskom mjestu četverostrukih fokusa jednog snopa ravninskih cirkularnih presjeka nekih ploha 3. i 4. reda. RAD JAZU, 292, (1953), 56-66.

[37] Cisoidalne plohe ravnine i kugle, njihove pratilice i neke njihove generalizacije. RAD JAZU. 302, (1955), 26-46.

[38] Die Brennpunktsfläche der Kegelschnitte des Plückerschen Konoids. GLASNIK mat. fiz. i astr.9, (1954), 251-257.

[39] Kompleks osi oskulacionih kružnih valjaka jedne kružnice i neke njegove plohe i kongruencije. RAD JAZU, 314, (1957), 92-109.

[40] Die Brennachsenkongruenz der Zylinder eines Kreises. GLASNIK mat. fiz. i astr. 11, (1956), 37-44.

[41] La science mathematique en Croatie, Bulletin scientif. 2(3), (1955), 68-72.

[42] Parametrische Sextupel Reyescher tetraedraler Strahlkomplexe eines und zweiter Haupttetraeder. GLASNIK mat. fiz. i astr. 13, (1958), 107-120.

[43] Reyevi tetraedralni kompleksi jednog, dvaju, triju i četiriju glavnih tetraedara. RAD JAZU, 314, (1959), 228-262.

[44] Modell der 27 Geraden einer Fläche 3. Ordnung. GLASNIK mat. fiz. i astr. 15, (1960), 107-111.

[45] Ein Beitrag zum F2-Bündel mit Polartetraeder. GLASNIK mat. fiz. i astr. 15, (1960), 179-188.

[46] Beiträge zum Büschel der Reyeschen tetraedralen Strahlkomplexe. RAD JAZU, 325, (1961), 26-48.

[47] Ergenzände Beiträge zum Majcenschen kubischen Srahlkomplex. RAD JAZU, 325, (1962), 106-125.

[48] Juraj Majcen, RAD JAZU, 325, (1962), 48-125.

[49] Novi prilozi Reyeovim tetraedralnim kompleksima, BULLETIN mat. fiz. SRS 14, (1962), 125-130.

[50] Über neue Eigenschaften der Büschel und der Bündel polarer Räume. GLASNIK mat. fiz. i astr. 17, (1962), 189-204.

[51] Kompleks osi valjak zraka tetraedralnih kompleksa u jednom pramenu takvih kompleksa. BULLETIN mat. fiz. SRS, 14 (1962), 123-124.

[52] Normalenkomplex der Flächen eines Flächenbüschels 2. Grades. GLASNIK mat. fiz i astr. 18, (1963), 255- 268.

[53] Über die Fusspunkte der Strahlen des achsenkomplexes eines Polarraumes. GLASNIK mat. fiz. i astr. 18, (1963), 269-278.

[54] Die Achsenkomplexe der in einem Büchsel sich befindenen Polarräume. GLASNIK mat. fiz. i astr. 19, (1964), 243-255.

[55] Über die kürzesten Tangentialwege zwischen den Flächen eines Flächenbüschels 2 Grades. RAD JAZU, 331, (1965), 144-172.

[56] Homothetische polare Räume. RAD JAZU, 343, (1966), 80-118.

[57] Koaxiale polare Räume. GLASNIK mat. fiz. i astr. 21, (1966), 223-243.

[58] Die Achsenregelfläche eines Flächenbüschels 2. Grades. GLASNIK mat. fiz i astr. 21, (1966), 215-221.

[59] Konzentrische polare Räume. GLASNIK MATEMATIČKI, 2 (22), (1967), 99-117.

[60] Die gemeinsamen Kongruenzen der vier Starhlkomplexe eines Polarraumbüschels. RAD JAZU, 347, (1968), 193-220.

[61] Eine neue Eigenschaft des Flächenbüschels 2. Grades. GLASNIK MATEMATIČKI 3. (23), (1968), 261-263.

[62] Das koaxiale Nullraumbüschel. RAD JAZU, 349, (1969), 13-31.

[63] Ein Beitrag zu den Sätzen von C. G. Jacobi, W. Fenchel und V. Avakumović. GLASNIK MATEMATIČKI 2 (24), (1969). 291-297.

[64] Neue Beiträge zu den Eigenschaften eines Polarraumbündels. GLASNIK MATEMATIČKI 2(24), (1969), 259-274.

[65] Noch einige Eigenschaften des Plückerschen Konoids. GLASNIK MATEMATIČKI 5(25), (1970), 309-318.

[66] Zusätzliche Betrachtugen mit ergänzenden Sätzen über den Tangentialkurzwegekomplex eines Flächenbüschels 2. Grades. RAD2), (1967), 99-117.

[67] Die Direktrixkongruenz der Kegelschnitte des Plückerschen Konoids. GLASNIK MATEMATIČKI 7(27), (1972), 269-276.

[68] Über eine Quasi-nullraumabbildung. RAD JAZU, 367 (1974), 37-55.

[69] Über die konstruktive Bahandlung einer rot. Kugelflächen 3. Ordnung. GLASNIK MATEMATIČKI 9. (1974), 303-315.

[70] Der kubische Nullraum zweier linear Kongruenzen. RAD JAZU 374 (1977), 5-31.

[71] Über die mittels der Polarfelder bestimmten Nullräume, RAD JAZU 396 (1982), 29-44.

Visokoškolski udžbenici, priručnici i monografije

[1] Deskriptivna geometrija. Šesto izdanje, Školska knjiga, Zagreb 1971.

[2] Perspektiva. Treće izdanj. Školska knjiga, Zagreb 1972.

[3] Uvod u sintetičku geometriju. Prvo izdanje. Školska knjiga, Zagreb 1956.

[4] F. Hohenberg: Konstruktivna geometrija u tehnici. Građevinska knjiga, Beograd 1966.. Prijevod s njemačkog jezika.

[5] I. Paál: Nacrtna geometrija u anaglifskim slikama. Tehnička knjiga, Zagreb 1966.. Prijevod s mađarskog jezika.

[6] Deskriptivna geometrija I i II. Školska knjiga, Zagreb 1979.

Sto godina po rođenja Vilka Ničea našla sam se u situaciji da za časopis “KoG”, kao jedna od njegovih urednica, priredim prigodni tekst. Učinila sam to najbolje što sam u ovom trenutku znala. Kad sam se zapitala u čije ja to ime uzimam sebi pravo ovdje nešto pisati, te tko su ti ljudi koji na različite načine vide Vilka Ničea kao svoga učitelja, nisam mogla do kraja sagledati tu zajednicu. Ona je mala ili velika, razjedinjena ili jedinstvena, ovisno o tome kako se na nju gleda, a iz svog kuta gledanja ne mogu sa sigurnošću reći da li se povećava ili smanjuje. Svakako postoji i ja joj pripadam. Onima kao što sam ja, koji nisu imali prilike osjetiti neposredno ljudsko djelovanje profesora Ničea, ostavio je literaturu na našem jeziku, za nas je prevodio s drugih jezika, skupljao važne knjige i ostavio nešto što sam oduvijek nazivala *Ničeovom knjižnicom*. Ovom prigodom pozivam sve članove naše zajednice da na stogodišnjicu rođenja Vilka Ničea zajedničkim snagama nađemo najbolje rješenje za to da knjige i članke koje nam je učitelj baštinio učinimo dostupnima svima koji ih žele čitati i u ovom stoljeću.

Originäre wissenschaftliche Arbeit
Angenommen am 04.04.2002

DANIEL LORDICK

Schattengrenzen krummer Flächen – Drehflächen, Schraubrohrfläche und Meridiankreisschraubfläche

Rastavnice oblih ploha - rotacijskih i zavojnih cikličkih

SAŽETAK

Uobičajeno je da se tangenta t na rastavnicu e oble plohe Φ konstruira na temelju činjnice da su t i zraka svetlosti l par konjugiranih dijametara tzv. DUPINOVE *indikatrise* u promatranoj točki P. Ovaj rad opisuje drukčiji pristup konstrukciji takve tangente: rastavnica e definira se kao prodorna krivulja plohe Φ i specijalne pravčaste plohe Ψ koja ovisi o Φ i snopu zraka svetlosti. Ψ se uvodi kao *pridružena pravčasta ploha* duž krivulje e. Taj pristup omogućuje jednostavnu, linearno i globalno primjenjivu konstrukciju tangente t za rotacijske i zavojne plohe, na način nacrtne geometrije. Metoda je također prikladna za klizne plohe isto kao i za centralnu rasvjetu. U nekim je slučajevima ploha Ψ pravčasta kvartika.

Ključne riječi: Dupinova indikatrisa, oble plohe, pravčaste plohe, sjene

Shade Lines of Curved Surfaces - Rotational and Helical Circular Surfaces

ABSTRACT

Typically a tangent t to the shade line e of a curved surface Φ is constructed by making use of the fact that t and the light ray l form a pair of *conjugate diameters* of the so-called DUPIN-*indicatix* of Φ at an investigated point P. This article describes a very different approach to developing such a tangent: The shade line e is defined as the intersection of Φ and a special ruled surface Ψ, which depends both on Φ and on the bundle of light rays. Ψ is introduced as *accompanying ruled surface* along e. This approach allows a simple, linear and globally applicable construction of t for rotational and helical surfaces by means of descriptive geometry. The method is also suitable for translation surfaces as well as for central illumination [4]. In a few cases Ψ is a ruled quartic.

Key words: curved surface, Dupin-indicatrix, ruled surface, shades and shadows

MSC 2000: 51M99, 51N05, 53A05

Der Artikel führt kurz in die *Begleitregelflächenmethode* zur Konstruktion von Tangenten an die Eigenschattengrenzen krummer Flächen ein und zeigt anschließend ihre Anwendung auf Drehflächen, Schraubrohrfläche und Meridiankreisschraubfläche. Weitere Einzelheiten werden in [4] dargestellt. Dort sind, neben der Behandlung der Schiebflächen und des Torus bei Zentralbeleuchtung, insbesondere die Begleitregelflächen selbst Gegenstand der Untersuchung.

1 Begleitregelflächenmethode

Nur auf regulären krummen Flächenstücken kann eine Eigenschattengrenze auftreten, die in Abhängigkeit von der Lichtrichtung variiert. Für die zu untersuchenden Flächenstücke wird deshalb vorausgesetzt, dass sie nicht eben sind und zu jedem Flächenpunkt genau eine Flächennormale existiert. Außerdem beschränken wir uns vorerst auf den Fall der Parallelbeleuchtung (Abb. 1). Die Lichtrichtung wird so angenommen, dass keine Flächengebiete in so genanntem *Streiflicht* existieren.

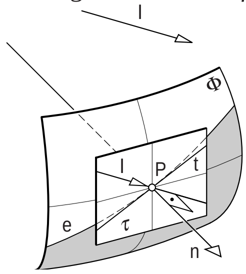

Abb. 1

Punkte der Eigenschattengrenze e einer Fläche Φ erhält man mit

Satz 1 *Bei Parallelbeleuchtung ist die Eigenschattengrenze einer regulären krummen Fläche der Ort jener Flächenpunkte, in denen die Flächennormalen zur Lichtrichtung normal sind.*

Die Flächennormalen längs e erfüllen eine *konoidale Regelfläche* Ψ, deren Richtebene zur Lichtrichtung normal ist (Abb. 2). Wenn e regulär ist, was wir voraussetzen wollen, muss Ψ in einem Umgebungsstreifen von e ebenfalls regulär sein.

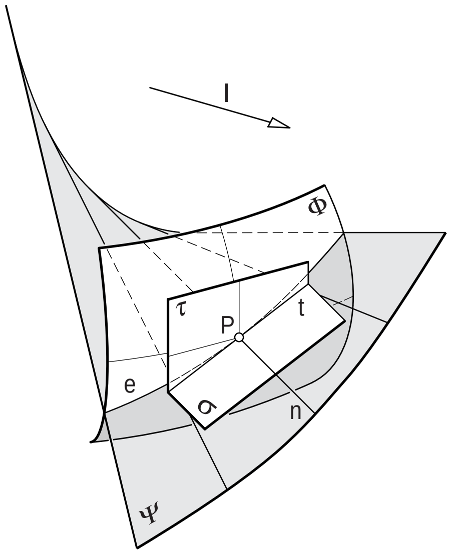

Abb. 2

Mit Ψ liegt eine Hilfsfläche vor, die Φ in e (normal) schneidet. In jedem Punkt von e kann die Tangente an e folglich als Schnittgerade der entsprechenden Tangentialebenen von Φ und Ψ konstruiert werden. Im Wesentlichen läuft das darauf hinaus, dass gewisse Tangentialebenen von Ψ unter Ausnutzung der *Berührkorrelation* verfügbar gemacht werden müssen.

Mit dem Ziel, eine konstruktiv leicht beherrschbare Regelfläche durch e zu erhalten, kann es gelegentlich, etwa bei Schiebflächen, sinnvoll sein, eine andere als die Normalenfläche zu betrachten. Wir berücksichtigen das durch folgende Bezeichnung:

Def. 1 *Eine durch Geraden erzeugte Hilfsfläche, die eine krumme Fläche Φ längs der Eigenschattengrenze von Φ schneidet, heißt eine Begleitregelfläche der Eigenschattengrenze.*

Sind die Erzeugenden der Begleitregelfläche Ψ Flächennormalen von Φ, so ist Ψ der Schnitt der Normalenkongruenz von Φ mit dem *planaren Normalenkomplex* der Lichtrichtung. Bleibt die Lichtrichtung konstant, so ist Ψ auch Begleitregelfläche aller Parallelflächen von Φ.

2 Tangenten an die Eigenschattengrenzen von Drehflächen

Bei jeder Drehfläche Φ ist die Normalenkongruenz eine Untermenge des Gebüsches durch die Drehachse a. Jede Begleitregelfläche von Φ liegt somit in der Schnittkongruenz dieses Gebüsches mit dem Normalenkomplex der Lichtrichtung. Weil beide Komplexe ersten Grades sind, erfüllt die Schnittkongruenz im Allgemeinen ein hyperbolisches Netz mit den Netzachsen a und l_∞, der Ferngeraden der Normalebenen zur Lichtrichtung ([5] S. 5 ff). Wenn die Lichtrichtung zu a normal ist, zerfällt das Netz und erfüllt eine Meridianebene.

Satz 2 *Die Begleitregelfläche einer Drehfläche bei Parallelbeleuchtung ist im Allgemeinen eine Netzfläche mit der Drehachse als Leitgerade und einer zur Lichtrichtung normalen Richtebene, das heißt sie ist ein schiefes Konoid.*

Nur beim Torus hat die Normalenkongruenz neben a eine zweite einfache Leitkurve, den Mittenkreis m. Die Begleitregelfläche des Torus ist folglich eine Netzfläche durch m und wegen der gegenseitigen Lage von a, l_∞ und m von viertem Grad und siebter STURMscher Art (Abb. 3).

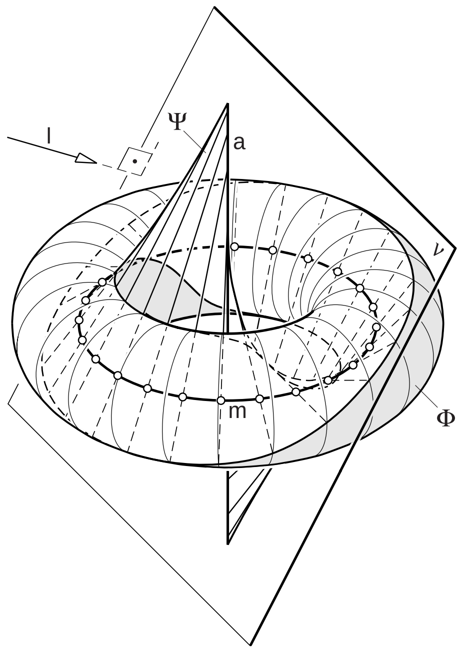

Abb. 3

In der Regel weist die Normalenkongruenz einer Drehfläche Φ anstelle von m eine koaxiale Leitdrehfläche (Brennfläche) Θ auf. Der Meridian von Θ ist die Evolute des Meridians von Φ. Jede Begleitregelfläche Ψ von Φ berührt Θ längs einer Raumkurve, deren Drehriss ein Teil der Evolute ist.

Durch die Leitgerade a, die Berührung mit Θ sowie die Fernleitgerade l_∞ sind zu jeder Erzeugenden n von Ψ in drei verschiedenen Punkten die Tangentialebenen gegeben, mit deren Hilfe die Berührkorrelation längs n vervollständigt werden kann. Dabei wird die Tangentialebene im Berührpunkt M von n mit Θ durch n und die Breitenkreistangente in M aufgespannt. Zugleich ist M der Mittelpunkt des Meridiankrümmungskreises im zu n gehörenden Flächenpunkt P von Φ. Für die Vervollständigung der Berührkorrelation ist demnach unerheblich, welche Eigenschaften Θ besitzt. Die Konstruktion ist durchführbar, sobald zu jedem untersuchten Punkt von Φ ein Meridiankrümmungskreis bekannt ist.

Wenn offensichtlich die Festlegung der Berührkorrelation längs einer Erzeugenden von Ψ – und damit verbunden die Konstruktion der Tangente an die Eigenschattengrenze – nur von der Meridiankrümmung und der Drehachse a sowie l_∞ abhängig ist, kann Φ lokal durch einen entsprechenden Torus und seine Begleitregelfläche ersetzt werden. Bekanntlich gilt:

Längs des Breitenkreises durch einen allgemeinen Punkt P einer Drehfläche Φ_1 wird Φ_1 von einem koaxialen Torus Φ_2 oskuliert, dessen Meridian der Meridiankrümmungskreis von Φ_1 in P ist. Das heißt in P stimmt das Schattengrenzenverhalten von Φ_1 und Φ_2 jedenfalls bis zur ersten Ordnung überein. Wir begnügen uns deshalb damit, den Torus bezüglich seiner Eigenschattengrenze näher in Augenschein zu nehmen.

Torus

Zu einem allgemeinen Punkt P der Eigenschattengrenze e eines Torus Φ soll die Tangente t von e im Normalriss in der Lichtmeridianebene, kurz *Lichtmeridianriss*, konstruiert werden (Abb. 4). Die Flächennormale n durch P ist eine Erzeugende der Begleitregelfläche Ψ von Φ längs e. Die gesuchte Tangente t ist die Schnittgerade der Tangentialebenen τ von Φ und σ_P von Ψ in P. Es ist darum sinnvoll, die Berührkorrelation längs n direkt in τ zu vervollständigen.

Zuerst benötigt man die Spuren der drei bekannten Tangentialebenen von n in τ. Das Bild der Spur s_∞ der asymptotischen Ebene fällt in der gewählten Aufstellung in den Meridianriss von n. Die Spur der Tangentialebene σ_M in M, die durch n und den Mittenkreis m aufgespannt wird, ist die Breitenkreistangente t_b in P. Die Tangentialebene σ_N im Schnittpunkt N von n mit der Drehachse a schneidet τ in der Meridiantangente t_k.

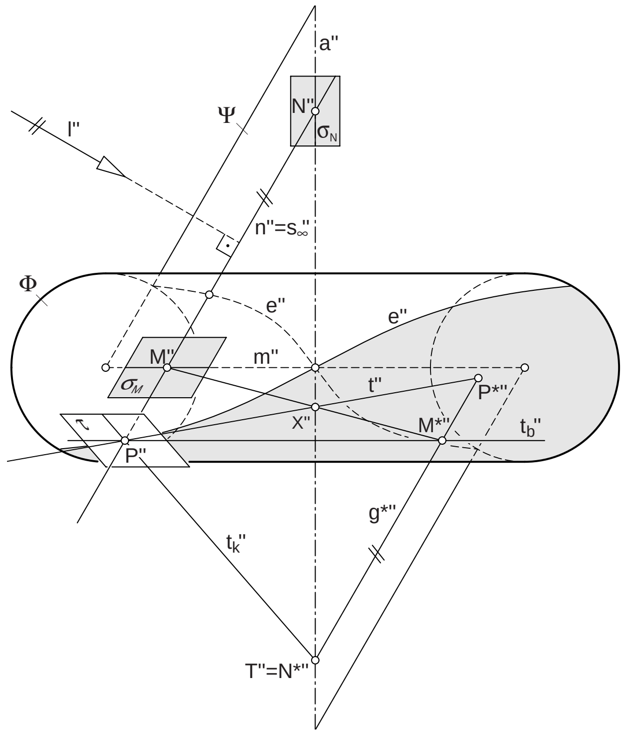

Abb. 4

Der Berührpunkt der asymptotischen Ebene ist der Fernpunkt von n. Damit läuft die Konstruktion auf eine Teilverhältnisübertragung, etwa mittels geeigneter Perspektivität (*Strahlensatz*), hinaus. Auf einer Hilfsgeraden g^* in τ parallel zu s_∞, die durch den Schnittpunkt T von t_k und a gelegt werden kann, liegen die Schnittpunkte $N^* := T$, $M^* := g^* \cap t_b$ und $P^* := g^* \cap t$, deren Teilverhältnis $TV(N^*, M^*, P^*)$ mit $TV(N, M, P)$ übereinstimmt. Somit ist der Strahlenschnittpunkt $X := NN^* \cap MM^*$ ein Punkt der gesuchten Tangente t.

Wenn man beachtet, dass M und N die Hauptkrümmungsmittelpunkte und t_k sowie t_b die Krümmungstangenten von P sind, so führt das auf folgenden allgemeinen

Satz 3 *In einem Punkt* P *der Eigenschattengrenze* e *einer krummen Fläche schneiden die Tangente* t *von* e *und die Krümmungstangenten* t_1 *und* t_2 *aus jeder in der Tangentialebene von* P *befindlichen und zum berührenden Lichtstrahl in* P *orthogonalen Geraden* g^* *mit* $P \notin g^*$ *jenes Teilverhältnis aus, das dem Teilverhältnis von* P *und den Hauptkrümmungsmittelpunkten* K_1 *und* K_2 *auf der Flächennormalen in* P *entspricht: Es ist mit* $P^* := g^* \cap t$, $K_1^* := g^* \cap t_2$ *und* $K_2^* := g^* \cap t_1$ *dann* $TV(P, K_1, K_2) = TV(P^*, K_1^*, K_2^*)$.

Dieser Satz gilt unverändert auch bei Zentralbeleuchtung. Man beachte aufmerksam, dass K_1^* auf der Krümmungstangente von K_2 liegt und K_2^* auf t_1.

Betrachten wir erneut den Lichtmeridianriss des Torus Φ (Abb. 5): In den Äquatorpunkten von Φ vereinfacht sich die Teilverhältnisübertragung zur Konstruktion der Tangenten an die Eigenschattengrenze e von Φ durch die direkt ablesbare Lage der Krümmungstangenten. Außerdem ist das jeweilige Teilverhältnis der Äquatorpunkte mit den Krümmungsmittelpunkten im Hauptmeridian gegeben. Mit wenigen Linien erhält man so die Tangenten im elliptischen und im hyperbolischen Punkt P_e bzw. P_h.

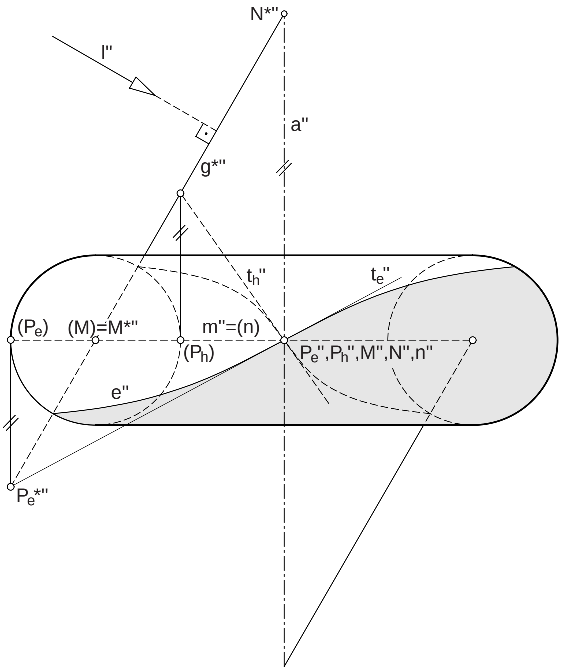

Abb. 5

Diese Konstruktion kann mit jener abgeglichen werden, die längs des Äquators oskulierende Drehquadriken einsetzt (Abb. 6, vgl. [6] und [2] S. 305; mögliche Umrisskonstruktionen der Drehquadriken sind gestrichelt wiedergegeben). Bekanntlich bilden sich der berührende Lichtstahl l und die Tangente t an die Eigenschattengrenze auf ein Paar konjugierter Durchmesser des Umrisses der oskulierenden Drehquadrik ab. Daraus folgt eine elementare Konstruktion konjugierter Durchmessergeraden bei Ellipse und Hyperbel.

Satz 4 *Die zu einer Durchmessergeraden* l *konjugierte Durchmessergerade einer Ellipse oder Hyperbel schneidet die durch einen Scheitelkrümmungsmittelpunkt gelegte Normale zu* l *in einem Punkt der zugehörigen Scheiteltangente.*

Eine Umkehrung von Satz 4 ist die übliche Scheitelkrümmungskreiskonstruktion der Ellipse aus dem Tangentenrechteck. Schließlich sind die Diagonalen im Rechteck zueinander konjugierte Durchmesser der Ellipse. Bei der Hyperbel wiederum ist der zu einer Asymptoten konjugierte Durchmesser die selbe Asymptote.

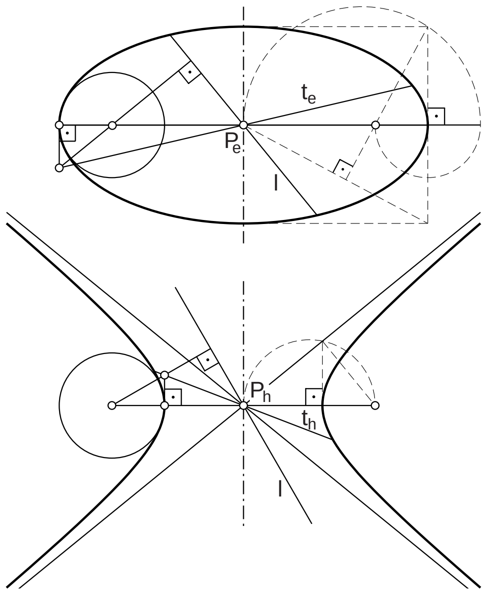

Abb. 6

3 Tangenten an die Eigenschattengrenzen von Schraubflächen

Auch die Normalenkongruenz einer Schraubfläche gehört einem linearen Komplex an, dem Normalenkomplex der Schraubung, kurz *Gewinde*. Folglich sind die Begleitregelflächen von Schraubflächen bezüglich Parallelbeleuchtung ebenfalls Netzflächen. Wie zuvor bei den Drehflächen gehört eine Netzachse, die Ferngerade l_∞, zum Normalenkomplex der Lichtrichtung. Die zweite Netzachse wird durch Einsatz des Drehfluchtprinzips greifbar. Schließlich schneiden alle Flächennormalen längs der Eigenschattengrenze einer Schraubfläche bei Parallelbeleuchtung die Achsenparallele l_0 durch den *Drehfluchtpunkt* der Lichtstrahlen (vgl. [7] S. 173 f). Das Netz ist im Allgemeinen hyperbolisch. Wird die Lichtrichtung jedoch normal zur Schraubachse a angenommen, so fallen die Netzachsen zusammen in eine a treffende Ferngerade l_∞. Es liegt dann ein parabolisches Netz vor, bei dem die Projektivität längs l_∞ durch das Gewinde induziert wird.

Satz 5 *Die Begleitregelfläche einer Schraubfläche ist im Allgemeinen eine Netzfläche mit einer achsenparallelen Leitgeraden durch den Drehfluchtpunkt der Lichtstrahlen und einer zur Lichtrichtung normalen Richtebene, das heißt sie ist ein schiefes Konoid.*

Dies impliziert Satz 2 zu den Drehflächen: Wenn der Schraubparameter null ist, fallen alle Drehfluchtpunkte in die Drehachse.

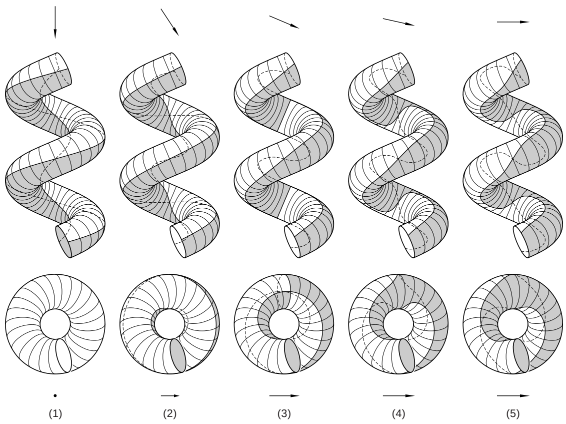

Abb. 7

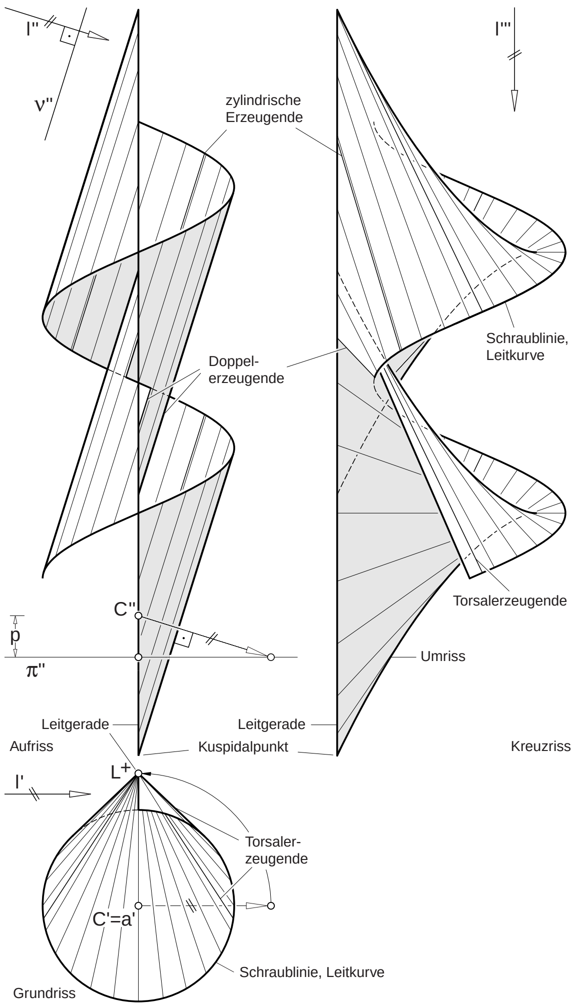

Abb. 8

Schraubrohrfläche

Die einzige Schraubfläche, deren Normalenkongruenz eine Leitkurve aufweist, ist die Schraubrohrfläche (Abb. 7). Jede Begleitregelfläche Ψ einer *Schraubrohrfläche* Φ ist folglich durch drei konstruktiv leicht beherrschbare Leitkurven gegeben: Die zwei Netzachsen (getrennt oder zusammenfallend) und die Mittenschraublinie m (Abb. 8). Für die Vervollständigung der Berührkorrelation ist folgendes bemerkenswert:

Bei jeder Erzeugenden n von Ψ schneidet die Tangentialebene in $\mathrm{N} := \mathrm{n} \cap l_0$ durch n und l_0 die zugehörige Tangentialebene τ von Φ in einer *Falltangente* (es wird von lotrechter Aufstellung der Schraubachse ausgegangen). Die Tangentialebene in M, die durch n und die Schraubtangente im Schnittpunkt von n und m aufgespannt wird, schneidet τ nach einer Krümmungstangente. Nach Festlegung der Berührkorrelation kann durch Teilverhältnisübertragung und unter Rückgriff auf Satz 3 der zweite Hauptkrümmungsmittelpunkt auf n bestimmt werden. In Abb. 9 erfolgt die Tangentenkonstruktion für einen allgemeinen Punkt P der Eigenschattengrenze e von Φ im Lichtmeridianriss.

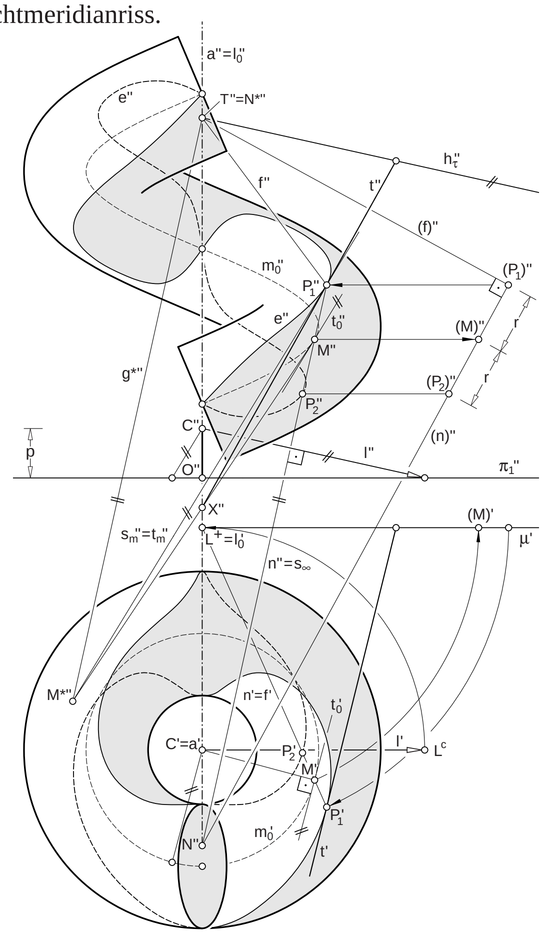

Abb. 9

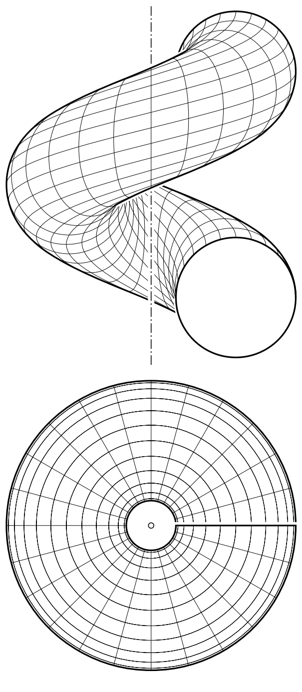

Abb. 10

Meridiankreisschraubfläche

Die Meridiankreisschraubfläche unterscheidet sich vom Torus dadurch, dass der Meridiankreis statt einer Drehung eine Schraubung erfährt (Abb. 10). Allerdings zieht diese kleine Modifikation einige konstruktive Schwierigkeiten bei der Festlegung der Begleitregelfläche nach sich. Um diese in den Griff zu bekommen, untersuchen wir zuerst die Normalenkongruenz der Meridiankreisschraubfläche Φ:

Die Flächennormalen längs eines erzeugenden Kreises k von Φ sind Gewindegeraden und gehören zugleich dem Gebüsch durch die Drehachse a_k von k an. Das Gewinde und a_k bestimmen ein Netz. Solange die Gebüschachse a_k keine Gewindegerade ist, sind die Netzachsen reell getrennt und das Netz ist hyperbolisch. Andernfalls ist das Netz parabolisch. Die Normalenfläche Ψ_k längs k wird demnach durch zwei Leitgeraden und den Leitkreis k festgelegt. Diese Feststellung kann auf alle Kreisschraubflächen ausgeweitet werden und gilt auch bei Drehung bzw. Schiebung:

Satz 6 *Die Normalenfläche längs eines erzeugenden Kreises einer zyklischen Bewegfläche ist im Allgemeinen eine Regelfläche vierten Grades siebter STURMscher Art.*

Für ein weiteres Vorgehen ist es nötig, die zweite Leitgerade von Ψ_k aufzuspüren: Genau wie die Meridiankreisschraubfläche ist Ψ_k zu jener Durchmessergeraden d von k axialsymmetrisch, welche die Schraubachse a orthogonal schneidet. Somit ist d die Doppelerzeugende von Ψ_k und die gesuchte Leitgerade q_0 normal zu d.

Weil q_0 zur Doppelkurve von Ψ_k gehört, schneiden sich die Flächennormalen paarweise in Punkten von q_0. Greift man zwei solche Erzeugende n_1 und n_2 heraus, deren Schnittpunkte P_1 und P_2 mit k auf einem Durchmesser von k liegen, so spannen sie eine Ebene durch a_k auf. Diese Ebene schneidet die zu d normale Meridianebene φ in einer Höhenlinie (Abb. 11). Zugleich müssen die Grundrissbilder von n_1 und n_2 durch den gemeinsamen Drehfluchtpunkt T^+ der zueinander parallelen Kreistangenten in P_1 und P_2 verlaufen. Daraus folgt: n_1 und n_2 schneiden φ in einem gemeinsamen Punkt Q und q_0 befindet sich in φ.

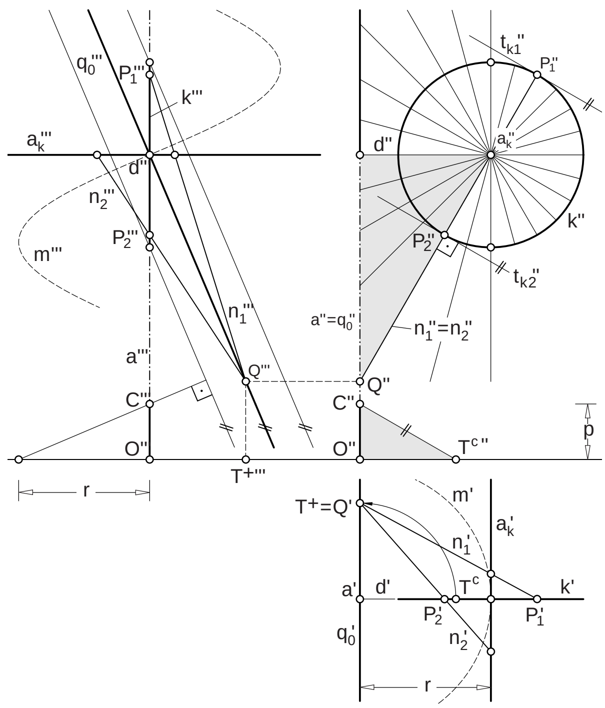

Abb. 11

Die Tangentialebenen von Φ in den Endpunkten des zu a parallelen Durchmessers von k sind zueinander parallel. Demnach sind auch die Erzeugenden von Ψ_k in diesen Punkten zueinander parallel und schneiden sich im Fernpunkt von q_0. Weil die Bahnkurven der betreffenden Punkte von k zur Mittenlinie m von Φ kongruent sind, kann formuliert werden:

Satz 7 *Die Normalenfläche längs eines erzeugenden Kreises einer Meridiankreisschraubfläche besitzt neben der Drehachse des Kreises eine zweite Leitgerade, nämlich die Schnittgerade der Bahnnormalebene des Kreismittelpunktes mit der zur Kreisebene normalen Meridianebene.*

Wird Ψ_k derselben Schraubung wie k unterworfen, so entsteht als Hüllfläche der Schraublagen von Ψ_k die Schraubfläche Θ. Folglich ist Θ die Brennfläche der Normalenkongruenz von Φ. In jeder Schraublage von Ψ_k berühren sich Ψ_k und Θ längs einer immer gleichen Flächenkurve c von Ψ_k, die *Eingriffslinie* oder *Charakteristik* genannt wird ([3] S. 194). Verschraubt man c, so entsteht Θ. Die gemeinsamen Tangentialebenen von Ψ_k und Θ längs c enthalten demnach jeweils eine Bahntangente der Schraubung.

Jede Begleitregelfläche Ψ von Φ berührt die Brennfläche Θ der Normalenkongruenz von Φ längs einer nicht näher spezifizierten Kurve. Jede Erzeugende n von Ψ gehört jedoch auch einer Schraublage von Ψ_k an, weshalb der Berührpunkt K von n mit Θ auf c liegt. Für die Vervollständigung der Berührkorrelation wird es also darum gehen, $K \in c$ auf Ψ_k zu bestimmen. Über die Schraubtangente in K und unter Rücksicht auf Satz 5 sind dann drei Tangentialebenen längs n bekannt. Um den konstruktiven Zugang zu vereinfachen bietet es sich an, analog zum Begriff *Zirkularprojektion* ([7] S. 68), den Begriff *Schraubprojektion* einzuführen. Dies geschieht allerdings nicht mit dem Ziel, eine Abbildung zu produzieren, die dann allgemein Schraubriss heißen könnte, sondern um die Kontur von Ψ_k unter Schraubprojektion zu untersuchen. Schließlich stimmt diese Kontur mit der Charakteristik c überein.

Def. 2 *Eine Abbildungsvorschrift, deren Projektionslinien die Bahnkurven einer Schraubung um die Achse* a *mit dem Schraubparameter* p *sind, heißt* Schraubprojektion *um die Achse* a *mit dem Schraubparameter* p. *Ein Punkt* K *einer Fläche heißt* Konturpunkt bezüglich *Schraubprojektion, wenn die Tangentialebene in* K *die Schraubtangente von* K *enthält.*

Jeder Punkt einer Schraubfläche ist ein Konturpunkt bezüglich Schraubprojektion (zur selben Schraubung). Unter Zuhilfenahme des Drehfluchtprinzips wird Def. 2 auch bei anderen Flächen erfüllt, wenn die Drehfluchtspur der Tangentialebene von K den Grundriss von K enthält. Diesen bekannten Sachverhalt lesen wir als

Satz 8 *Fällt in einem Punkt* K *einer Fläche der Grundriss der Flächennormalen in die Drehfluchtspur der Tangentialebene von* K, *so ist* K *ein Konturpunkt bezüglich Schraubprojektion.*

Das kann nun folgendermaßen ausgenutzt werden: Die Drehfluchtspuren aller Tangentialebenen längs einer Erzeugenden n der Normalenfläche Ψ_k enthalten den Drehfluchtpunkt N^+ von n. Die Flächennormalen längs n bilden dagegen ein *Normalenparaboloid* Γ ([5] S. 69). Im Grundriss hüllen die Bilder der Flächennormalen längs n in der Regel eine Umrissparabel u′ ein ([7] S. 29). Flächennormalen von Ψ_k durch Konturpunkte bezüglich Schraubprojektion zeigen sich im Grundriss folglich als Tangenten aus N+ an u′. Dafür gibt es zu jeder Erzeugenden von Ψ_k im algebraischen Sinne zwei Lösungen.

Wir werden nun die Umrissparabel u′ von Γ im Grundriss unter Hinweis auf ihre Leitlinie und mithilfe eines Parabelpunktes mit Tangente bestimmen. Dazu ist es nötig, zuerst ein Berührparaboloid Γ_B längs n festzulegen (Abb. 12 am Hauptmeridiankreis k):

Setzt man die Leitgeraden q_0 und a_k von Ψ_k als Erzeugende von Γ_B ein, so ist die Richtebene von Γ_B grund- und aufrissprojizierend. In P findet man eine weitere Erzeugende g_P von Γ_B über die Tangentialebene σ_P von Ψ_k. Die Tangentialebene σ_P wird durch n und die Kreistangente t_k aufgespannt. Eine Höhenlinie h_P von σ_P verläuft durch den Schnittpunkt von t_k mit der Doppelerzeugenden d und den Schnittpunkt von n mit a_k.

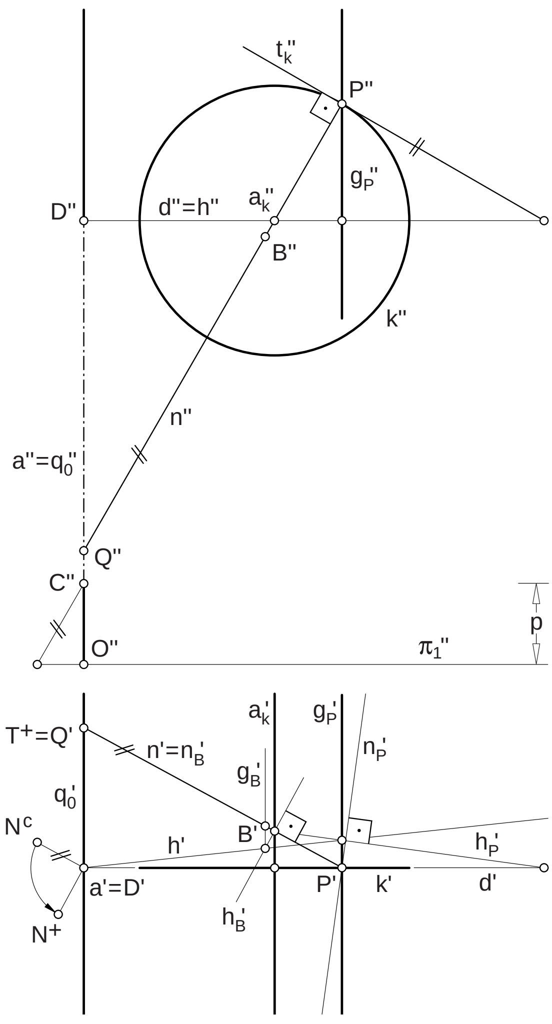

Abb. 12

Besonders nützlich für das weitere Vorgehen ist die horizontale Erzeugende h von Γ_B aus der Schar von n. Sie befindet sich in der Höhenebene durch a_k und schneidet q_0 im Fußpunkt D von d sowie g_P im Schnittpunkt von g_P mit h_P. Die Erzeugende h ist deshalb so wertvoll, weil die Leitlinie von u' in h' fällt. Dies wird in [4] S. 188 f, 191 und194 f begründet.

Um einen Punkt B' von u' und die dazugehörige Tangente n'_B zu erhalten, suchen wir den Konturpunkt B von Γ zu n auf. Dabei muss das Grundrissbild der Flächennormalen n_B von Ψ_k (und Γ_B) in B (mithin eine Erzeugende von Γ) mit n' zur Deckung kommen. Das heißt die Grundrissbilder aller Höhenlinien der Tangentialebene σ_B von Γ_B in B müssen zu n' orthogonal sein. Legt man eine solche Höhenlinie h_B durch den Schnittpunkt von n mit a_k vor, so trifft h_B die horizontale Erzeugende h in einem Punkt jener Erzeugenden g_B von Γ_B, die n im Berührpunkt B von σ_B schneidet (Abb. 12).

Im Wesentlichen benötigt man außer der Leitlinie h' noch den Brennpunkt F von u' (Abb. 13). Dabei ist $n' = n'_B$ Symmetriegerade zu F und dem Fußpunkt des Lotes aus B' zu h'.

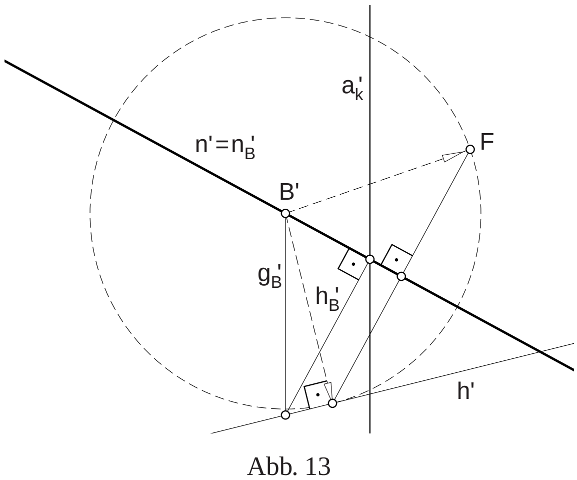

Abb. 13

Zu guter Letzt werden jetzt die Parabeltangenten n'_{K_1} und n'_{K_2} aus N^+ an u' konstruiert ([1] S. 208 f). Ein Hilfskreis um N^+ durch F schneidet h' in den Gegenpunkten G_1 und G_2 (Abb. 14). Die Geraden FG_1 und FG_2 sind zu n'_{K_1} bzw. n'_{K_2} normal. Nach Satz 8 sind n'_{K_1} und n'_{K_2} die Grundrissbilder der Flächennormalen n_{K_1} und n_{K_2} von Ψ_k in den Konturpunkten K_1 und K_2 bezüglich Schraubprojektion auf der Erzeugenden n von Ψ_k. (Die Konturpunkte bezüglich Schraubprojektion auf der Doppelerzeugenden d von Ψ_k werden in [4] S. 198 gesondert behandelt.)

Die Konstruktion der Tangente an die Eigenschattengrenze e der Meridiankreisschraubfläche Φ in einem Punkt P von e läuft nun wieder auf eine Teilverhältnisübertragung in der Tangentialebene τ von P hinaus. Dabei ist folgender Zusammenhang erwähnenswert:

In P spannen die Bahntangente von P und die Meridiankreistangente t_k die Tangentialebene τ auf. Die Erzeugende n der Begleitregelfläche längs e durch P ist Bahnnormale zu jedem ihrer Punkte. Folglich sind auch die Bahntangenten in den Konturpunkten bezüglich Schraubprojektion zu τ parallel.

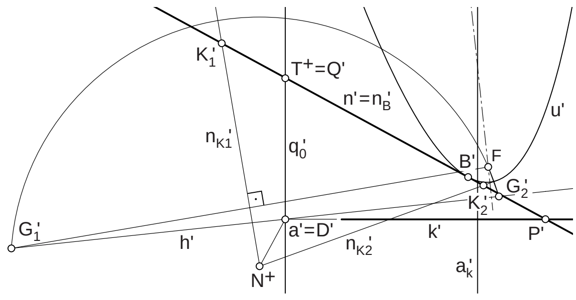

Abb. 14

Schlussbemerkungen

Um Tangenten an die Eigenschattengrenzen krummer Flächen in den Griff zu bekommen wird in der Regel *lokal* das Instrumentarium der konstruktiven Differentialgeometrie eingesetzt. Dabei werden Zusammenhänge quadratischer Form ausgenutzt. Dagegen erfasst die hier vorgestellte *Begleitregelflächenmethode* Eigenschattengrenzen *global* als Schnittkurven und führt zu linearen Lösungen. Die Methode greift, sobald man die Normalenkongruenz der untersuchten Fläche konstruktiv beherrscht. Bei nächster Gelegenheit soll ergänzend vorgeführt werden, dass auch der Einsatz solcher Begleitregelflächen sinnvoll sein kann, deren Erzeugenden im Allgemeinen keine Flächennormalen sind.

Irgend zwei Lagen einer Kurve im Raum lassen sich stets durch eine Schraubung ineinander überführen ([7] S. 158). Diese fundamentale Eigenschaft der Schraubung muss auch für zwei benachbarte Lagen der erzeugenden Kurve k einer allgemeinen Bewegfläche Φ gelten, woraus folgt: Ist P ein Punkt der Eigenschattengrenze von Φ, so kann immer eine Kreisschraubfläche gefunden werden, die Φ in P oskuliert und deren erzeugender Kreis der Krümmungskreis von k ist. Bei der Betrachtung der Meridiankreisschraubfläche wurde bereits skizziert, dass jede Kreisschraubfläche mit der Begleitregelflächenmethode erfasst wird. Konstruktiv ist das mit einigem Aufwand verbunden. Es bleibt zu vergleichen, ob hier der Einsatz der DUPIN*schen Indikatrix* nicht zweckmäßiger ist.

Für Bewegflächen, insbesondere für die vorgeführten Spezialfälle, ist die *Begleitregelflächenmethode* auch zur Bestimmung von *Isophotentangenten* verwendbar und kann gelegentlich zu durchaus einfachen Konstruktionen Anlass geben.

Literatur

[1] BEREIS, RUDOLF: Darstellende Geometrie I; Akademie Verlag, Berlin 1964

[2] BRAUNER, HEINRICH: Lehrbuch der Konstruktiven Geometrie; Springer-Verlag, Wien, New York 1986

[3] HOHENBERG, FRITZ: Konstruktive Geometrie in der Technik; 3. verb. Aufl. Springer-Verlag, Wien 1966

[4] LORDICK, DANIEL: Konstruktion der Schattengrenzen krummer Flächen mithilfe von Begleitflächen; Shaker, Aachen 2001 (zugl. Karlsruhe, Univ., Diss. 2001)

[5] MÜLLER, EMIL; KRAMES, JOSEF LEOPOLD: Konstruktive Behandlung der Regelflächen; in: Vorlesungen über Geometrie, Band III; Franz Deuticke, Leipzig, Wien 1931

[6] STACHEL, HELLMUTH: Zum Umriss der Drehflächen; in: Anzeiger der math.-naturw. Klasse der Österreichischen Akademie der Wissenschaften, Nr. 10; Wien 1972

[7] WUNDERLICH, WALTER: Darstellende Geometrie II; Bibliographisches Institut, Mannheim 1967

Daniel Lordick
Institut für Geometrie
Technische Universität Dresden
Zellescher Weg 12-14, D 01096 Dresden
e-mail: lordick@math.tu-dresden.de

Original scientific paper
Accepted 28.06.2002

ATTILA BÖLCSKEI
MÓNIKA SZÉL-KOPONYÁS

Construction of D-Graphs Related to Periodic Tilings

Konstrukcija D-grafova kod periodičkih popločavanja

SAŽETAK

U radu je dan algoritam koji teoretski omogućuje izvođenje metoda za klasifikaciju periodičkih popločavanja u svakoj dimenziju. Pomoću toga se može provjeriti raniji rezulatat dan u radu (e. g. [BM98, BM00]). Primjenom algoritma prikazana je potpuna klasifikacija neizomorfnih trodimenzionalnih $D-$grafova s 5 elemenata.

Ključne riječi: Delaney-Dress simbol, popločavanje u n-dimenzijama

Construction of D-Graphs Related to Periodic Tilings

ABSTRACT

This paper presents an algorithm which allows to derive classification methods concerning periodic tilings in any dimension, theoretically. By the help of this, one can check former results of the topic (e. g. [BM98, BM00]). An implementation of the algorithm yields the complete enumeration of non-isomorphic three-dimensional $D-$graphs with 5 elements, given as illustration.

Key words: Delaney-Dress symbol, tiling in n-dimensions

MSC 2000: 52C22, 57N16, 68R99

1 Introduction

The paper contains the description of an algorithm by which one can solve combinatorial classification problems for tilings in any dimension. The method is based on the well-known concept of Delaney-Dress symbol (or $D-$symbol, shortly, suggested by E. Molnár). This is nothing but a concise representation of the combinatorics and periodicity of a tiling. The symbol consists of a colored graph ($D-$graph) and a matrix function. The theory has been elaborated for the 2-dimensional case in more details (see e. g. [DS84], [DHZ92], [Hus93], [BH96]), however, beside results ([DHM93], [Mol96], [Del95], to name a few) there are a lot of open questions in higher dimensions.

In the following we shall briefly recall the points that are necessary to understand the algorithm. Helping the visual imagination we parallelly work out a spatial example.

Assume that a group Γ acts from the right discretely on a $d-$dimensional, simply connected manifold X^d in such a way that one can find a $\Gamma-$*equivariant cell decomposition*. That is, if we denote the set of cells by $\mathcal{T}$, then $\mathcal{T} = \mathcal{T}^\gamma := \{A^\gamma : A \in \mathcal{T}\}$ holds for all $\gamma \in \Gamma$. The elements of $\mathcal{T}$ are the so-called *cells*. Every point of X^d belongs to at least one tile and no two tiles have an inner point in common. The points of X^d, belonging to exactly two tiles, constitute the $(d-1)$-hyperfaces, or *facets* of $\mathcal{T}$. By intersections we consequently define $(d-2)$-faces, ..., r-faces, ..., 1-faces or *edges*, then 0-faces or *vertices*, as usual for compact (topological) d-politopes. The above pair $(\mathcal{T},\Gamma)$ is called *equivariant tiling*. In our examinations the *symmetry group* Γ contains at least d independent translations, so it is always *periodic*.

Two tilings $(\mathcal{T},\Gamma)$ and $(\mathcal{T}',\Gamma')$, will be considered equivalent if they are topologically equivariant (homeomeric). It means that there exists a homeomorphism ψ that maps $\mathcal{T}$ onto $\mathcal{T}'$ preserving all incidences of tiles, r-faces $(0 \le r \le d-1)$ such that $\psi^{-1}\Gamma\psi = \Gamma'$.

Our Fig. 1 shows a periodic tiling of regular tetrahedra and octahedra filling the Euclidean 3-space. The construction can be derived from a particioned cube by reflecting it in each of its faces, step by step. (See Fig. 2.) "Melting" tiles together we may get octahedra from 8 corner tetrahedra. It is easy to see that the (periodic) space group $Fm\bar{3}m =: \Gamma$ acts on the tiles forming the pair $(\mathcal{T},\Gamma)$ to be equivariant.

We can speak about the vertices, edges and faces of the tetrahedra and octahedra in a usual sense.

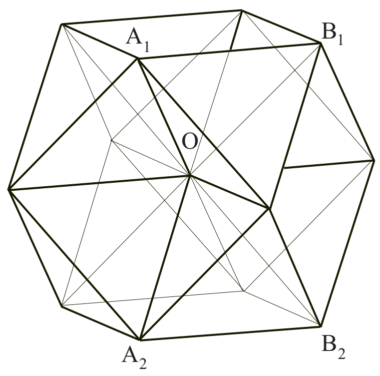

Fig. 1 The tiling can be constructed as follows. Take first 8 regular tetrahedra in the position illustrated above. Then extend the configuration with reflections on the planes A_1A_2O, B_1B_2O, the bisector plane of the segment A_1A_2 and the planes determined by the squares around. Finally we get a tiling with regular tetrahedra and octahedra.

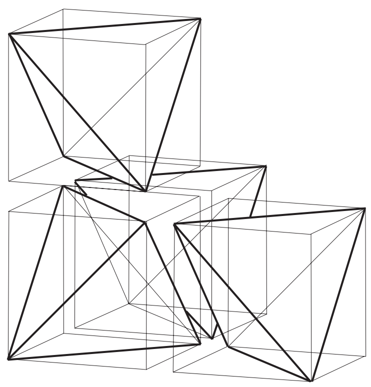

Fig. 2 Take a cube and a tetrahedron in it. In order to get the tiling reflect the bodies in the faces of the cube. The octahedra are divided into 8 smaller simplices.

Now we define the *formal barycentric subdivision* of $\mathcal{T}$ in the usual way: For every $r-$dimensional constituent of $\mathcal{T}$ $(r = 0,\dots,d)$ we choose an interior point, called *r*-center of $\mathcal{T}$ $(r = 0,\dots,d)$. Consider a fixed tile, one of its $(d-1)$-faces; an incident $(d-2)$-face, $\dots$, finally an incident vertex. These $(d+1)$ centers form the vertices of a $d-$dimensional simplex. Other sequence of $r-$centers leads to other simplex in the tile. Using the method for every tile we finally get the barycentric subdivision made up by simplices called *chambers*. The chamber-system is denoted by $\mathcal{C}$. Every chamber has an *i-face* opposite to its $i-$vertex ($i \in I := \{0,\dots,d\}$). It is obvious that for every chamber $C_1 \in \mathcal{C}$ there exists exactly one chamber C_2 such that their $i-$face is common. In this case we say that C_1 and C_2 are $i-$*adjacent* or $i-$*neighbors*. These adjacencies imply the so-called *adjacency operations* σ_i for $i = 0,\dots,d$:

$$\sigma_i : \mathcal{C} \to \mathcal{C}, \quad C \mapsto \sigma_i C$$

that maps every $C \in \mathcal{C}$ onto its *i*-neighbor.

The adjacency operations form a free Coxeter group:

$$\Sigma_I := \langle \sigma_i \big| 1 = \sigma_i\sigma_i = \sigma_i^2 : i = 0,\dots,d \rangle$$

that acts transitively from the left on $\mathcal{C}$, if Γ acts from the right, by our convention.

Our Fig. 3 illustrates how the barycentric subdivision can be built up from the given tiling. As an interior point of an $r-$face we have chosen the midpoint for every $r \in \{0,1,2,3\}$.

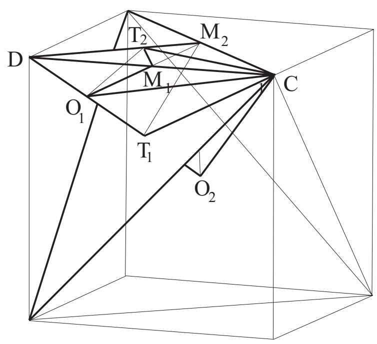

Fig. 3 Take the centers of the two solids (O_1 and O_2), the centers of two faces (T_1 and T_2), the midpoints of edges (M_1 and M_2) and two vertices in common (C,D). The barycentric simplices are $O_2T_1M_2C$, $O_1T_1M_2C$, $O_1T_2M_2C$, $O_1T_2M_1C$, $O_1T_2M_1D$, numbered as 1, 2, 3, 4, 5, respectively, in Fig. 5. O_2M_2CD is the fundamental domain of $Fm\bar{3}m$.

Note that the chamber system $\mathcal{C}$ can always be constructed in a way compatible with the action of Γ on $\mathcal{T}$, and suppose in the following that this is the case. Take a chamber $C \in \mathcal{C}$ and form its *orbit* by Γ:

$$C^\Gamma := \{C^\gamma : \gamma \in \Gamma\}.$$

Our Fig. 4 a−d try to visualize the different simplex orbits by equally coloring the $\Gamma-$equivalent chambers. To avoid any confusion we restrict our attention just to a small part of the tiling.

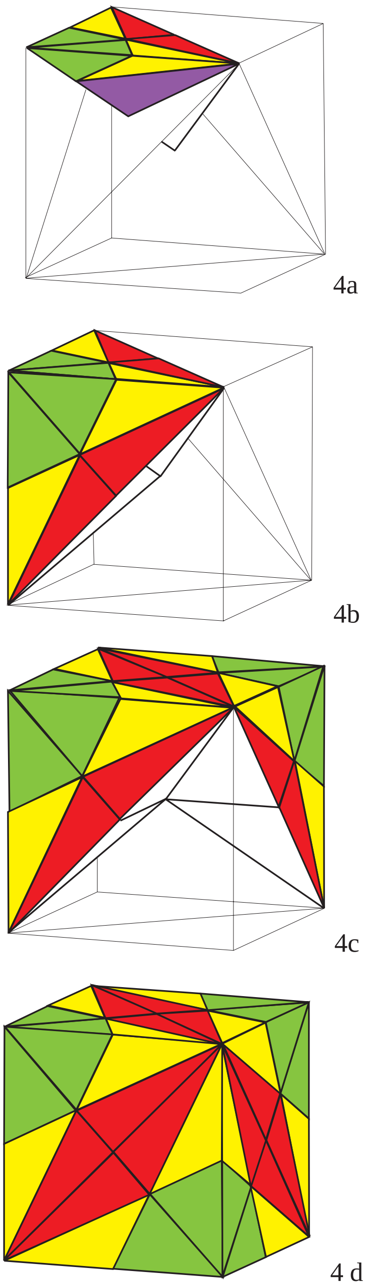

Fig. 4 Take first the 5 simplices above and let act $Fm\bar{3}m$ on them. The polyhedra which can be mapped onto each other are colored in the same way. Step by step we have filled the cube. By reflections we can develop the tiling further.

Fig. 3 shows a polyhedron O_2M_2CD containing barycentric simplices of each kind. This reflection simplex O_2M_2CD can serve as a fundamental domain for Γ. By the so-called Poincare-algorithm one can confirm that the corresponding symmetry group is just $Fm\bar{3}m$ (for more details, see e. g. [Mol83]).

Let $\mathcal{D} := \mathcal{C}/\Gamma$ be the set of different chamber orbits under Γ and let D_k be any orbit ($1 \leq k \leq n$, now $n = 5$). Any $\gamma \in \Gamma$ maps i-neighbors onto i-neighbors, hence the operations σ_i commute with Γ on $\mathcal{C}$, for any i. Thus we can introduce the concept of *i-adjacencies of D_k's*: D_j and D_k are i-adjacent or i-neighbor iff for any $C_j \in D_j$ there exists $C_k \in D_k$ such that $C_k = \sigma_i C_j$ holds.

The set $\mathcal{D}$ and the mappings σ_i define a finite, connected, $(d+1)$-colored graph in which the nodes refer to the orbits and two nodes are linked by an i-colored edge ($i = 0, \dots, d$) if the corresponding orbits are i-neighbors. Such a graph is called a *Delaney-Dress graph (diagram)* or shortly *D-graph*. Of course, $D = \sigma_i D$ is also possible, in this case we get an $i-$loop.

In Fig. 5, where the loops are not indicated, we can see the $D-$graph of our spatial example from which the Reader may identify the correspondence between colors and numberings.

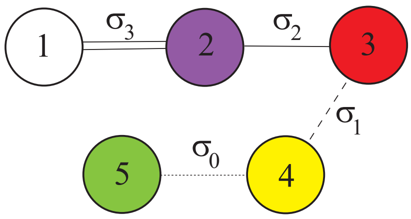

Fig. 5 The D-graph of our example. The loops are not indicated. The colors and numbers are in correspondence with the numbers of matrices and with Fig. 4.

For short D_k will simply be denoted by $k, (k = 1, 2, \dots, 5)$ in the following.

Let us introduce a matrix function $(m_{ij}) : \mathcal{D} \rightarrow \mathbf{N}_{I \times I}$ in the following way. For any $D \in \mathcal{D}$ let

$$m_{ij}(D) := \min \left\{ m \middle| (\sigma_j \sigma_i)^m C = C, \quad C \in D \subset \mathcal{C} \right\}, \qquad (0 \leq i \leq j \leq d).$$

It is easy to see that in a tiling this function has the properties 1-5:

1. $m_{ii}(D) = 1$;
2. $m_{ij}(D) = m_{ji}(D)$;
3. $m_{ij}(D) = m_{ij}(\sigma_i D) = m_{ij}(\sigma_j D)$;
4. $m_{ij}(D) = 2$, if $|i - j| > 1$;
5. $m_{ij}(D) > 2$, if $|i - j| = 1$ in the usual tilings.

Here we give the matrix function m in our example:

$$m(1) = m(2) = m(3) = \begin{bmatrix} 1 & 3 & 2 & 2 \\ 3 & 1 & 3 & 2 \\ 2 & 3 & 1 & 6 \\ 2 & 2 & 6 & 1 \end{bmatrix},$$

$$m(4) = m(5) = \begin{bmatrix} 1 & 3 & 2 & 2 \\ 3 & 1 & 3 & 2 \\ 2 & 3 & 1 & 4 \\ 2 & 2 & 4 & 1 \end{bmatrix}.$$

A pair $(\mathcal{D};m)$, consisting of a finite, connected, colored D-graph and the matrix function fulfilling the properties 1-5, is called a *d-dimensional Delaney-Dress symbol*, or shortly *D-symbol*.

Two D-symbols $(\mathcal{D};m)$, $(\mathcal{D}';m')$ are called *isomorphic* if there exists a bijection $\pi : \mathcal{D} \to \mathcal{D}'$ such that $\sigma_k(D^\pi) = (\sigma_k D)^\pi$ moreover, $m'_{ij}(D^\pi) = m_{ij}(D)$ hold for any $D \in \mathcal{D}$, $0 \le k \le d$, $0 \le i \le j \le d$.

The following basic lemma provides the advantages of D-symbols concerning classification problems :

Lemma 1 *Two tilings $(\mathcal{T},\Gamma)$ and $(\mathcal{T}',\Gamma')$ are equivariantly equivalent (homeomeric, or lying in the same homeomorphism equivariance class), if and only if the corresponding D-symbols $(\mathcal{D};m)$and $(\mathcal{D}';m')$ are isomorphic.* [Dre87] □

Analogously as before, we can introduce other important matrix functions r and v:

$r : \mathcal{D} \to \mathbf{N}_{I\times I} \qquad r_{ij}(D) := \min\left\{r : (\sigma_j\sigma_i)^r D = D\right\}$

for any $D \in \mathcal{D}$, $(0 \le i \le j \le d)$; and

$v : \mathcal{D} \to \mathbf{N}_{I\times I} \qquad v_{ij}(D) := m_{ij}(D)/r_{ij}(D),$

where the above division is meant for the elements of matrices.

These functions have the following values in our example (Fig. 5).

$$r(1) = \begin{bmatrix} 1 & 1 & 1 & 2 \\ 1 & 1 & 1 & 2 \\ 1 & 1 & 1 & 3 \\ 2 & 2 & 3 & 1 \end{bmatrix},\ r(2) = \begin{bmatrix} 1 & 1 & 2 & 2 \\ 1 & 1 & 3 & 2 \\ 2 & 3 & 1 & 3 \\ 2 & 2 & 3 & 1 \end{bmatrix},$$

$$r(3) = \begin{bmatrix} 1 & 3 & 2 & 1 \\ 3 & 1 & 3 & 2 \\ 2 & 3 & 1 & 3 \\ 1 & 2 & 3 & 1 \end{bmatrix},\ r(4) = \begin{bmatrix} 1 & 3 & 2 & 2 \\ 3 & 1 & 3 & 2 \\ 2 & 3 & 1 & 1 \\ 2 & 2 & 1 & 1 \end{bmatrix},$$

$$r(5) = \begin{bmatrix} 1 & 3 & 2 & 2 \\ 3 & 1 & 1 & 1 \\ 2 & 1 & 1 & 1 \\ 2 & 1 & 1 & 1 \end{bmatrix};$$

$$v(1) = \begin{bmatrix} 1 & 3 & 2 & 1 \\ 3 & 1 & 3 & 1 \\ 2 & 3 & 1 & 2 \\ 1 & 1 & 2 & 1 \end{bmatrix},\ v(2) = \begin{bmatrix} 1 & 3 & 1 & 1 \\ 3 & 1 & 1 & 1 \\ 1 & 1 & 1 & 2 \\ 1 & 1 & 2 & 1 \end{bmatrix},$$

$$v(3) = \begin{bmatrix} 1 & 1 & 1 & 2 \\ 1 & 1 & 1 & 1 \\ 1 & 1 & 1 & 2 \\ 2 & 1 & 2 & 1 \end{bmatrix},\ v(4) = \begin{bmatrix} 1 & 1 & 1 & 1 \\ 1 & 1 & 1 & 1 \\ 1 & 1 & 1 & 4 \\ 1 & 1 & 4 & 1 \end{bmatrix},$$

$$v(5) = \begin{bmatrix} 1 & 1 & 1 & 1 \\ 1 & 1 & 3 & 2 \\ 1 & 3 & 1 & 4 \\ 1 & 2 & 4 & 1 \end{bmatrix}.$$

It is easy to see that r and v have the properties 1-3 of the matrix function m, as well. We emphasize that 4 and 5 do not necessarily hold but r_{ij} has to be the divisor of m_{ij}. Particularly, $r_{ij}(D) = 1$ or 2, if $|i-j| > 1$. This observation has a basic role in the following algorithm and results in theorems 1 and 2.

2 An algorithm for creating D-graphs

The point of this section is to describe an algorithm by that we can derive D-graphs for any number of nodes in any dimension. On the one hand the method provides us checking previously published results ([BM98, BM00] - made by hands, in a different way), on the other hand we get new results given at the end of the paper.

In order to construct D-graphs firstly we describe them algebraically. Let be given a D-graph. Suppose that the nodes have already been numbered. Any adjacency operation (or, the set of i-colored edges of the graph) refers to an involutive permutation. This $i-$permutation will be encoded by a sequence of $n := \left|\mathcal{D}\right|$ numbers as follows: the j-th number for σ_i expresses the number of the node with whom the node number j is $i-$adjacent, i. e. is linked by an $i-$colored edge. Let a_n denote the number of all involutive permutations of n elements.

For calculation of a_n we have the formulas:

$a_0 = 1, a_1 = 1, a_2 = 2$

and for $n \geq 3$:

$a_n = a_{n-1} + (n-1)a_{n-2}$, i. e.

$$a_n = 1 + \sum_{k=1}^{n} \frac{(2n)(2n-1)\dots(2n-[2k-1])}{2^k k!}.$$

The complexity of a_n is at most $O(n^{\frac{n}{2}})$.

Proof Pick out a node. If it is adjacent to itself (loop), then we have a_{n-1} permutations. If it is adjacent to any other node, then we have a_{n-2} permuatations for the $(n-1)$ possibilities each. The second formula comes from combinatorics easily.

Now we give rough estimates for a_n.

$$\begin{aligned} a_n &= a_{n-1} + (n-1)a_{n-2} \\ &= a_{n-2} + (n-2)a_{n-3} + (n-1)a_{n-2} \\ &= na_{n-2} + (n-2)a_{n-3} \end{aligned}$$

$na_{n-2} < a_n < n(a_{n-2} + a_{n-3}) < 2na_{n-2}$.

If n is odd ($n = 2t+1$), then

$$a_{2t+1} > (2t+1)a_{2t-1} > \dots$$
$$\dots > (2t+1)(2t-1) \quad \dots \overbrace{a_1}^{1} = \frac{(2t+1)!}{2^t t!},$$

and analogously

$$\frac{2^t(2t+1)!}{2^t t!} > a_{2t+1}.$$

If n is even ($n = 2t$), then

$$a_{2t} > 2ta_{2t-2} > \dots > 2t(2t-2)\dots \overbrace{a_2}^{2} = 2^t t!,$$

and

$$2^{2t-1}t! > a_{2t}, \text{ respectively.}$$

By the Stirling-formula $\left(t! \approx (\frac{t}{e})^t \sqrt{2\pi t}\right)$ we get:

$$\frac{(2t+1)^{2t+1}}{t^t e^{t+1}} \sqrt{\frac{2t+1}{t}} > a_{2t+1} > \frac{(2t+1)^{2t+1}}{(2t)^t e^{t+1}} \sqrt{\frac{2t+1}{t}},$$

and

$$\left(\frac{4t}{e}\right)^t \sqrt{\frac{\pi t}{2}} > a_{2t} > \left(\frac{2t}{e}\right)^t \sqrt{\frac{\pi t}{2}}.$$

From these estimates we see that $a_n = O(n^{\frac{n}{2}})$, indeed. □

Remark The above calculations give us just a rough asymptotics for a_n. There are several conjectures of E. Makai concerning this problem. In his opinion $a_n = \frac{n^{\frac{n}{2}}}{e^{\frac{n}{2}}} e^{\sqrt{n}+o(1)}$ or, even better $a_n \approx c\frac{n^{\frac{n}{2}}}{e^{\frac{n}{2}}} e^{\sqrt{n}}\sqrt{n}$.

Here we sketch the main steps of our algorithm. In this approach the candidates of a D-graph are represented as ordered $(d+1)$-tuples of involutive permutations. The number of entries depends on the dimension d of the tiling. Having all the possible $(d+1)$-tuples we exclude those ones which do not provide connected D-graph, and for which the property $r_{ij}(D) = 1$ or 2 does not hold. Since many different $(d+1)$-tuple can describe the same graph (according to the numberings) at the end we have to choose representants. More precisely the algoritm will be the following.

ALGORITHM

Assume that the D-graph to be constructed has n nodes and dimension d, i. e. $d+1$ colors.

- Construct first the a_n involutive permutations for a given fixed numbering and order them (e. g. lexicographically).

- Subsequently form ordered $(d+1)$-tuples of involutive permutations in such a way that the $(i+1)$-th element of a $(d+1)$-tuple can not be less than the i-th element according to the order above. (We do not need the $(d+1)$-tuples as a set!) Therefore the $(d+1)$-tuples themselves are ordered.

- Consider a $(d+1)$-tuple and decide whether it is connected. If no, then step back and form the next $(d+1)$-tuple. If yes, then step further.

- Take an element of the symmetric group S_n, conjugate all the involutive permutations of the $(d+1)$-tuple and order them. If this latter one is less then the original $(d+1)$-tuple of permutations (according to the ordering of $(d+1)$-tuples), then continue from the previous item. If no then choose another element of S_n, step by step. If no derived $(d+1)$-tuple is less than the original one, then store it and continue from the previous item. At the end we have a set of $(d+1)$-tuples that will be called the set of representants.

- Choose a representant and permute all the $d+1$ involutive permutations in it. In any case check whether the square of the product of two permutations standing on the k-th and $(k+2)$-th places is the identity. If this property holds for all the products, we store the representant, otherwise continue with another representant.

- Work with this subset of representants further and adopt to them a procedure similar to that before two items. However, there is a big difference, namely the $(d+1)$-tuples are not ordered more. In this way one have to compare the conjugate in question to each of the stored $(d+1)$-tuples. Having used up all the elements of S_n finally we get the representants of non-isomorphic d-dimensional D-graphs with n nodes.

Theorem 1 *Using the ALGORITHM one can construct all the non-isomorphic D-graphs with n nodes and of dimension d.*

Proof Using lexicographic ordering for permutation $(d+1)$-tuples (by that of the involutive permutations) we could considerably reduce the number of cases to be treated with. E. g. if all the involutive permutations of a $(d+1)$-tuple are different, then it is enough to check the connectedness of just one $(d+1)$-tuple instead of $(d+1)!$ ones. The involutive permutations are made inductively, as in the proof of Lemma 2 above. The connectedness procedure is the following.

Take the $(d+1)$-tuple in question. Consider the first number in every involutive permutation. Now we have the numbers of those nodes with whom the first node is linked at all. Take these new numbers (if they exist) and collect the numbers from the involutive permutations which stand on the places whose number is as much as these new numbers. Continue this procedure until new numbers appear. If we get all the numbers, then the $(d+1)$-tuple is connected, otherwise not.

However, since the numbers of the nodes were fixed, it is possible that different $(d+1)$-tuples describe the same graph. The fourth item of the algorithm provides us to avoid this phenomenon. It is easy to see that each renumbering can be presented by a permutation from S_n. Conjugating the involutive permutations, we have another involutive ones, according to the change of numbering. Using the fact that each graph has a a minimal $(d+1)$-tuple according to the ordering, it is enough to find this minimal one. At the end of the procedure we get the representants of connected graphs of each kind.

Beside the advantages of the ordering of $(d+1)$-tuples there is a huge disadvantage, too. That is, the adjacency operations of a graph ought to be distinguished. It means that we have to take into consideration any coloring of the edges, any sequence of the $(d+1)$ involutive permutations of any representant.

Since the product of adjacencies refers algebraically to the product of permutations we can apply the previously mentioned restriction ($r_{ij}(D)=1$ or 2, if $|i-j|>1$) by comparing the square of any $(d+1)$-tuple with the identity.

Finally, since we fail the restriction of being ordered we have to search for the representants, again.

In this way the proof of the algorithm is complete. We mention that this relatively complicated structure of the algorithm seems to be the most effective in practice.

The complexity of our algorithm is at most $O(n^{d\frac{n}{2}})$, asymptotically. $\square$

We have implemented our algorithm to computer. We found the earlier results of [BM98] and [BM00] correct. As a new result we get the complete enumeration of the 3-dimensional D-graphs with 5 barycentric simplex orbits.

Theorem 2 *The number of non-isomorphic 3-dimensional D-graphs with 5 simplex orbits is 33. The table below contains the permutation description of them. (The permutations refer to the adjacency operations in the following order: $\sigma_0, \sigma_1, \sigma_2, \sigma_3$.)* $\square$

12345,12345,13254,21435	12345,13254,21435,12345
13254,21435,12345,12345	12345,12354,21435,13245
12345,13245,21435,12354	12354,21435,13245,12345
13245,21435,12354,12345	12345,12354,21435,13254
12345,13254,21435,12354	12354,21435,13254,12345
13254,21435,12354,12345	12345,12354,42513,13254
12345,13254,42513,12354	12354,42513,13254,12345
13254,42513,12354,12345	12345,21435,12354,34125
21435,12354,34125,12345	12345,13254,21435,13254
13254,21435,13254,12345	12345,13254,21354,14523
12345,14523,21354,13254	13254,21354,14523,12345
14523,21354,13254,12345	12345,13254,21435,14523
13254,21435,14523,12345	12354,12435,13245,21345
12354,12435,13254,21345	21345,13254,12435,12354
12354,43215,21354,13245	12354,45312,13245,21354
21354,13245,45312,12354	12354,14523,21354,13254
13254,21354,14523,12354	

We mention that the introductory example of tiling of regular octahedra and tetrahedra is just of the type $12354, 12435, 13245, 21345$ (No. 30 in the table) which has Euclidean realization with the earlier described function *m*.

We hope that our algorithm can further be developed in a reasonable way for more number of orbits or for higher dimensions.

Acknowledgement

We are very grateful to prof. Emil Molnár for his valuable remarks.

References

[BH96] L. Balke - D. H. Huson: Two-dimensional groups, orbifolds and tilings, *Geom. Dedicata* **60** (1996), 89–106.

[BM98] A. Bölcskei - E. Molnár: How to Design Nice Tilings? *KoG, Scientific and Professional Information Journal of Croatian Society for Constructive Geometry and Computer Graphics* **3** (1998), 21–28.

[BM00] A. Bölcskei - E. Molnár: On classification of tilings in the planes of constant curvature by $D-$symbols, In *Proceedings of the* 4^{rd} *International Conference on Applied Informatics (2000)*, 117–128.

[DHZ92] O. Delgado Friedrichs - D. H. Huson - E. Zamorzaeva: The classification of 2-isohedral tilings of the plane, *Geom. Dedicata* **42** (1992), 43–117.

[Del95] O. Delgado Friedrichs: Euclidicity criteria for three-dimensional branched triangulations, PhD thesis, 1995

[Dre87] A. W. M. Dress: Presentations of discrete groups, acting on simply connected manifolds, *Adv. in Math.* **63** (1987), No. 2, 196–212.

[DHM93] A. W. M. Dress - D. H. Huson - E. Molnár: The classifications of face-transitive periodic three-dimensional tilings, *Acta Crystallographica* **A 49** (1993), 806–817.

[DS84] A. W. Dress - R. Scharlau: Zur Klassifikation äquivarianter Pflasterungen, *Mitteilungen aus dem Math. Seminar Giessen* **164** (1984), Coxeter-Festschrift

[Hus93] D. H. Huson: The generation and classification of tile-*k*-transitive tilings of the Euclidean plane, the sphere and hyperbolic plane, *Geom. Dedicata* **47** (1993), 269–296.

[Mol83] E. Molnár: Konvexe Fundamentalpolyeder und einfache D-V-Zellen für 29 Raumgruppen, die Coxetersche Spiegelungsuntegruppen enthalten. *Beitr. Algebra u. Geometrie* **14** (1983), 33–75.

[Mol96] E. Molnár: Discontinuous groups in homogeneous Riemannian spaces by classification of $D-$symbols, *Publicationes Math. Debrecen* **49** (1996) 3-4, 265–294.

Attila Bölcskei
Dept. of Geometry, TU Budapest
H-1521 Budapest
e-mail: bolcskei@math.bme.hu

Mónika Szél-Koponyás,
Dept. of Geometry, TU Budapest
H-1521 Budapest
e-mail: mszel@freemail.hu

Original scientific paper
Accepted 15. 07. 2002.

Damir Lazarević
Josip Dvornik
Krešimir Fresl

Contact Detection Algorithm for Discrete Element Analysis

Algoritam određivanja kontakata za metodu diskretnih elemenata

SAŽETAK

U radu je opisana inačica na mreži utemeljenog algoritma za nalaženje parova čestica između kojih se može pojaviti međudjelovanje kratkoga dometa, posebno prilagođena numeričkim analizama velikih sustava čestica podjednakih promjera, ravnomjerno raspodijeljenih u prostoru. Algoritam je primijenjen u modeliranju punjenja i pražnjenja silosa s granularnim materijalom.

Ključne riječi: metoda diskretnih elemenata, određivanje kontakata, sortiranje, pretraživanje

Contact Detection Algorithm for Discrete Element Analysis

ABSTRACT

The grid based variation of the contact detection algorithm, with corresponding data structures, is described. This variation is tuned for numerical analysis of large, homogenously distributed assemblages of particles of fairly equal diameters. As an example, algorithm is used in the modelling of granular material silo filling and discharge.

Key words: discrete element method, contact detection, sorting, searching

MSC 2000: 68P10, 70E55, 70F35

1 Introduction

Silos are industrial structures which experience a significant percentage of damage and collapse in comparison with other engineering structures: over 1000 silos, bins and hoppers fail in North America each year [7]. The main reason for such a state lies in the fact that a satisfactory theory about the motion of granular materials in silos has not yet been fully developed [5, 6, 11].

More or less validated differential equations (versions of Janssen–Koenen equation) and their exact or approximate solutions exist for filling stages and content at rest [13]. As the moving part of the total mass is small (only cap of the contents moves in form of avalanches) and the arching is negligible, these states do not cause significant dynamic effects; principles of continuum mechanics excluding inertial forces are therefore acceptable.

On the other hand, in the course of the discharge stages the usual state of the content is that of a nonuniform, relatively slow flow of material, characterized by arching and a large number of collisions between particles, and, therefore, by high dissipation of energy which leads to potential instabilities in solving equations derived from thermodynamical or hydrodynamical analogies (these analogies are more appropriate for the rapid flow of the content, but, unfortunately, prerequisites for its occurrence are rare in the regimes of silo usage) [4].

Recently, new computational methods, usually called *discrete* or *distinct element methods*, were developed with the aim to more closely model the behaviour of multibody (N–body) or particle assemblages [2, 18, 19].

These discrete numerical approaches comprise three main parts: (i) interaction model, (ii) determination of the interacting bodies, and (iii) numerical integration of the governing equations.

With respect to the interactions between bodies, discrete systems can be broadly classified into three groups [17]:

1. systems governed by long range forces, e. g. gravitational systems, where coupling is all–to–all,
2. systems in which interactions are medium range, e. g. molecular systems, and, finally,

3. systems with short range, mostly impact and contact, interactions, as the one with which we are concerned here, where each particle is usually coupled with dozen particles or thereabout.

The shapes of the particles can be approximated using various geometric solids [17], but the complexity of the form severely influences the computational time needed to determine the geometric details of the contact. Therefore, we opted for the simplest shape, the ball. However, to avoid crystalization, balls are given varying radii

$$r_i = r_{\min} + (r_{\max} - r_{\min})\,\mathtt{rnd}(), \tag{1}$$

where $r_{\max}$ and $r_{\min}$ are predefined extreme radii and $\mathtt{rnd}()$ is the random number generator with a uniform distribution on the unit segment. (If more complex shapes are needed, they can be realized by connecting two or more balls with some overlap. Similar idea was used to model the silo wall, section 4.)

The number of balls currently in the system will be denoted by $n(t)$.

If friction is omitted, rotational degrees of freedom need not be taken into account. Equations of motion of the centroid of the ith particle are then

$$\ddot{\mathbf{u}}_i(t) = \mathbf{M}_i^{-1}\mathbf{f}_i(t) + \mathbf{g}, \tag{2}$$

where $\ddot{\mathbf{u}}_i(t)$ is the acceleration of the centroid, $\mathbf{M}_i$ the diagonal mass matrix and $\mathbf{g}$ is the acceleration vector due to the gravity. The total applied force vector $\mathbf{f}_i(t)$ on the centroid of the particle i, interacting with the $k_i(t)$ particles, is given by

$$\mathbf{f}_i(t) = \sum_{\substack{j=1 \\ j\neq i}}^{k_i(t)} f_{i,j}(t)\,\mathbf{n}_{i,j}(t). \tag{3}$$

The short range interaction force $f_{i,j}(t)$ between particles i and j is modelled by the linear spring and the viscous damper in parallel (the so-called viscoelastic Kelvin or Voigt body) if the balls overlap and by the linear spring (Hookean body) if they are within the reach of cohesion and move apart. Maximum overlap or minimum distance between two balls is given by

$$\delta_{i,j}(t) = r_i + r_j - |\mathbf{u}_i(t) - \mathbf{u}_j(t)|, \tag{4}$$

where $\mathbf{u}_i(t)$ and $\mathbf{u}_j(t)$ are position vectors of the balls' centers. Clearly, the overlap $\delta_{i,j}(t) > 0$ is the numerical/geometrical counterpart of the squeezing of the balls during contact. The unit vector $\mathbf{n}_{i,j}(t)$ on the line joining centers of the balls is defined by

$$\mathbf{n}_{i,j}(t) = \frac{\mathbf{u}_{i,j}(t)}{|\mathbf{u}_{i,j}(t)|} = \frac{\mathbf{u}_i(t) - \mathbf{u}_j(t)}{|\mathbf{u}_i(t) - \mathbf{u}_j(t)|}. \tag{5}$$

System of equations (2) for $i = 1,\ldots,n(t)$ is an approximate description of the large displacements and strains problem. Although material linearity is assumed, the geometric nonlinearity still remains. Because of the frequent collisions, the paths, velocities and accelerations are not smooth functions. Not only the magnitudes, but also the types of the interaction forces between particles depend on the particles' positions and velocities and therefore change intensively in time. Described nonlinear problem has no analytical solution and some step by step technique should be used to numerically integrate equations of motion (our approach, a variation of the predictor–corrector method, is described in [9]).

What is more, neighbours of the ith particle, needed to perform the summation in (3), are not known in advance, but, as the particle system is in permanent motion, must be determined in each time step. Contact detection algorithm which facilitate efficient determination of the interacting particles will be more fully described in the sequel.

2 On spatial sorting and searching

The neighbour is defined here as a particle which is close enough to the observed particle so that any of the aforementioned short range interactions can be 'activated'. Determination of the interacting particles is called *contact detection*. More generally, contact detection is a determination of contact or overlap among members of a set of n geometric entities in an m–dimensional (Euclidean) space. Thus, it is a fundamental operation in a wide variety of diverse computation areas such as computational geometry and computer graphics (including CAD), particle physics and astrophysics, cartography and medical imaging, robotics and computational mechanics... And in particular, in computational mechanics contact detection is not restricted to discrete element methods. Finite element modelling of discontinous contact and fracture phenomena, unstructured multilevel/multigrid solution procedures, mesh generation algorithms, adaptive remeshing and remeshing necessitated by large mesh distortions (even in applications to 'oldfashioned' continuum mechanics) all require some form of contact detection. Closely related algorithms are used in recently developed meshless methods to obtain nodal connectivity and cloud overlap information, too.

The straightforward algorithm to find interacting particle pairs is to simply test each particle against every other in a nested loops:

for $i \leftarrow 1$ to $n(t)-1$ **do**
  for $j \leftarrow i+1$ to $n(t)$ **do**
    test particle i against particle j
  end for
end for

Obviously, for a system containing $n(t)$ particles, the number of required tests is proportional to $n(t)^2$, denoted by $O(n(t)^2)$. This is a very time consuming process for systems with many discrete elements (say 10 000 or more).[1] It was estimated that even with the most sophisticated contact detection algorithms these operations can amount to almost 60% of the total calculation time for large, short range, dynamic discrete systems [17].

These more advanced algorithms usually consist of two (possibly overlapping) phases called *spatial* or *neighbour searching* and *contact* or *geometric resolution* [17]. Spatial searching is the identification of the potential neighbours, while contact resolution determines whether candidate pairs actually interact, i. e. distances between candidates or depths of their mutual penetrations are calculated and compared to threshold values.[2] As the number of potential neighbours is small, the computational cost of contact resolution depends almost only on the complexity of the geometric representation of particles.

On the other hand, the cost of neighbour searching is dependent on the total number $n(t)$ of particles. Irregularly shaped particles are approximated with bounding boxes or bounding spheres, or even with equivalent spheres whose radius is obtained by taking the size of the largest particle in the system, e. g. [12].

Again, spatial searching is commonly performed in two steps. In the first step the complete set of particles is spatially ordered using some sorting algorithm and appropriate data structure is built. Then, in the second step, this sorted set is searched for potential neighbours. Spatial sorting and searching algorithms and corresponding data structures are mainly based on spatial decomposition. They can be roughly divided into two categories: region of interest (so-called search space) is either 'covered' with a grid, or partitioned in a hierarchical manner. Hierarchical decompositions, e. g. octrees and 3*d*–trees [1, 3], are spatial generalizations of the well known one–dimensional binary search trees [8, 15]; average time complexity of neighbour searching is thus $O(n(t)\log n(t))$, although it can degrade to $O(n(t)^2)$ for highly unbalanced trees. Grid techniques, on the other hand, have time complexity $O(n(t))$, but they are much more sensitive to the uneven distribution of particles (clusters and empty space) and to the ball size variances, i. e. the ratio $r_{\max}/r_{\min}$ [12, 14].

3 Fixed cubes scheme

Silo content is densely packed and evenly distributed, except maybe in small areas under arches and vaults (and, of course, above the heap in filling phase). It is also reasonable to assume that particles have approximately equal sizes, i. e. that we can take for balls' radii $r_{\max}/r_{\min} \approx 1.05$. Therefore we developed a variation of the grid based spatial sorting and searching algorithm.

The main idea of the fixed cubes scheme is to cover the search space with cubes (figure 1a) and sort balls in them. Then, during the calculation of forces, contact resolution is made only through the contents of the cubes which intersect the observed ball, and not through the whole region of the silo model. The cube that contains the center of the observed ball will be called *the central cube*.

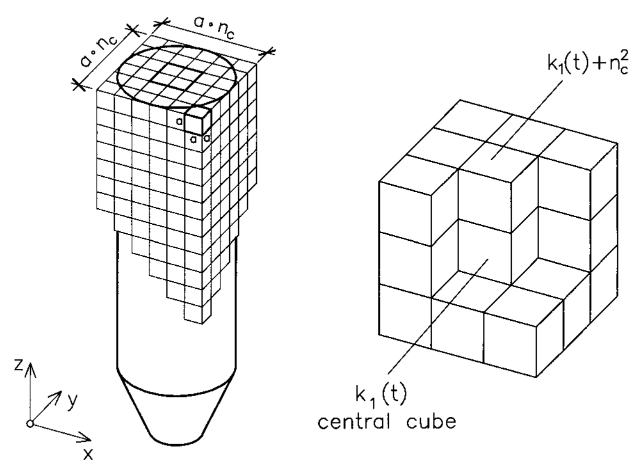

(a) (b)

Figure 1: Fixed cubes scheme: (a) covering the region of calculation, (b) central cube and its 26 neighbours (6 cubes are omitted for clearness).

If the size a of a cube is selected such that

$$a = 2\,r_{\max} + \Delta, \tag{6}$$

where $\Delta \geq 0$ is some small number, then all possible neighbours of the ball must be completely or partially contained in 26 cubes around the central cube ($3\times3\times3$ cubes subspace). These cubes will be called *surrounding cubes*.

[1] With respect to time, discrete systems can be pseudo–static, where relative position of particles do not change appreciably in time, or dynamic, where individual particles move significantly [12]. If the system is pseudo–static, the performance of a searching algorithm is not very important, because neighbours must be determined only once or occasionally, after several time steps.

[2] In our application, as the cohesion can be activated only if particles move apart, directions of motion and/or velocities should be determined, too.

It should be noted that the efficiency of this scheme requires careful selection of the size Δ. If Δ is too large, we have larger cubes, so that smaller number of surrounding cubes contain neighbours (i. e. more than 19 cubes can be immediately eliminated from the search, subsection 3.2), but there are more particles in each cube and contact resolution will be too long. On the other hand, assuming small time steps and small velocities, sorting procedure can be performed before the predictor phase only, but too small Δ (or $\Delta = 0$) may cause overlapping of the cubes by balls in the corrector phase, resulting in incorrect neighbour detection.

3.1 Central cube and its neighbours

According to the coordinates of the ball center $x_i(t)$, $y_i(t)$, $z_i(t)$, integer coordinates of the central cube are obtained from:

$$k_x(t) = \left\lceil \frac{x_i(t)}{a} \right\rceil, \; k_y(t) = \left\lceil \frac{y_i(t)}{a} \right\rceil, \; k_z(t) = \left\lceil \frac{z_i(t)}{a} \right\rceil, \quad (7)$$

where $\lceil \cdot \rceil$ means 'ceiling' of the given quotient [8]. Then the cube is assigned a unique index according to the formula

$$k_1(t) = n_c^2\big(k_z(t) - 1\big) + n_c\big(k_y(t) - 1\big) + k_x(t), \quad (8)$$

where n_c denotes the number of cubes in the global x and y directions (figure 1a). Now, depending on $k_1(t)$ and n_c it is easy to find indices of the remaining 26 cubes. For example, a cube above the central cube has an index given by $k_1(t) + n_c^2$ (figure 1b).

3.2 Elimination of 19 cubes

The condition (6), which can be rewritten as $a > 2r_{\max}$, gives three additional rules which arise from one another:

1. one ball cannot touch two opposite faces of the central cube at the same time,
2. ball can intersect up to three faces, three edges and contain one corner of the central cube,
3. ball can intersect up to 7 neighbouring cubes.

From the given statements it can be recognized that, depending on the position of the ball center in the local coordinate system (or octants/cells) of the central cube (figure 2a), one can eliminate 19 of 26 cubes. This is done by examining inequalities

$$d_x(t) \gtreqless 0, \qquad d_y(t) \gtreqless 0, \qquad d_z(t) \gtreqless 0, \quad (9)$$

where $d_x(t)$, $d_y(t)$ and $d_z(t)$ are local coordinates of the ball center given by

$$\begin{aligned} d_x(t) &= x_i(t) - a\left[k_x(t) - \frac{1}{2}\right], \\ d_y(t) &= y_i(t) - a\left[k_y(t) - \frac{1}{2}\right], \\ d_z(t) &= z_i(t) - a\left[k_z(t) - \frac{1}{2}\right]. \end{aligned} \quad (10)$$

For example, in the case of the ball center placed in the eighth cell (hatched in figure 2b), parts of the corresponding ball can be contained in up to seven cubes, denoted by $k_2(t), \ldots k_8(t)$, whose elements are jointed with the elements of the observed cell, or bound the observed cell, as presented in figure 2b. Similarly, other cells have their own seven neighbouring cubes.

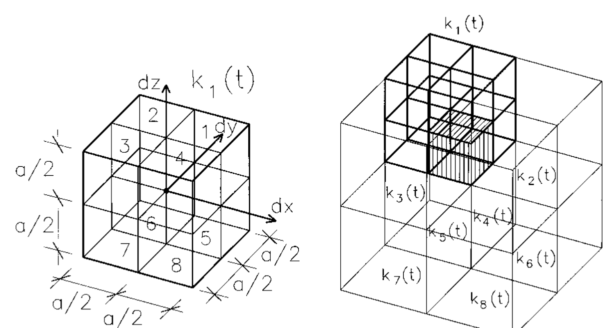

(a) (b)

Figure 2: Example of elimination: (a) local coordinate system (cells) of the central cube, (b) the eighth cell – remaining cubes

3.3 Intersected cubes

Finally, it is now possible to determine which of the 7 candidates $k_i(t)$ intersect the observed ball. This is done by examining distances between the surface of the ball, i. e. sphere, and faces, edges and corner of the observed cell, which also belong to remaining 7 cubes.

First, distances between the center of the ball and the faces of the cell are calculated,

$$\begin{aligned} \delta_x(t) &= \frac{1}{2}a - |d_x(t)|, \\ \delta_y(t) &= \frac{1}{2}a - |d_y(t)|, \\ \delta_z(t) &= \frac{1}{2}a - |d_z(t)|, \end{aligned} \quad (11)$$

followed by an examination of distances between the sphere and faces,

$$\begin{aligned} \Delta_x(t) &= r_i - \delta_x(t) \gtreqless 0, \qquad k_2(t), \\ \Delta_y(t) &= r_i - \delta_y(t) \gtreqless 0, \qquad k_3(t), \\ \Delta_z(t) &= r_i - \delta_z(t) \gtreqless 0, \qquad k_5(t), \end{aligned} \tag{12}$$

edges,

$$\begin{aligned} \Delta_{x,y}(t) &= r_i - \sqrt{\delta_x^2(t) + \delta_y^2(t)} \gtreqless 0, \\ &\qquad k_2(t), k_3(t), k_4(t), \\ \Delta_{x,z}(t) &= r_i - \sqrt{\delta_x^2(t) + \delta_z^2(t)} \gtreqless 0, \\ &\qquad k_2(t), k_5(t), k_6(t), \\ \Delta_{y,z}(t) &= r_i - \sqrt{\delta_y^2(t) + \delta_z^2(t)} \gtreqless 0, \\ &\qquad k_3(t), k_5(t), k_7(t), \end{aligned} \tag{13}$$

and corner of that cell,

$$\begin{aligned} \Delta_{x,y,z}(t) &= r_i - \sqrt{\delta_x^2(t) + \delta_y^2(t) + \delta_z^2(t)} \gtreqless 0, \\ &k_2(t), k_3(t), k_4(t), k_5(t), k_6(t), k_7(t), k_8(t), \end{aligned} \tag{14}$$

as shown in the example of the eighth cell depicted in figure 3. For each test (12)–(14), satisfaction of the criterion > 0 means that the ball intersects listed cubes.

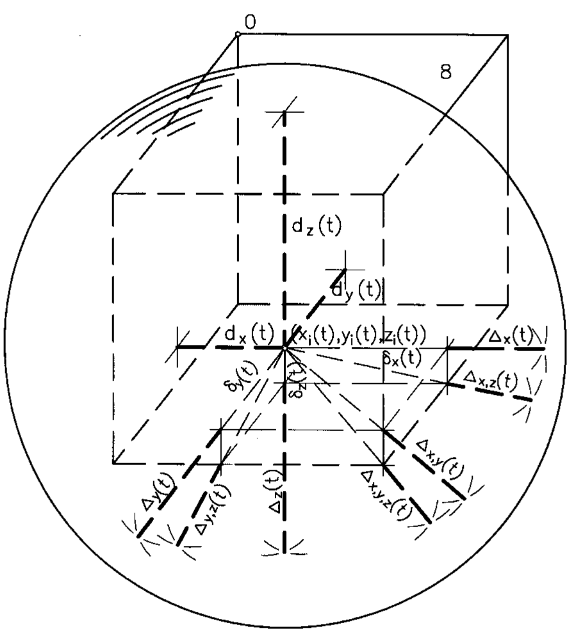

Figure 3: The center of the ball placed in the eighth cell

It should be pointed out that the ball, which do not intersect a face of the cell, can reach neither edges nor corners of that face. Therefore, (12)–(14) should be examined in the following order:

$$\text{faces} \to \text{edges} \to \text{corner}. \tag{15}$$

This logic (avoiding time argument t) can then be written as

$$\Delta_x \to \Delta_y \to \Delta_{x,y} \to \Delta_z \to \Delta_{x,z} \to \Delta_{y,z} \to \Delta_{x,y,z}. \tag{16}$$

Of course, during examinations, cube indices $k_i(t)$ must correspond to the chronology of examining distances given by (16). According to our convention (t is omitted), it holds that:

$$k_2 \to k_3 \to k_4 \to k_5 \to k_6 \to k_7 \to k_8. \tag{17}$$

As mentioned in the subsection 3.1, these indices are, depending on $k_1(t)$ and n_c, known a apriori and could be easily determined, as given by algorithm 1.

Algorithm 1: Forming the vector **k** of indices of cubes which could be intersected by the ball whose center is in the eighth cell.

cell_8 $(n_c, k_x, k_y, k_z) \;\mapsto\; \mathbf{k}$
$k_1 \leftarrow n_c^2(k_z - 1) + n_c(k_y - 1) + k_x$ {central cube; (8)}
$k_2 \leftarrow k_1 + 1$ {$\Delta_x > 0$; 1st eq. in (12)}
$k_3 \leftarrow k_1 - n_c$ {$\Delta_y > 0$; 2nd eq. in (12)}
$k_4 \leftarrow k_1 - n_c + 1$ {$\Delta_{x,y} > 0$; 1st eq. in (13)}
$k_5 \leftarrow k_1 - n_c^2$ {$\Delta_z > 0$; 3rd eq. in (12)}
$k_6 \leftarrow k_1 - n_c^2 + 1$ {$\Delta_{x,z} > 0$; 2nd eq. in (13)}
$k_7 \leftarrow k_1 - n_c^2 - n_c$ {$\Delta_{y,z} > 0$; 3rd eq. in (13)}
$k_8 \leftarrow k_1 - n_c^2 - n_c + 1$ {$\Delta_{x,y,z} > 0$; (14)}

Cubes which bind other cells can be similary found and stored using appropriate procedure **cell_i**, $1 \le i \le 8$.

3.4 Special configurations and ambiguous cases

There exist some limiting, very rare, but in the case of a large number of balls possible positions, where indices of the central cube, the cell and the remaining cubes are geometrically ambiguous or undefined if no additional decisions are provided.

Undefined central cube If the center of the ball falls on the common face, at the edge or at the corner of some cubes, that is, if one or more expressions

$$\begin{aligned} x_i(t) \bmod a &= 0, \\ y_i(t) \bmod a &= 0, \\ z_i(t) \bmod a &= 0, \end{aligned} \tag{18}$$

are satisified, it is easy to verify that because of the 'ceiling' operations in (7), equation (8) chooses the cube with the highest integer coordinates (the highest index) as central.

Undefined cell If the center of the ball falls on the plane, on the axis, or at the origin of the local coordinate system of the central cube, that is one or more of the following equalities holds,

$$d_x(t) = 0, \qquad d_y(t) = 0, \qquad d_z(t) = 0 \tag{19}$$

(equalities in (9)), we decided to choose the same cell as in the > 0 case.

This is deemed reasonable because the procedure given by (11)–(14) will in the case of the positions of the center described in this and previous paragraph provide all remaining cubes irrespective of the central cube and cell index. In these positions, *one* possible cube is used as central, and *one* of its cells is adopted. It is irrelevant which of these cubes/cells is used.

It is interesting to note that described positions can provide indices of all remaining cubes immediately, without additional searching. For example, coordinates of the center placed at the common corner of the (eight) cubes must fulfill (18) and, with the index of the central cube given in previous paragraph, seven remaining cubes can directly be found using (8). Similarly, local coordinates of the ball center placed at the center of the central cube must fulfill (19), which means that the central cube is the only cube, because it contains the entire ball. Analogously, by recognizing single relations in (18) and (19), other specific positions of the ball center (on the face, at the edge, or on local axis) can be found and remaining cubes directly determined. However, as these special positions are very rare, additional tests needed to recognize them introduce unnecessary computational burden and is therefore omitted.

Undefined remaining cubes If the ball touches a face, an edge or a corner of the chosen cell, that is, if one or more equalities appear in (12)–(14), it is considered that the corresponding cubes also contain the ball, as in the > 0 case, because possible touching between ball and its neighbours in such a cube could activate the cohesion force.

3.5 A kind of a binary tree

It follows from the previous section that it is unnecessary to treat equalities in (9) and (12)–(14) independently. It is sufficient to add them to the $>$ case and always examine only *two* possibilities ($\geq$ and $<$) in given relations.

This fact, with (16), gives for every moving ball in the system search structure which resembles the known binary tree [8, 15]. The flow chart of the searching procedure for one ball is, according to (17), partially presented in figure 4.

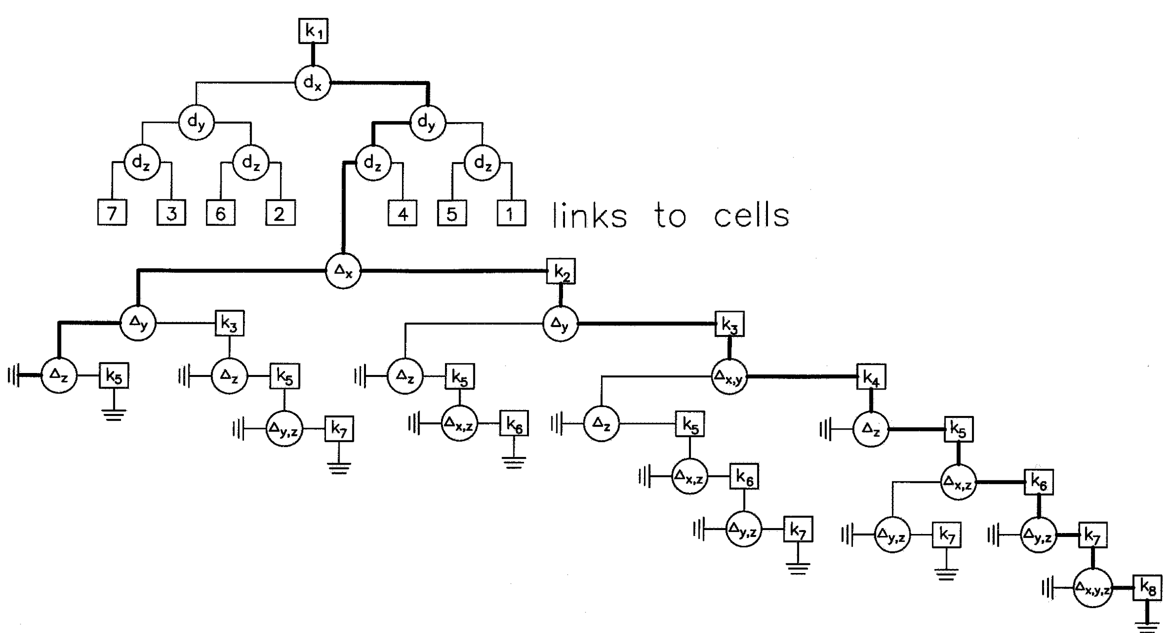

Figure 4: Shape and indexing of the search tree when the ball's center is placed in the eighth cell. Extreme search paths are marked.

The remaining seven subtrees denoted with the cell numbers rather than drawn are of the same shape but contain indices of the other, for certain cell neighbouring, cubes. The analysis of the tree shows that for extreme searching situations 6 examinations are needed if the ball is fully contained in the cube (this is a rare position and the shortest branch in the tree) and 10 examinations if the ball contains a corner of the cube (this is more frequent and the longest branch in the tree). These paths are marked in figure 4.

3.6 Programming strategy for sorting procedure

Memory organization of the procedures which will be described by pseudocode is now defined.[3]

The number of cubes $a_i(t)$ intersected by ball i and, *vice versa*, balls $b_k(t)$ by cube k, are saved as components of vectors $\mathbf{a}(t)$ and $\mathbf{b}(t)$, respectively. Indices i and k are saved as components of the matrix $\mathbf{B}(t)$ and $\mathbf{A}(t)$, that is $b_{k,b_k(t)}(t)$ and $a_{i,a_i(t)}(t)$. Thus, all temporary relations between cubes and balls in the system are stored. The filling procedure for adopted vectors and matrices is given by the algorithm 2.

Algorithm 2: Saving cube k that intersect ball i and vice versa.

cube $(i,k,\mathbf{a},\mathbf{b},\mathbf{A},\mathbf{B}) \mapsto [\mathbf{a},\mathbf{b},\mathbf{A},\mathbf{B}]$
$a_i \leftarrow a_i + 1$ {add new cube}
$a_{i,a_i} \leftarrow k$ {store new cube index}
$b_k \leftarrow b_k + 1$ {add new ball}
$b_{k,b_k} \leftarrow i$ {store new ball index}

Matrices $\mathbf{A}(t)$ and $\mathbf{B}(t)$ could also be represented as vectors using the linked allocation procedure [8]. This is not a problem for the matrix $\mathbf{A}(t)$ because balls are sorted in cubes successively, in increasing order, so that the matrix is filled from left to right and row by row. But, simultaneously, the matrix $\mathbf{B}(t)$ is filled almost randomly, so it is necessary to use one of the insertion techniques (for example bisection) for placing the ball index at the correct place of the equivalent vector. Of course, this storage scheme saves the amount of memory space because zeroes are not stored (though some additional vectors for addressing are needed), but also increases the amount of time taken for sorting phase. However, the silo contents has a relatively uniform density distribution, so that matrices $\mathbf{A}(t)$ and $\mathbf{B}(t)$ are always well populated and 'classical' array representation suffices.

The complete search algorithm is given by pseudocode 3 and the sorting procedure by pseudocode 4.

Algorithm 3: Searching for cubes that intersect given ball i.

search $(i,\Delta_x,\Delta_y,\Delta_{x,y},\Delta_z,\Delta_{x,z},\Delta_{y,z},\Delta_{x,y,z},\mathbf{k},\mathbf{a},\mathbf{b},\mathbf{A},\mathbf{B}) \mapsto [\mathbf{a},\mathbf{b},\mathbf{A},\mathbf{B}]$
$[\mathbf{a},\mathbf{b},\mathbf{A},\mathbf{B}] \leftarrow$ **cube** $(i,k_1,\mathbf{a},\mathbf{b},\mathbf{A},\mathbf{B})$ {cube k_1}
if $\Delta_x \geq 0$ **then** {cube k_2}
  $[\mathbf{a},\mathbf{b},\mathbf{A},\mathbf{B}] \leftarrow$ **cube** $(i,k_2,\mathbf{a},\mathbf{b},\mathbf{A},\mathbf{B})$
  if $\Delta_y \geq 0$ **then** {cube k_3}
    $[\mathbf{a},\mathbf{b},\mathbf{A},\mathbf{B}] \leftarrow$ **cube** $(i,k_3,\mathbf{a},\mathbf{b},\mathbf{A},\mathbf{B})$
    if $\Delta_{x,y} \geq 0$ **then** {cube k_4}
      $[\mathbf{a},\mathbf{b},\mathbf{A},\mathbf{B}] \leftarrow$ **cube** $(i,k_4,\mathbf{a},\mathbf{b},\mathbf{A},\mathbf{B})$
      if $\Delta_z \geq 0$ **then** {cube k_5}
        $[\mathbf{a},\mathbf{b},\mathbf{A},\mathbf{B}] \leftarrow$ **cube** $(i,k_5,\mathbf{a},\mathbf{b},\mathbf{A},\mathbf{B})$
        if $\Delta_{x,z} \geq 0$ **then** {cube k_6}
          $[\mathbf{a},\mathbf{b},\mathbf{A},\mathbf{B}] \leftarrow$ **cube** $(i,k_6,\mathbf{a},\mathbf{b},\mathbf{A},\mathbf{B})$
          if $\Delta_{y,z} \geq 0$ **then** {cube k_7}
            $[\mathbf{a},\mathbf{b},\mathbf{A},\mathbf{B}] \leftarrow$ **cube** $(i,k_7,\mathbf{a},\mathbf{b},\mathbf{A},\mathbf{B})$
            if $\Delta_{x,y,z} \geq 0$ **then** {cube k_8}
              $[\mathbf{a},\mathbf{b},\mathbf{A},\mathbf{B}] \leftarrow$ **cube** $(i,k_8,\mathbf{a},\mathbf{b},\mathbf{A},\mathbf{B})$
        else {$\Delta_{x,z} < 0$}
          if $\Delta_{y,z} \geq 0$ **then** {cube k_7}
            $[\mathbf{a},\mathbf{b},\mathbf{A},\mathbf{B}] \leftarrow$ **cube** $(i,k_7,\mathbf{a},\mathbf{b},\mathbf{A},\mathbf{B})$
    else {$\Delta_{x,y} < 0$}
      if $\Delta_z \geq 0$ **then** {cube k_5}
        $[\mathbf{a},\mathbf{b},\mathbf{A},\mathbf{B}] \leftarrow$ **cube** $(i,k_5,\mathbf{a},\mathbf{b},\mathbf{A},\mathbf{B})$
        if $\Delta_{x,z} \geq 0$ **then** {cube k_6}
          $[\mathbf{a},\mathbf{b},\mathbf{A},\mathbf{B}] \leftarrow$ **cube** $(i,k_6,\mathbf{a},\mathbf{b},\mathbf{A},\mathbf{B})$
        if $\Delta_{y,z} \geq 0$ **then** {cube k_7}
          $[\mathbf{a},\mathbf{b},\mathbf{A},\mathbf{B}] \leftarrow$ **cube** $(i,k_7,\mathbf{a},\mathbf{b},\mathbf{A},\mathbf{B})$
  else {$\Delta_y < 0$}
    if $\Delta_z \geq 0$ **then** {cube k_5}
      $[\mathbf{a},\mathbf{b},\mathbf{A},\mathbf{B}] \leftarrow$ **cube** $(i,k_5,\mathbf{a},\mathbf{b},\mathbf{A},\mathbf{B})$
      if $\Delta_{x,z} \geq 0$ **then** {cube k_6}
        $[\mathbf{a},\mathbf{b},\mathbf{A},\mathbf{B}] \leftarrow$ **cube** $(i,k_6,\mathbf{a},\mathbf{b},\mathbf{A},\mathbf{B})$
else {$\Delta_x < 0$}
  if $\Delta_y \geq 0$ **then** {cube k_3}
    $[\mathbf{a},\mathbf{b},\mathbf{A},\mathbf{B}] \leftarrow$ **cube** $(i,k_3,\mathbf{a},\mathbf{b},\mathbf{A},\mathbf{B})$
    if $\Delta_z \geq 0$ **then** {cube k_5}
      $[\mathbf{a},\mathbf{b},\mathbf{A},\mathbf{B}] \leftarrow$ **cube** $(i,k_5,\mathbf{a},\mathbf{b},\mathbf{A},\mathbf{B})$
      if $\Delta_{y,z} \geq 0$ **then** {cube k_7}
        $[\mathbf{a},\mathbf{b},\mathbf{A},\mathbf{B}] \leftarrow$ **cube** $(i,k_7,\mathbf{a},\mathbf{b},\mathbf{A},\mathbf{B})$
  else {$\Delta_y < 0$}
    if $\Delta_z \geq 0$ **then** {cube k_5}
      $[\mathbf{a},\mathbf{b},\mathbf{A},\mathbf{B}] \leftarrow$ **cube** $(i,k_5,\mathbf{a},\mathbf{b},\mathbf{A},\mathbf{B})$

[3] Fortran 77 is chosen as implementation language. Therefore, given algorithms and corresponding data structures are in a sense not very 'contemporary' or 'fashionable'.

Algorithm 4: Sorting balls in cubes and vice versa.

1: **sort** $(n, n_w, n_c, a, \mathbf{x}, \mathbf{y}, \mathbf{z}, \mathbf{r}) \mapsto [\mathbf{a}, \mathbf{b}, \mathbf{A}, \mathbf{B}]$
2: **for** $i \leftarrow n_w + 1$ to n **do** {sorting movable balls}
3: $\quad k_x \leftarrow \lceil x_i/a \rceil$; $k_y \leftarrow \lceil y_i/a \rceil$; $k_z \leftarrow \lceil z_i/a \rceil$
$\quad$ {integer coordinates of the central cube; (7)}
4: $\quad d_x \leftarrow x_i - a(k_x - 1/2)$; $d_y \leftarrow y_i - a(k_y - 1/2)$;
$\quad d_z \leftarrow z_i - a(k_z - 1/2)$
$\quad$ {local coordinates of the center; (10)}
5: $\quad$ **if** $d_x \geq 0$ **then** {finding the cell; (9)}
6: $\quad\quad$ **if** $d_y \geq 0$ **then**
7: $\quad\quad\quad$ **if** $d_z \geq 0$ **then** {cell 1}
8: $\quad\quad\quad\quad$ $\mathbf{k} \leftarrow$ **cell_1** (n_c, k_x, k_y, k_z)
9: $\quad\quad\quad$ **else** {cell 5}
10: $\quad\quad\quad\quad$ $\mathbf{k} \leftarrow$ **cell_5** (n_c, k_x, k_y, k_z)
11: $\quad\quad$ **else** $\{d_y < 0\}$
12: $\quad\quad\quad$ **if** $d_z \geq 0$ **then** {cell 4}
13: $\quad\quad\quad\quad$ $\mathbf{k} \leftarrow$ **cell_4** (n_c, k_x, k_y, k_z)
14: $\quad\quad\quad$ **else** {cell 8}
15: $\quad\quad\quad\quad$ $\mathbf{k} \leftarrow$ **cell_8** (n_c, k_x, k_y, k_z)
16: $\quad$ **else** $\{d_x < 0\}$
17: $\quad\quad$ **if** $d_y \geq 0$ **then**
18: $\quad\quad\quad$ **if** $d_z \geq 0$ **then** {cell 2}
19: $\quad\quad\quad\quad$ $\mathbf{k} \leftarrow$ **cell_2** (n_c, k_x, k_y, k_z)
20: $\quad\quad\quad$ **else** {cell 6}
21: $\quad\quad\quad\quad$ $\mathbf{k} \leftarrow$ **cell_6** (n_c, k_x, k_y, k_z)
22: $\quad\quad$ **else** $\{d_y < 0\}$
23: $\quad\quad\quad$ **if** $d_z \geq 0$ **then** {cell 3}
24: $\quad\quad\quad\quad$ $\mathbf{k} \leftarrow$ **cell_3** (n_c, k_x, k_y, k_z)
25: $\quad\quad\quad$ **else** {cell 7}
26: $\quad\quad\quad\quad$ $\mathbf{k} \leftarrow$ **cell_7** (n_c, k_x, k_y, k_z)
27: $\quad \delta_x \leftarrow a/2 - |d_x|$; $\delta_y \leftarrow a/2 - |d_y|$; $\delta_z \leftarrow a/2 - |d_z|$
$\quad$ {position of the centroid in the cell; (11)}
28: $\quad \Delta_x \leftarrow r_i - \delta_x$; $\Delta_y \leftarrow r_i - \delta_y$; $\Delta_z \leftarrow r_i - \delta_z$
$\quad$ {distances between the sphere and faces of the cell; (12)}
29: $\quad \Delta_{x,y} \leftarrow r_i - \sqrt{\delta_x^2 + \delta_y^2}$; $\Delta_{x,z} \leftarrow r_i - \sqrt{\delta_x^2 + \delta_z^2}$;
$\quad \Delta_{y,z} \leftarrow r_i - \sqrt{\delta_y^2 + \delta_z^2}$
$\quad$ {distances between the sphere and edges of the cell; (13)}
30: $\quad \Delta_{x,y,z} \leftarrow r_i - \sqrt{\delta_x^2 + \delta_y^2 + \delta_z^2}$
$\quad$ {distance between sphere and corner of the cell; (14)}
31: $\quad [\mathbf{a}, \mathbf{b}, \mathbf{A}, \mathbf{B}] \leftarrow$
$\quad\quad$ **search** $(i, \Delta_x, \Delta_y, \Delta_{x,y}, \Delta_z, \Delta_{x,z}, \Delta_{y,z}, \Delta_{x,y,z}, \mathbf{k}, \mathbf{a}, \mathbf{b}, \mathbf{A}, \mathbf{B})$
$\quad$ {searching for intersected cubes}

The efficiency of given algorithms for the densest observed packing ($b_k(t) = 20$) and, theoretically, the sparsest packing ($b_k(t) = 1$) of the system with various numbers of balls, is shown on diagrams in figure 5. They show that sorting time is almost of order $O\big(n(t)\big)$ as expected [15, 12, 14] for a well distributed (not clustered) system as the one presented here.

3.7 Contact resolution and geometry

After spatial sorting is completed, contact resolution may be of the $O\big(\tilde{n}^2(t)\big)$ order, because of the small number of possible neighbours in cubes that intersect the observed ball (in our calculations $\tilde{n}(t) = b_k(t) \leq 20$).

Finally, it is quite simple to solve for geometry needed for determining interaction forces between balls i and j. As indicated in the introduction, two examinations to find if they overlap or possibly stick to each other are needed:

$$\delta_{i,j}(t) > 0, \tag{20}$$

$$-N^c_{\max;i,j}/k_{i,j} \leq \delta_{i,j}(t) \leq 0, \tag{21}$$

where distance $\delta_{i,j}(t)$ is given by (4), $N^c_{\max;i,j}$ is the maximum cohesion force and $k_{i,j}$ is the stiffness of the collision model. In the latter case, an additional testing is whether they are going apart or approaching one another along the line joining their centers:

$$d^n_{i,j}(t) = \dot{\mathbf{u}}_{i,j}(t) \cdot \mathbf{u}_{i,j}(t) < 0. \tag{22}$$

4 Boundary conditions

The model of the silo wall is made of fixed overlapping balls with randomized radii, again to prevent crystalization of balls representing silage material. This model also imitates friction due to roughness and geometric imperfections on the surface of the wall. Thus, in the absence of an expensive model of friction between balls (characterized by a friction coefficient), the aim was to simulate at least the geometric part of this phenomena. Boundary balls are generated with separate procedure **wall** $(d_h, h_h, d_c, h_c, k_w, c_w, n_w, \mathbf{k}, \mathbf{c}, \mathbf{x}, \mathbf{y}, \mathbf{z}, \mathbf{r}, \dot{\mathbf{x}}, \dot{\mathbf{y}}, \dot{\mathbf{z}})$, not shown here. Values d_h, h_h and d_c, h_c are diameters and heights of conical and cylindrical parts of the silo and k_w, c_w are stiffness and viscosity of the wall model. The number of boundary wall balls is n_w. Their velocities are, of course, zero.

Two additional things must be mentioned here. First, it is sufficient to execute the sorting procedure and store the boundary balls in the appropriate cubes only once, in the beginning of the calculation, as they do not move. Thus, the sorting procedure must always be performed for the moving balls only, as indicated in the line 2 of the algorithm 4.

Second, the algorithm 2 requires that vectors $\mathbf{a}(t)$, $\mathbf{b}(t)$ and matrices $\mathbf{A}(t)$, $\mathbf{B}(t)$ should always be set to zero before

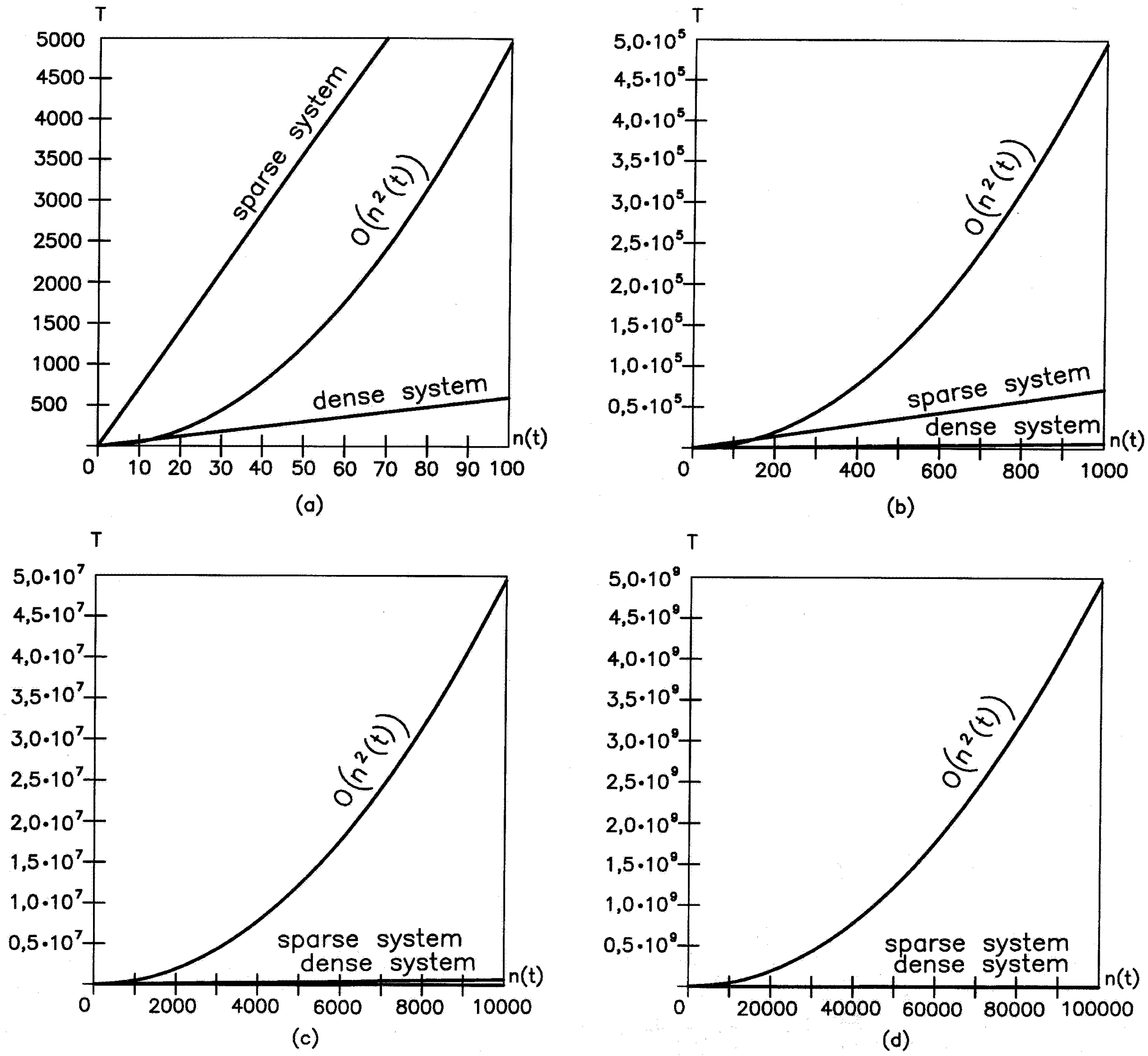

Figure 5: Efficiency of fixed cubes algorithm for sparse and dense systems in comparison with $O\left(n^2(t)\right)$ for various numbers of balls: (a) $n(t) \leq 100$, (b) $n(t) \leq 1000$, (c) $n(t) \leq 10000$, (d) $n(t) \leq 100000$.

the sorting procedure is executed. But from the previous comment it follows that this process should also be performed for moving balls only. Therefore indices of boundary balls must be saved and their cubes stored in $\mathbf{A}(t)$ and $\mathbf{B}(t)$. This is done by using the total number of boundary balls n_w (given by the procedure **wall**) and saving numbers of boundary balls in every cube $\mathbf{w}$ (given by first call of the procedure **sort** after **wall** is executed).

5 Calculation of interactions

Now, naïve nested loops from section 2 can be written as given in algorithm 5, where ball pairs are denoted by i and m instead of by i and j.

To avoid multiple interactions logical vector $\mathbf{s}(t)$ is used with additional testing to determine the cube which, according to (7) and (8), contains the midpoint of the line segment between centers:

$$x_s = \frac{1}{2}(x_i + x_m),\; y_s = \frac{1}{2}(y_i + y_m),\; z_s = \frac{1}{2}(z_i + z_m). \quad (23)$$

Once sorted, interactions between boundary and moving balls in the sense of the algorithm 5 are nothing special. Assuming zero velocities for boundary balls, all other constants of the collision model are obtained.

It should be mentioned that given vectors and matrices could be (in a more 'modern' implementation) allocated dynamically, because the system moves, so their sizes vary during calculation, i. e. $n(t) \geq 1$, $b_k(t) \geq 1$, $1 \leq a_i(t) \leq 8$.

Algorithm 5: Loops over sorted balls.

loops $(n, n_w, n_c, \mathbf{s}, \mathbf{a}, \mathbf{b}, \mathbf{A}, \mathbf{B}, \mathbf{x}, \mathbf{y}, \mathbf{z}, \mathbf{r})$
for $i \leftarrow n_w + 1$ to n **do** {movable balls}
  $s_i \leftarrow$ `true` {solving ball i}
  for $j \leftarrow 1$ to a_i **do** {intersected cubes}
    $k \leftarrow a_{i,j}$ {current cube index}
    for $l \leftarrow 1$ to b_k **do** {all balls in intersected cubes}
      $m \leftarrow b_{k,l}$ {current ball index}
      if $s_m \equiv$ `false` **then** {ball m is not solved}
        $x_s \leftarrow (x_i + x_m)/2;\ \ y_s \leftarrow (y_i + y_m)/2;$
        $z_s \leftarrow (z_i + z_m)/2$
        {midpoint coordinates; (23)}
        $k_x \leftarrow \lceil x_s/a \rceil;\ \ k_y \leftarrow \lceil y_s/a \rceil;\ \ k_z \leftarrow \lceil z_s/a \rceil$
        {integer coordinates of cube with the midpoint; (7)}
        $k_s \leftarrow n_c^2(k_z - 1) + n_c(k_y - 1) + k_x$ {cube index; (8)}
        if $k_s = k$ **then** {midpoint in the current cube}
          test particle i against particle m

The total number of cubes is fixed during the calculation due to the fixed cubes scheme used here, but it can be given as the input parameter.

6 Example

Described algorithms were implemented in Fortran 77 (version by Absoft) and incorporated in a computer program which simulates various regimes during silo exploatation. Also, for better visualization of results fast perspective routines using PGPLOT graphics library were programmed.

Some snapshots during silo filling and discharge are given in figures 6 and 7, respectively. For graphical presentation the silo model was cut with a plane through its vertical axis and only half of the model was rendered so that the insides of the silo can be seen. Input data of the presented example are given in table 1.

Table 1: Main data of the model.

$r_{\min}$	$0,215$ m
$r_{\max}$	$0,225$ m
a	$0,500$ m
Δ	$0,050$ m
$n_{\max}^{\text{contents}}$	22741
n_w	3821
γ	$1250\ \text{kg/m}^3$
k_c	10^7 N/m
k_w	10^9 N/m
c_c	10^8 Ns/m
c_w	10^7 Ns/m
$\Delta t_{\text{filling}}$	10^{-4} s
$\Delta t_{\text{discharge}}$	10^{-5} s

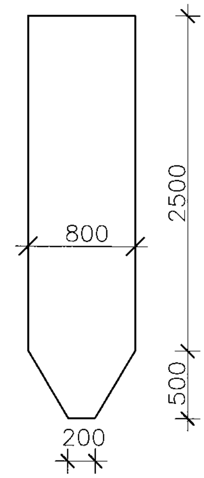

7 Conclusions

There is no universal spatial sorting and searching algorithm whose performance is (completely) independant of the characteristics of the analysed discrete system. Namely, discrete systems can be densely or sparsely packed, and, what is more important, particles can be evenly distributed or clustered. Furthermore, the range of bounding spheres' radii (i. e. whether spheres have equal, approximately equal or considerably differing radii) must be taken into account. In particular, theoretical $O(n)$ performance of grid based algorithms cannot be attained if particles are clustered in few cells only, because there are many unused cells which nevertheless must be tested. Furthermore, the ball size variances lead to the so-called over–reporting problem as the size of the cells are determined by the largest particle in the system.

But silo content has homogenous spatial distribution while grains can be assumed to have fairly equal sizes and, therefore, prerequisites for the optimal behaviour of grid techniques are realised. Majority of computational time in discrete element simulations is spent in contact detection and it is, therefore, sensible to develop highly specialised algorithm tuned for discrete numerical modelling of silo exploatation.

References

[1] BONET, J.; PERAIRE, J.: *An Alternating Digital Tree (ADT) Algorithm for 3D Geometric Searching and Intersection Problems*, International Journal for Numerical Methods in Engineering, **31** (1991), pp. 1–17.

[2] CUNDALL, P. A.; STRACK, O. D. L.: *A Distinct Element Model for Granular Assemblies*, Geotechnique, **29** (1979), pp. 47–65.

[3] FENG, Y. T.; OWEN, D. R. J.: *A Spatial Digital Tree Based Contact Detection Algorithm*, Proceedings of ICADD–4, Fourth International Conference on Analysis of Discontinuous Deformation (ed. Bićanić, N.), June 6th–8th, 2001, University of Glasgow, Scotland, UK, pp. 221–238.

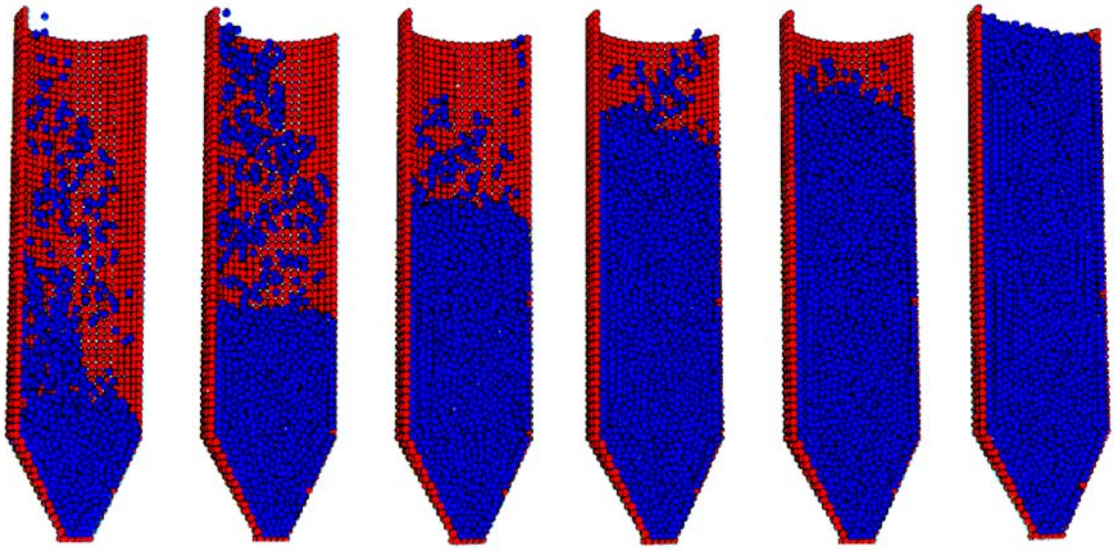

Figure 6: Silo filling.

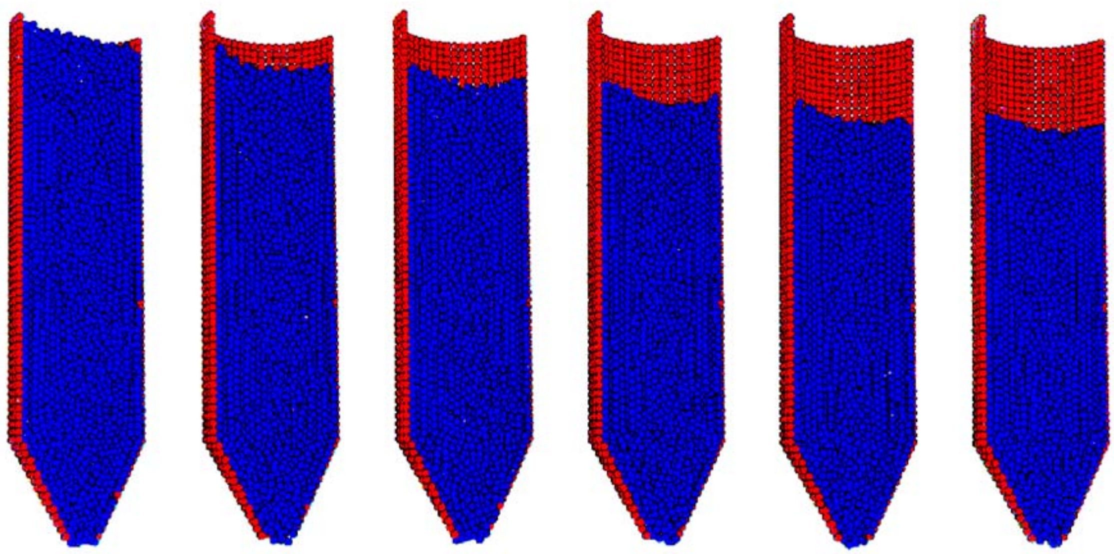

Figure 7: Silo discharge.

[4] JAEGER, H. M.: *Chicago Experiments on Convections, Compaction, and Compression*, Physics of Dry Granular Media (eds. Herrmann, H. J.; Hovi, J.–P.; Luding, S.), Kluwer Academic Publishers, Dordrecht, 1997, pp. 553–583.

[5] JAEGER, H. M.; NAGEL, S. R.: *Physics of the Granular State*, Science, **255** (1992), pp. 1523–1531.

[6] JAEGER, H. M.; NAGEL, S. R.; BEHRINGER, R. P.: *Granular Solids, Liquids and Gases*, Reviews of Modern Physics, **68** (1996), pp. 1259–1273.

[7] KNOWLTON, T. M.; CARSON, J. W.; KLINZING, G. E.; YANG, W-C.: *The Importance of Storage, Transfer, and Collection*, Chemical Engineering Progress, **90** (1994), pp. 44–54.

[8] KNUTH, D. E.: *The Art of Computer Programming. Volume 3: Sorting and Searching*, Addison–Wesley, Reading, Massachusetts, 1973.

[9] LAZAREVIĆ, D.; DVORNIK, K.; FRESL, K.: *Diskretno numeričko modeliranje opterećenja silosa*, Građevinar, **54** (2002) pp. 135–144.

[10] Mark, J.; Holst, F. G.; Rotter, J. M.; Ooi, J. Y.; Rong, G. H.: *Numerical Modeling of Silo Filling. II: Discrete Element Analyses*, Journal of Engineering Mechanics, **125** (1999) pp. 104–110.

[11] Mehta, A.; Barker, G. C.: *The Dynamics of Sand*, Reports on Progress in Physics, 1994, pp. 383–416.

[12] Munjiza, A.; Andrews, K. R. F.: *NBS Contact Detection Algorithm for Bodies of Similar Size*, International Journal for Numerical Methods in Engineering, **43** (1998), pp. 131–149.

[13] Nedderman, R. M.: *Statics and Kinematics of Granular Materials*, Cambridge University Press, Cambridge, New York, USA, 1992.

[14] Perkins, E.; Williams, J.: *CGrid: Neighbor Searching for Many Body Simulation*, Proceedings of ICADD–4, Fourth International Conference on Analysis of Discontinuous Deformation (ed. Bićanić, N.), June 6th–8th, 2001, University of Glasgow, Scotland, UK, pp. 427–438.

[15] Sedgewick, R.: *Algorithms*, Addison–Wesley, Reading, Massachusetts, 1989.

[16] *Silos, Hoppers, Bins & Bunkers for Storing Bulk Materials*, The Best of Bulk Solids Handling. Selected Articles, Trans Tech Publications, Volume A/86, Clausthal–Zellerfeld, Germany, 1986.

[17] Williams, J. R., O'Connor, R.: *Discrete Element Simulation and the Contact Problem*, Archives of Computational Methods in Engineering, **6** (1999), pp. 279–304.

[18] Williams, J. R.; Hocking, G.; Mustoe, G. E.: *The Theoretical Basis of the Discrete Element Method*, NUMETA 85, Numerical Methods in Engineering: Theory and Applications, (eds. Middleton, J.; Pande, G. N.), Proceedings of the International Conference on Numerical Methods in Engineering: Theory and applications, Swansea, January 7th–11th, 1985, pp. 897–906.

[19] Yserentant, H.: *A New Class of Particle Methods*, Numerische Mathematik, **76** (1997), pp. 87–109.

Damir Lazarević
e-mail: damir@grad.hr

Josip Dvornik
e-mail: dvornik@grad.hr

Krešimir Fresl
e-mail: fresl@grad.hr

University of Zagreb
Faculty of Civil Engineering

Original scientific paper
Accepted 07. 08. 2002.

MÁRTA SZILVÁSI-NAGY
TERÉZ P. VENDEL
HELLMUTH STACHEL

C^2 Filling of Gaps by Convex Combination of Surfaces under Boundary Constraints

C^2 popunjavanje praznina pomoću konveksne kombinacije ploha pod rubnim ograničenjima

SAŽETAK

Dane su dvije metode za izvođenje ploha. Jedna za povezivanje dviju ploha sa C^2 neprekinutošću koja odgovara i dvjema graničnim linijama, a druga za G^1 popunjavanje posebnog slučaja trostrane rupe. Plohe se izvode kao konveksna kombinacija plošnih i krivuljnih sastvanih dijelova sa odgovarajućom korektivnom funkcijom, a dane su u parametarskom obliku.

Ključne riječi: C^2 neprekinutost, konveksna kombinacija, Coonsove plohe, popunjavanje rupa, plošno modeliranje

C^2 Filling of Gaps by Convex Combination of Surfaces under Boundary Constraints

ABSTRACT

Two surface generation methods are presented, one for connecting two surfaces with C^2 continuity while matching also two prescribed border lines on the free sides of the gap, and one for G^1 filling a three-sided hole in a special case. The surfaces are generated as convex combination of surface and curve constituents with an appropriate correction function, and are represented in parametric form.

Key words: C^2 continuity, Convex combination, Coons surfaces, Filling of holes, Surface modelling

MSC 2000: 65D17, 68U07

1 Introduction

In this paper trigonometric convex combinations of surfaces and curves are applied for filling gaps between two surfaces and holes bounded by three surfaces. Trigonometric blending functions have been applied for G^1 curve construction already by Bär (1977), then for defining G^2 spline curves as convex combinations of arcs and straight line segments by Szilvási-Nagy and P.Vendel (2000). An extension of those curve constructions to surfaces has been given by Szilvási-Nagy (2000). Continuity conditions and a rational parametric form of the blending functions are presented here.

Convex combinations of points, curves or surfaces are frequently used for solving interpolation problems, for example Little (1983). Well-known interpolating surfaces defined by convex combination of boundary curves are the Coons surfaces (see e.g. in Farin 1990). Curves defined over triangles are interpolated by a C^2 surface using quintic polynomials by Alfeld and Barnhill (1984). Here, similarly to Coons's method, the input data are "wire frame data" consisting of curves and first and second cross-boundary derivatives. A transfinite blending function interpolant for the simplex in $\mathbf{R}^n$ is decribed by Gregory (1985). The term transfinite means that the interpolant matches function and derivative values given on all faces of the simplex. That is, surfaces appear in the combination. The method is based on an explicit representation of a finite dimensional Hermite interpolation polynomial for the simplex.

The surface generation methods presented in this paper formally follow the construction method of Coons by building a convex combination of the boundary data and applying proper correction functions. However, the geometric concept of our construction is rather similar to the transfinite interpolation surface of Gregory. The use of surface patches in a Coons-type blend is novel in our algorithms. The surfaces in the combination are defined over the same parameter domain. The resulting surface matches one bordering line of each surface and the tangent planes along this line. Moreover, the second cross-derivatives are also equal along the contact curves in the rectangular case (first algorithm). This fact can be used for filling a gap between two surfaces or a hole between three surfaces. The constituents are either the extensions of the surfaces bordering the gap or the hole, or patches (two or three) joining C^1 or C^2 continuously to one of the surfaces which are to be connected. In this way these patches transfer the boundary data to the convex combination. There are several known methods for C^1 or C^2 fitting of rectangular and triangular patches (Farin, 1990, Chapter 19 and Hoschek, 1992, Chapter 7). These constructions will not be the subject of this paper.

2 Blending surface between two surfaces with boundary constraints

A blending surface is one that smoothly connects two given surfaces and satisfies additional geometric constraints. Filip (1989) applied cubic Hermite blend of two boundary curves of the given surfaces and two arbitrary rail curves. The literature describes many different methods for constructing blending surfaces, recently Hartmann (2001) used rational functions. Some of these methods are extended to three or more surfaces, for example that of Schichtel (1993). These blending surfaces defined as linear combinations of given curves or surfaces with one parameter blending functions are different from both the Coons and our patches, they are not the subject of this paper.

In this algorithm two regular surfaces $\mathbf{r}_1(u,v)$ and $\mathbf{r}_2(u,v)$ and two curves $\mathbf{r}_3(v)$ and $\mathbf{r}_4(v)$ are given. The curves join the corresponding corner points of the two surfaces as boundary lines of the required surface patch. The blending surface is defined over the parameter domain $(u,v) \in [0,1]\times[0,1]$ such that its boundary curves for $v=0$ and $v=1$ match the boundaries of the gap determined from the left by $\mathbf{r}_1(u,0)$ and from the right by $\mathbf{r}_2(u,1)$, respectively, while the upper border line for $u=0$ coincides with the curve $\mathbf{r}_3(v)$ and the lower border line for $u=1$ coincides with the curve $\mathbf{r}_4(v)$ ($v\in[0,1]$) (Fig. 1). The drawn parts of the given underlying surfaces in Fig. 2 are parametrized as follows: $\mathbf{r}_1(u,v)$: $(u,v)\in[0,1]\times[-1,0]$, and $\mathbf{r}_2(u,v)$: $(u,v)\in[0,1]\times[1,2]$.

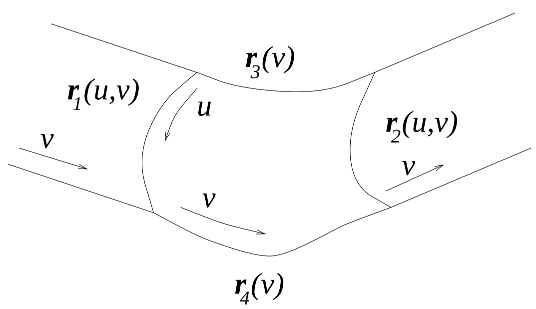

Figure 1: Two surfaces and two curves bordering a gap.

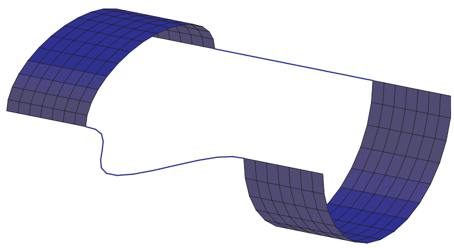

Figure 2: The input surfaces and curves determining a gap.

The blending surface $\mathbf{f}(u,v)$ is generated by a trigonometric convex combination of the surfaces and curves and by an appropriate correction function (Fig. 3).

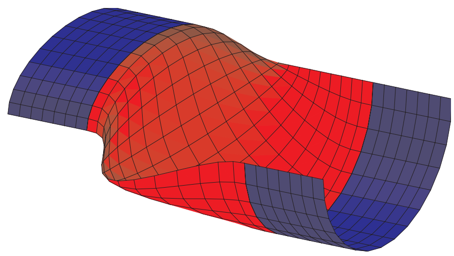

Figure 3: The filled gap shown in Fig. 2.

Theorem 1 *Let two surfaces be given by the differentiable vector functions $\mathbf{r}_1(u,v)$ and $\mathbf{r}_2(u,v)$ over a parameter domain containing the unit square $[0,1]\times[0,1]$ moreover, two curve segments given by the differentiable vector functions $\mathbf{r}_3(v)$ and $\mathbf{r}_4(v)$, $v\in[0,1]$. In the corner points*

$$\mathbf{r}_1(0,0)=\mathbf{r}_3(0), \quad \mathbf{r}_1(1,0)=\mathbf{r}_4(0),$$
$$\mathbf{r}_2(0,1)=\mathbf{r}_3(1), \quad \mathbf{r}_2(1,1)=\mathbf{r}_4(1)$$

are required.
Then the surface defined by the following vector equation

$$\begin{aligned}\mathbf{f}(u,v) &= \cos^2(\frac{\pi}{2}\cdot v)\mathbf{r}_1(u,v)+\sin^2(\frac{\pi}{2}\cdot v)\mathbf{r}_2(u,v)\\ &+ \cos^2(\frac{\pi}{2}\cdot u)\mathbf{r}_3(v)+\sin^2(\frac{\pi}{2}\cdot u)\mathbf{r}_4(v)\\ &- \mathbf{q}(u,v),\end{aligned} \tag{1}$$

$$\begin{aligned}\textit{where}\quad \mathbf{q}(u,v) &= [\cos^2(\frac{\pi}{2}\cdot v)\mathbf{r}_1(0,v)\\ &+ \sin^2(\frac{\pi}{2}\cdot v)\mathbf{r}_2(0,v)]\cos^2(\frac{\pi}{2}\cdot u)\\ &+ [\cos^2(\frac{\pi}{2}\cdot v)\mathbf{r}_1(1,v)\\ &+ \sin^2(\frac{\pi}{2}\cdot v)\mathbf{r}_2(1,v)]\sin^2(\frac{\pi}{2}\cdot u),\\ \textit{and}\quad (u,v) &\in [0,1]\times[0,1],\end{aligned}$$

is differentiable and fits the boundary curves $\mathbf{r}_1(u,0)$, $\mathbf{r}_2(u,1)$, $\mathbf{r}_3(v)$ and $\mathbf{r}_4(v)$.

Proof. The border lines of the patch $\mathbf{f}(u,v)$ are to be checked by substituting $u=0$, $u=1$, $v=0$, and $v=1$ into the equation (1) in turn. The computation results with $\mathbf{f}(0,v)=\mathbf{r}_3(v)$, $\mathbf{f}(1,v)=\mathbf{r}_4(v)$, $\mathbf{f}(u,0)=\mathbf{r}_1(u,0)$, $\mathbf{f}(u,1)=\mathbf{r}_2(u,1)$, $u\in[0,1]$, $v\in[0,1]$ as stated in the Theorem. $\diamond$

Theorem 2 *The surface defined in (1) joins to the given surface $\mathbf{r}_1(u,v)$ with first order (C^1) continuity along the boundary line $\mathbf{r}_1(u,0)$, $u\in[0,1]$, when the curves $\mathbf{r}_3(v)$ and $\mathbf{r}_4(v)$ join with C^1 continuity to the border lines $u=0$ and $u=1$ of the surface $\mathbf{r}_1(u,v)$, respectively.*

Proof. According to the conditions $\mathbf{r}_{1,v}(0,0)=\mathbf{r}_{3,v}(0)$ and $\mathbf{r}_{1,v}(1,0)=\mathbf{r}_{4,v}(0)$, where the subscript v denotes the differentiation with respect to v. According to Theorem 1 $\mathbf{f}(u,0)=\mathbf{r}_1(u,0)$, therefore the partial derivatives $\mathbf{f}_u(u,0)$ and $\mathbf{r}_{1,u}(u,0)$ are equal along the common boundary curve $v=0$, $u\in[0,1]$. The tangent vector of a v parameter line of the surface $\mathbf{f}(u,v)$ at a point of this curve is

$$\begin{aligned}\mathbf{f}_v(u,0) &= \mathbf{r}_{1,v}(u,0)+\cos^2(\frac{\pi}{2}\cdot u)(\mathbf{r}_{3,v}(0)-\mathbf{r}_{1,v}(0,0))\\ &+ \sin^2(\frac{\pi}{2}\cdot u)(\mathbf{r}_{4,v}(0)-\mathbf{r}_{1,v}(1,0)).\end{aligned}$$

By assumption, the second and third terms are zero vectors, consequently $\mathbf{f}_v(u,0)=\mathbf{r}_{1,v}(u,0)$ at the points of the connection line. This means C^1 continuity between $\mathbf{f}(u,v)$ and $\mathbf{r}_1(u,v)$ at the points $v=0$, $u\in[0,1]$. Therefore, the tangent planes of the two surfaces along the connection line are obviously the same. $\diamond$

Remark 1. The analogous statement about the C^1 connection of the blending surface $\mathbf{f}(u,v)$ defined in (1) and $\mathbf{r}_2(u,v)$ along the connection line $v=1$ yields if $\mathbf{r}_3(v)$ and $\mathbf{r}_4(v)$ join with C^1 continuity to the border lines $u=0$ and $u=1$ of $\mathbf{r}_2(u,v)$, respectively. The proof is similar to that of Theorem 2.

Remark 2. In the case if $\mathbf{r}_1(u,v)$ (and analogously $\mathbf{r}_2(u,v)$) is a cylindrical surface, G^1 continuous connection between $\mathbf{r}_1(u,v)$ (or $\mathbf{r}_2(u,v)$) and $\mathbf{f}(u,v)$ can be assured under weaker conditions, namely, when $\mathbf{r}_{3,v}(0)$ is parallel to $\mathbf{r}_{1,v}(0,0)$ and $\mathbf{r}_{4,v}(0)$ is parallel to $\mathbf{r}_{1,v}(1,0)$ (G^1 condition instead of C^1). As the derivatives with respect to v of the cylindrical surface $\mathbf{r}_1(u,v)$ (see Fig. 4) are all parallel, the terms in the expression of $\mathbf{f}_v(u,0)$ are parallel to $\mathbf{r}_{1,v}(u,0)$, which ensures the parallelity of the normals $\mathbf{f}_u(u,0)\times\mathbf{f}_v(u,0)$ and $\mathbf{r}_{1,u}(u,0)\times\mathbf{r}_{1,v}(u,0)$.
The tangent plane continuity is equivalent to the G^1 continuity. In this case the joining surface patches admit a local reparametrisation in which the joining surfaces are C^1 (Boehm, 1988 and Gregory, 1989).

The conditions in Remark 2 allow flexible constructions of blending surfaces between cylindrical surfaces. In the next example the upper and lower curves connect the border lines of the two cylindrical surfaces with G^1 continuity. The convex combination surface generated in the rational parametric form of the trigonometric blendig functions (see in Section 4.) fits the prescribed boundary curves and joins with tangential continuity (G^1) to the two cylindrical surfaces (Fig. 4.). Similar modelling problems occur e.g. in planning canals over a landscape by joining cylindrical or toroidal surfaces while also matching prescribed bordering curves.

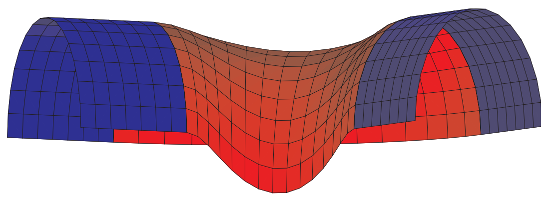

Figure 4: G^1 continuous input data result G^1 connection.

Theorem 3 *If the boundary curves $\mathbf{r}_3(v)$ and $\mathbf{r}_4(v)$ join C^2 continuously to the boundary lines $u=0$ and $u=1$ of the surfaces $\mathbf{r}_1(u,v)$ and $\mathbf{r}_2(u,v)$ at the corner points, then adding the correction function*

$$\begin{aligned}\mathbf{m}(u,v) &= s(v)\cdot[\mathbf{r}_1(u,v)-\mathbf{r}_2(u,v)\\ &- \cos^2(\frac{\pi}{2}\cdot u)(\mathbf{r}_1(0,v)-\mathbf{r}_2(0,v))\\ &- \sin^2(\frac{\pi}{2}\cdot u)(\mathbf{r}_1(1,v)-\mathbf{r}_2(1,v))]\end{aligned}$$

to the expression of $\mathbf{f}(u,v)$ in (1), where

$$s(v)=\frac{1}{16}(-2v+1)^3\sin^2(\pi(2v+1))$$

results C^2 connection of $\mathbf{f}(u,v)$ with $\mathbf{r}_1(u,v)$ and $\mathbf{r}_2(u,v)$.

Proof. The requirements of Theorem 2 are obviously fullfilled for both surfaces $\mathbf{r}_1(u,v)$ and $\mathbf{r}_2(u,v)$. As the values of $s(v)$ and $s'(v)$ at $v=0$ and $v=1$ are zero, the new term $\mathbf{m}(u,v)$ in (1) does not influence the C^0 and C^1 continuities. The second derivatives are $s_{vv}(0)=1$ and $s_{vv}(1)=-1$ therefore, the differences $\mathbf{f}_{vv}(u,0)-\mathbf{r}_{1,vv}(u,0)$ and $\mathbf{f}_{vv}(u,1)-\mathbf{r}_{2,vv}(u,1)$ become zero. $\diamond$

C^2 continuous filling of a gap is shown in Fig. 5. This example shows also the shape influence of the underlying surfaces, where the surface $\mathbf{r}_1(u,v)$ has periodic bulges and $\mathbf{r}_2(u,v)$ is planar. The resulting surface is the combination of such a bulge and a planar rectangle and two bordering straight line segments.

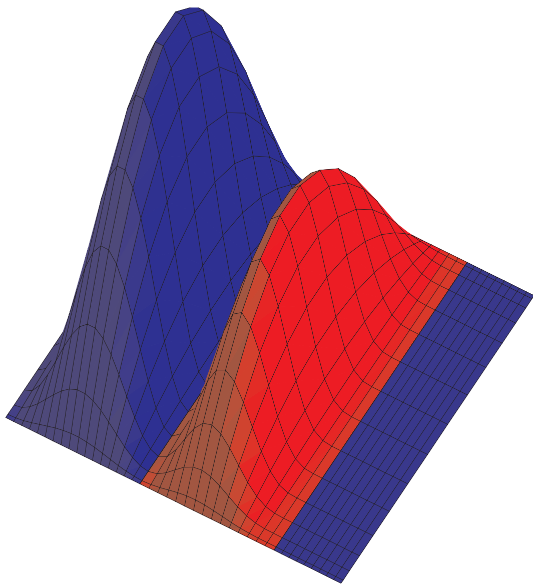

Figure 5: Shape influence of the constituents, C^2 connection.

Several experiments have shown that monoton polynomial parameter transformations of the underlying surfaces in v direction have no noticeable influence on the shape of the resulting surface.

3 Combination of three surfaces

The two parameter representation of the sphere has inspired the following trigonometric convex combination of three surfaces defined over the unit square $(u,v) \in [01,] \times [0,1]$.

Theorem 4 *If three surfaces represented by the differentiable vector functions $\mathbf{r}_1(u,v)$, $\mathbf{r}_2(u,v)$ and $\mathbf{r}_3(u,v)$ over the unit square $(u,v) \in [0,1] \times [0,1]$ have common corner points at $(u,v) = (1,0)$ and $(u,v) = (1,1)$, then the surface described by the vector function*

$$\begin{aligned} \mathbf{f}(u,v) &= \cos^2(\frac{\pi}{2}\cdot u)\cos^2(\frac{\pi}{2}\cdot v)\mathbf{r}_1(u,v) \\ &+ \cos^2(\frac{\pi}{2}\cdot u)\sin^2(\frac{\pi}{2}\cdot v)\mathbf{r}_2(u,v) \\ &+ \sin^2(\frac{\pi}{2}\cdot u)\mathbf{r}_3(u,v) - \mathbf{q}(u,v), \qquad (2) \end{aligned}$$

where

$$\begin{aligned} \mathbf{q}(u,v) &= \sin^2(\frac{\pi}{2}\cdot u)\cos^2(\frac{\pi}{2}\cdot v)[\mathbf{r}_3(u,0) - \mathbf{r}_1(u,0)] \\ &+ \sin^2(\frac{\pi}{2}\cdot u)\sin^2(\frac{\pi}{2}\cdot v)[\mathbf{r}_3(u,1) - \mathbf{r}_2(u,1)] \\ \text{and} \quad & (u,v) \in [0,1] \times [0,1] \end{aligned}$$

is differentiable and fits the boundary curves $\mathbf{r}_1(u,0)$, $\mathbf{r}_2(u,1)$ and $\mathbf{r}_3(1,v)$.

Proof. The boundary lines of the blending surface $\mathbf{f}(u,v)$ are to be computed by substituting the parameter values according to the bordering lines of the unit square in the u,v parameter plane in turn.

$$\begin{aligned} \mathbf{f}(1,v) &= \mathbf{r}_3(1,v) - \cos^2(\frac{\pi}{2}\cdot v)[\mathbf{r}_3(1,0) - \mathbf{r}_1(1,0)] \\ &- \sin^2(\frac{\pi}{2}\cdot v)[\mathbf{r}_3(1,1) - \mathbf{r}_2(1,1)] = \mathbf{r}_3(1,v), \\ \mathbf{f}(u,0) &= \cos^2(\frac{\pi}{2}\cdot u)\mathbf{r}_1(u,0) + \sin^2(\frac{\pi}{2}\cdot u)\mathbf{r}_3(u,0) \\ &- \sin^2(\frac{\pi}{2}\cdot u)[\mathbf{r}_3(u,0) - \mathbf{r}_1(u,0)] = \mathbf{r}_1(u,0), \\ \mathbf{f}(u,1) &= \cos^2(\frac{\pi}{2}\cdot u)\mathbf{r}_2(u,1) + \sin^2(\frac{\pi}{2}\cdot u)\mathbf{r}_3(u,1) \\ &- \sin^2(\frac{\pi}{2}\cdot u)[\mathbf{r}_3(u,1) - \mathbf{r}_2(u,1)] = \mathbf{r}_2(u,1), \end{aligned}$$

since the corner points standing in the same brackets are equal. ⋄

In Fig. 6 Three cylindrical surfaces are given obeying the conditions of Theorem 4. The drawn pieces are in turn $\mathbf{r}_1(u,v)$: $(u,v) \in [0,1] \times [-1,0]$, $\mathbf{r}_2(u,v)$: $(u,v) \in [0,1] \times [1,2]$ and $\mathbf{r}_3(u,v)$: $(u,v) \in [1,2] \times [0,1]$. The generated surface patch joins continuously to the three neighbours along their boundary curves.

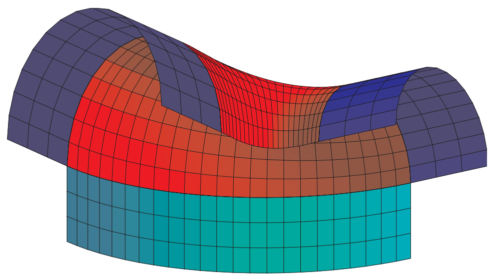

Figure 6: Combination of three surfaces, G^1 connection

The filling of a three-sided hole with a surface joining continuously to the surrounding surfaces is a classical problem, the so called suit case corner problem. The method presented here also gives a solution for this problem in a special case. The restriction in the algorithm is that two of the patches in the convex combination are three-sided degenerate surfaces meeting with their singular points at a corner of the hole. These are e.g. parts of two different rotational surfaces represented as degenerate rectangular patches (this is usually the case in CAD systems), or triangular patches, each joining with G^1 continuity to one bordering surface, then reparametrized. Such a reparametrization of a triangular domain described by the barycentric coordinates $0 \leq u,v,w \leq 1$, $u+v+w = 1$, is given by $u = t - s\cdot t$, $v = s\cdot t$, $0 \leq s,t \leq 1$.

The surface generated by equation (2) fills the three-sided hole. It is a degenerate rectangular patch, where the boundary line $u=0$ is just a point, i.e. one corner point of the triangular hole. Surfaces with singular points (e.g. cones) are also allowed in the construction, therefore nothing can be stated about the tangent plane at the singular point in general.

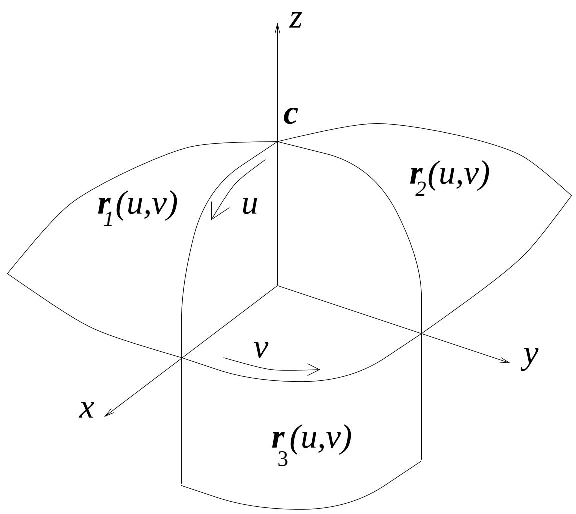

Figure 7: Three-sided hole formed by three surfaces.

In Fig. 7 a sketch of three surfaces is shown.

Theorem 5 *Let three surfaces be given by the differentiable vector functions $\mathbf{r}_1(u,v)$, $\mathbf{r}_2(u,v)$ and $\mathbf{r}_3(u,v)$ over a parameter domain containing the unit square $[0,1]\times[0,1]$ such that $\mathbf{r}_1(0,v)=\mathbf{r}_2(0,v)=\mathbf{c}$, $\mathbf{r}_1(1,0)=\mathbf{r}_3(1,0)$ and $\mathbf{r}_2(1,1)=\mathbf{r}_3(1,1)$ hold. Then the surface described by the vector function (2) is differentiable and fits the boundary curves $\mathbf{r}_1(u,0)$, $\mathbf{r}_2(u,1)$ and $\mathbf{r}_3(1,v)$.*

Proof. The equation of the boundary line $u=0$ is

$$\mathbf{f}(0,v)=\cos^2(\frac{\pi}{2}\cdot v)\cdot\mathbf{r}_1(0,v)+\sin^2(\frac{\pi}{2}\cdot v)\cdot\mathbf{r}_2(0,v).$$

Hence the corner points are

$$\mathbf{f}(0,0)=\mathbf{r}_1(0,0),\quad \mathbf{f}(0,1)=\mathbf{r}_2(0,1).$$

The parameter line $u=0$ collapses into a point only in the case when $\mathbf{r}_1(0,v)$ and $\mathbf{r}_2(0,v)$, $v\in[0,1]$ collapse also into the same point $\mathbf{c}$. The other three boundary curves are as in Theorem 4. $\diamond$

Corollary 1 *If the surfaces surrounding the hole are parts of the same sphere in the same parametrization, then the surface defined in (2) is also lying on this sphere.*

Theorem 6 *If for the given three surfaces the conditions of Theorem 5, moreover the following parallelity conditions*

$$\mathbf{r}_{1,v}(u,0)\,||\,\mathbf{r}_{3,v}(u,0)\quad \mathbf{r}_{2,v}(u,1)\,||\,\mathbf{r}_{3,v}(u,1),$$

and the equalities

$$\mathbf{r}_{1,u}(1,0)=\mathbf{r}_{3,u}(1,0)\quad \mathbf{r}_{2,u}(1,1)=\mathbf{r}_{3,u}(1,1)$$

are satisfied, then the blending surface $\mathbf{f}(u,v)$ given in (2) fills the hole G^1 continuously. (The subscripts u and v denote the differentiation with respect to u and v, respectively.)

Proof. According to Remark 2 the surface normals of the blending surface and the given surfaces are to be computed along the connection lines. The partial derivatives along the connection line $v=0$ are

$$\mathbf{f}_u(u,0)=\mathbf{r}_{1,u}(u,0)$$

and

$$\mathbf{f}_v(u,0)=\cos^2(\frac{\pi}{2}\cdot u)\mathbf{r}_{1,v}(u,0)+\sin^2(\frac{\pi}{2}\cdot u)\mathbf{r}_{3,v}(u,0).$$

Since $\mathbf{r}_{1,v}(u,0)$ and $\mathbf{r}_{3,v}(u,0)$ are by assumption parallel, the surface normals of $\mathbf{f}(u,v)$ and $\mathbf{r}_1(u,v)$ are also parallel along the connection line $0<u\leq 1$. The continuity between $\mathbf{f}(u,v)$ and $\mathbf{r}_2(u,v)$ along the border line $v=1$ of the hole can be checked in a similar way.

The partial derivatives along the connection line $u=1$ due to the conditions on the derivatives are

$$\mathbf{f}_u(1,v)=\mathbf{r}_{3,u}(1,v)$$

and

$$\mathbf{f}_v(1,v)=\mathbf{r}_{3,v}(1,v),$$

which result the G^1 continuity of the two surfaces.

At the singular point $u=0$ two cases can be differentiated. If one of the surfaces $\mathbf{r}_1(u,v)$ and $\mathbf{r}_2(u,v)$ has no tangent plane or they have different tangent planes at the singular point then the resulting surface has no tangent plane at this point either.

If the point $u=0$ of the surfaces $\mathbf{r}_1(u,v)$ and $\mathbf{r}_2(u,v)$ is singular only in the parametrization, then the unit vector of the surface normal at the singular point can be defined as $\lim_{u\to 0}(\mathbf{r}_{1,u}(u,v_0)\times\mathbf{r}_{1,v}(u,v_0))^0$ and $\lim_{u\to 0}(\mathbf{r}_{2,u}(u,v_0)\times\mathbf{r}_{2,v}(u,v_0))^0$, respectively, where $v_0\in[0,1]$ and the 0 in the exponent denotes the normalization of the vectors. This definition of the surface normal at singular points has been applied also by Reif (1995). By assumption, the two surfaces have a common tangent plane at the corner point of the hole, consequently these two vectors are equal to the common surface normal denoted by $\mathbf{n}$. We show that the resulting surface $\mathbf{f}(u,v)$ has the same tangent plane at this point (Fig. 10). Namely,

$$\begin{aligned}\lim_{u\to 0}\mathbf{f}_u(u,v_0) &= \cos^2(\frac{\pi}{2}v_0)\cdot\lim_{u\to 0}\mathbf{r}_{1,u}(u,v_0)\\ &+ \sin^2(\frac{\pi}{2}v_0)\cdot\lim_{u\to 0}\mathbf{r}_{2,u}(u,v_0)\end{aligned}$$

and similarly

$$\begin{aligned}\lim_{u\to 0}\mathbf{f}_v(u,v_0) &= \cos^2(\frac{\pi}{2}v_0)\cdot\lim_{u\to 0}\mathbf{r}_{1,v}(u,v_0)\\ &+ \sin^2(\frac{\pi}{2}v_0)\cdot\lim_{u\to 0}\mathbf{r}_{2,v}(u,v_0), \qquad v_0\in[0,1].\end{aligned}$$

Moving along a $v=v_0$ parameter line into the singular point, the surface normal defined as $\lim_{u\to 0}(\mathbf{f}_u(u,v_0)\times\mathbf{f}_v(u,v_0))^0$ is also parallel to $\mathbf{n}$, because all the vector components in this expression are perpendicular to $\mathbf{n}$. Consequently, the constructed blending surface $\mathbf{f}(u,v)$ has the same tangent plane at $(u,v)=(0,0)$ as the surfaces $\mathbf{r}_1(u,v)$ and $\mathbf{r}_2(u,v)$. $\diamond$

In Fig. 8 the three-sided surfaces are ellipsoids and the third one is a cylindrical surface. The drawn parts are parametrized as follows. $\mathbf{r}_1(u,v)$: $(u,v)\in[0,1]\times[-1,0]$; $\mathbf{r}_2(u,v)$: $(u,v)\in[0,1]\times[1,2]$; $\mathbf{r}_3(u,v)$: $(u,v)\in[1,3]\times[0,1]$.

The example in Fig. 10. illustrates the G^1 continuous filling of the three-sided hole shown in Fig. 8. Fig. 9 shows the surface patches used in equation (2).

Similar modelling problems occur e.g. in planning a roof by joining a conic and a planar part smoothly around a corner, while also matching a third surface (a part of a wall or eaves).

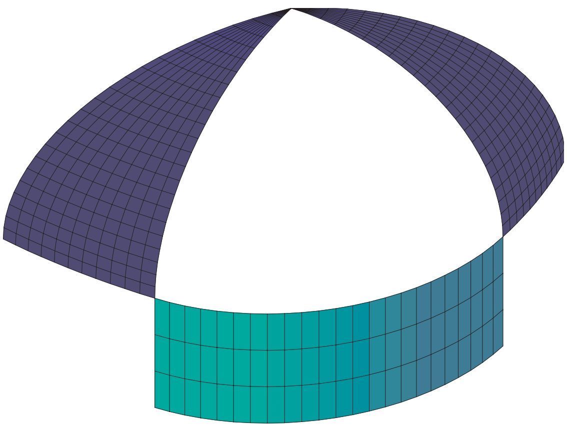

Figure 8: Two ellipsoids and a cylinder around the hole.

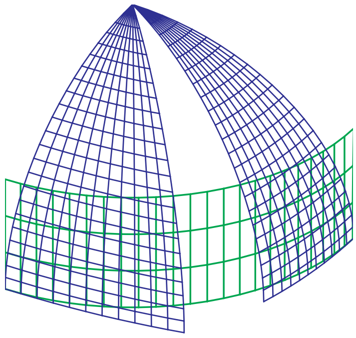

Figure 9: The combined surface pieces.

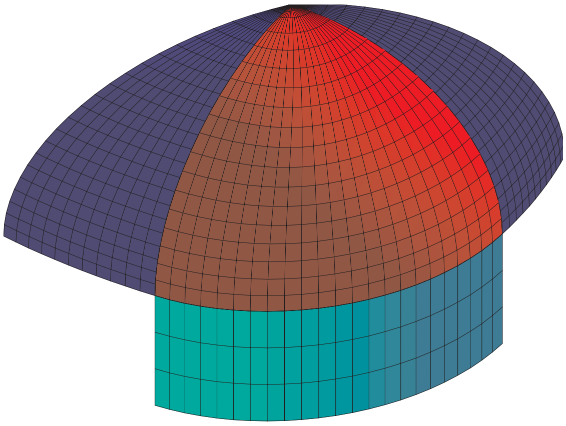

Figure 10:Filling the hole shown in Fig. 8.

4 Rational parametrization of the trigonometrical blending functions

In the algorithms shown in Sections 2 and 3 there are no restrictions on the type of the parametric vector functions describing the surfaces bordering the gap or the hole. However, the implementations in the praxis usually work with polynomial or rational spline functions. Consequently, when the curves and surfaces are described by rational functions, the blending functions in the convex combination should be also given in polynomial or rational form. Based on the rational parametrization of the circle and fundamental identities the trigonometric blending functions in (1) and (2) can be replaced as follows. Choosing the function

$$\mu(t)=\frac{4t^2}{(1+t^2)^2}, \qquad 0\le t\le 1,$$

the substitutions

$$\sin^2(\frac{\pi}{2}\cdot t)=\mu(t) \quad\text{and}\quad \cos^2(\frac{\pi}{2}\cdot t)=1-\mu(t) \tag{3}$$

(t is standing instead of u or v) lead to an equivalent definition of the surface in (1) or in (2). The Theorems and the Remarks above yield further on, since the functions in (3) behave equally at $t = 0$ and $t = 1$. Of course, the parametrization of the resulting surface will be different. The higher numerical stability of the rational blending functions in the neighbourhood of the singular point yields smoother surfaces than the trigonometric functions. However, the investigation of the boundary values of the functions and their derivatives is more transparent in the trigonometric form.

The surfaces shown in Figs. 4, 6 and 10 are generated in this rational form. Similarly, the rational form is used in the next example of a three-sided hole. The surface on the right-hand side is a planar triangle (Fig. 11.), on the left-hand side an ellipsoide and the lower one is a cylindrical surface with a quintic Bézier generator curve. The blending surface filling the hole joins with G^1 continuity to the three given surfaces.

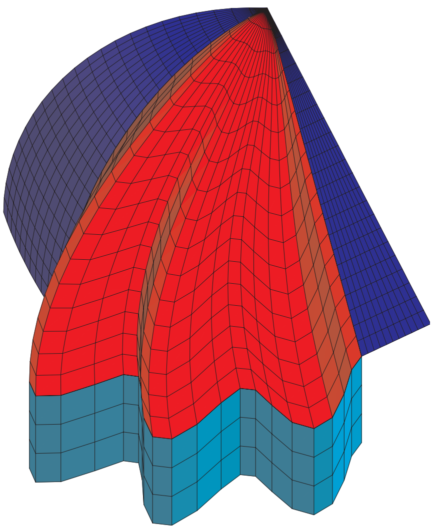

Figure 11: Filling the hole formed by an ellipsoid, a planar triangle and a cylindrical surface by rational blending.

5 Conclusions

The given methods for generating surfaces filling a gap between two surfaces or a three-sided hole are based on convex combinations of the surfaces surrounding the gap or the hole, respectively. This concept is a new approach of Coons's blending methods. The resulting surfaces fit the given surfaces along the connection curves with C^0, C^1, G^1 or C^2 continuity depending on the geometric inputs and correction functions. Both surface constructions are of importance in the practice, when traditional methods (subdivision algorithms in the first case or construction of control points in the second case) do not work. As CAD-systems frequently use degenerate rectangular patches which cannot be handle by methods developed for triangular surfaces, our method for C^1 or G^1 filling of a three sided hole is useful in such applications.

The assumptions in the Theorems allow parameter transformations on the constituents of the convex combination. Our experiments have shown that some parameter transformations do not influence the shape of the resulting surface. This shape influence of different parametrizations and weaker continuity conditions could be the subject of further investigations.

The computations and the drawings have been made by the symbolical algebraic program package Maple V R5.

Aknowledgements

The authors thank to Prof. Gunter Weiß for his valuable suggestions concerning rational parametrization of trigonometric blending functions.

References

Alfeld, P. and Barnhill, R.E. (1984), A transfinite C^2 interpolant over triangles, Rocky Mountain Journal of Mathematics 14, 17-39.

Bär, G. (1977) Parametrische Interpolation empirischer Raumkurven. ZAMM 57, 305-314

Boehm, W. (1988) Visual continuity. Computer-aided Design 20, 307-311

Farin, G. (1990) Curves and Surfaces for Computer Aided Geometric Design, A Practical Guide. Academic Press, Inc., San Diego

Filip, D. J. (1989) Blending Parametric Surfaces. ACM Transactions on Graphics, 8, 164-173

Gregory, J.A. (1985) Interpolation to boundary data on the simplex. Computer Aided Geometric Design 2, 43-52

Gregory, J.A. (1989) Geometric continuity. In: T. Lyche and L. Schumaker eds. (1989) Mathematical methods in CAGD. Academc Press, New York, pp. 353-371

Hartmann, E. (2001) Parametric G^n blending of curves and surfaces. Visual Computer, 17, 1-13

Hoschek, J. and Lasser, D. (1992) Grundlagen der geometrischen Datenverarbeitung. 2. Aufl., B.G. Teubner, Stuttgart

Little, F.F. (1983) Convex Combination Surfaces In: R.F. Barnhill and W. Boehm eds. (1983) Surfaces in CAGD. North-Holland Publishing Company, pp. 99-107

Reif, U. (1995) A unified approach to subdivision algorithms near extraordinary vertices. Computer Aided Geometric Design 12, 153-174

Schichtel, M. (1993) G^2 Blend Surfaces and Filling of N-Sided Holes. IEEE Computer Graphics & Applications 13, 68-73

Szilvási-Nagy, M. and P.Vendel, T. (2000) Generating curves and swept surfaces by blended circles. Computer Aided Geometric Design 17, 197-206

Szilvási-Nagy, M. (2000) Konstruktion von Verbindungsflächen mittels trigonometrischer Bindefunktionen. 25. Süddeutsches Differentialgeometrie-Kolloquium den 2.6.2000, Institut für Geometrie Technische Universität Wien (to appear)

Márta Szilvási-Nagy
Dept. of Geometry
Budapest University of Technology and Economics
H-1521 Budapest, Hungary
e-mail: szilvasi@math.bme.hu

Teréz P. Vendel
Dept. of Mathematics,
University of Pécs
Boszorkány u. 2, H-7624 Pécs, Hungary
vendel@witch.pmmf.hu

Hellmuth Stachel
Inst. of Geometry
Vienna University of Technology
Wiedner Hauptstrasse 8-10, A-1040 Wien, Austria
e-mail: stachel@geometrie.tuwien.ac.at

Stručni rad
Prihvaćeno 18.02.2002.

MILJENKO LAPAINE

Krivulja središta i krivulja fokusa u pramenu konika zadanom pomoću dviju dvostrukih točaka u izotropnoj ravnini

Krivulja središta i krivulja fokusa u pramenu konika zadanom pomoću dviju dvostrukih točaka u izotropnoj ravnini

SAŽETAK

Razmatraju se pramenovi konika zadani s pomoću dviju dvostrukih točaka. Dokazuje se da se krivulja središta raspada na dva pravca od kojih jedan prolazi dvostrukim temeljnim točkama pramena, a drugi točkom u kojoj se sijeku zajedničke tangente svih konika pramena i polovištem dužine koja spaja temeljne točke. Nadalje, dokazuje se da se krivulja fokusa raspada na pravac i koniku. Taj pravac i konika prolaze dvostrukim temeljnim točkama pramena, a konika još i točkom u kojoj se sijeku zajedničke tangente svih konika pramena.

Ključne riječi: izotropna ravnina, krivulja fokusa, krivulja središta, pramen konika

The Curve of Centres and the Curve of all Isotropic Focal Points in the Conic Section Pencil Given by Two Double Points of an Isotropic Plane

ABSTRACT

Conic section pencils given by two double points are discussed. It is proved that the curve of centres decomposes into two straight lines, one of which is passing through the two double base points, while the other is passing through the intersection of common tanget lines of all conics of the pencil and through the centre of the straight segment joining the base points. Furthermore, it is proved that the curve of all isotropic focal points decomposes into a straight line and a conic. These straight line and conic are passing through the double base points of pencil, and the conic through the intersection of common tangent lines of all conics of the pencil.

Key words: conic section pencil, curve of centres, curve of all isotropic focal points, isotropic plane

MSC 2000: 51N20, 51N15

1 Uvod

Pramen konika određen je općenito s četiri realne i različite točke A, B, C i D koje se nazivaju temeljnim točkama pramena. Pramen konika tipa VI (Ščurić 1996) karakteriziran je svojstvom da se temeljne točke A i B podudaraju i da se temeljne točke C i D podudaraju. Kažemo da je pramen određen s dvije dvostruke točke. U tim točkama sve konike pramena imaju zajedničke tangente.

Grafički prikaz pramena konika može se učinkovito ostvariti primjenom računala i plotera. Matematička osnova razvijenog softvera za pramenove konika opisana je u prethodnom radu (Lapaine 1997) i više puta primijenjena (Lapaine i Lapaine 1998; Lapaine 2001).

Pri klasifikaciji pramenova konika mogu se primijeniti krivulja središta m^2 i krivulja fokusa k_f. Te su krivulje primjenjivane pri klasifikaciji pramenova konika tipa IV izotropne ravnine (Ščurić-Čudovan i Sachs 1995, 1997) i pri klasifikaciji pramenova konika tipa VI izotropne ravnine (Ščurić 1996).

Pri određivanju krivulje središta pramenova konika tipa VI može se primijeniti opći pristup određivanja krivulje središta pramena konika bilo kojeg tipa na način opisan u radu (Lapaine i Lapaine 1998). Drugi način određivanja krivulje središta za pramen konika tipa VI opisan je u ovome radu. Koristeći svojstvo da se radi baš o pramenu tipa VI, dokazuje se da se krivulja središta raspada na dva pravca od kojih jedan prolazi temeljnim dvostrukim točkama pramena, a drugi točkom u kojoj se sijeku zajedničke tangente svih konika pramena i polovištem dužine koja spaja temeljne točke.

U radu (Lapaine i Ščurić 1994) pokazuje se da je izotropna krivulja fokusa k_f pramena konika općenito krivulja trećeg reda, te se izvode i diskutiraju jednadžbe takvih krivulja u parametarskom obliku za 3 slučaja koji obuhvaćaju sve one tipove tih krivulja koji se pojavljuju pri klasifikaciji pramenova konika tipa IV. U ovome se radu dokazuje da se za pramenove tipa VI krivulja fokusa raspada na pravac i koniku. Taj pravac i konika prolaze temeljnim dvostrukim točkama pramena, a konika još i točkom u kojoj se sijeku zajedničke tangente svih konika pramena.

2 Konike

Najopćenitija jednadžba drugog stupnja od dvije varijable x i y može se napisati u obliku

$$F(x,y) = ax^2+2bxy+cy^2+2dx+2ey+f=0, \tag{1}$$

gdje su a,b,c,d,e i f realni brojevi, i barem jedan od brojeva a,b i c različit od nule. Skup nul-točaka polinoma $F=F(x,y)$ zove se krivuljom 2. reda, konusnim presjekom, konikom ili čunjosječnicom.

Pretpostavimo da je bar jedan od brojeva a,b,c različit od nule. Pomoću rotacije ravnine oko ishodišta i translacije ravnine moguće je svaku koniku prikazati u standardnom ili kanonskom obliku (vidi npr. Lapaine i Jovičić 1996).

3 Pramen konika

Neka su

$$F(x,y) = a_1x^2+2b_1xy+c_1y^2+2d_1x+2e_1y+f_1=0, \tag{2}$$

$$G(x,y) = a_2x^2+2b_2xy+c_2y^2+2d_2x+2e_2y+f_2=0, \tag{3}$$

jednadžbe dviju konika. Za proizvoljni $\mu\in\mathbf{R}$, sastavimo polinom

$$H(x,y) = F(x,y)+\mu G(x,y). \tag{4}$$

Polinom $H=H(x,y)$ je oblika

$$H(x,y) = ax^2+2bxy+cy^2+2dx+2ey+f, \tag{5}$$

gdje smo označili

$$a=a_1+\mu a_2,\, b=b_1+\mu b_2,\, \ldots,\, f=f_1+\mu f_2. \tag{6}$$

Za svaki pojedini $\mu\in\mathbf{R}$, izraz

$$H(x,y) = F(x,y)+\mu G(x,y)=0 \tag{7}$$

je jednadžba konike u smislu definicije iz prethodnog poglavlja, ako je barem jedan od brojeva a, b i c različit od nule. Za zadane realne brojeve $a_1,b_1,\ldots,f_1,a_2,b_2,\ldots,f_2$, i $\mu\in\mathbf{R}$ skup svih konika obuhvaćenih jednadžbom (7) zove se pramenom konika. Konike pomoću kojih je pramen definiran i kojima odgovaraju jednadžbe $F(x,y)=0$ i $G(x,y)=0$ zovu se osnovnim konikama pramena.

4 Krivulja središta pramena konika

Neka je

$$H(x,y) = F(x,y)+\mu G(x,y)=0 \tag{8}$$

jednadžba pramena konika, gdje su osnovne konike pramena određene jednadžbama

$$F(x,y) = a_1x^2+2b_1xy+c_1y^2+2d_1x+2e_1y+f_1=0, \tag{9}$$

$$G(x,y) = a_2x^2+2b_2xy+c_2y^2+2d_2x+2e_2y+f_2=0. \tag{10}$$

Tada je $H=H(x,y)$ polinom oblika

$$H(x,y) = ax^2+2bxy+cy^2+2dx+2ey+f, \tag{11}$$

gdje smo označili

$$a=a_1+\mu a_2,\, b=b_1+\mu b_2,\, \ldots,\, f=f_1+\mu f_2. \tag{12}$$

Reći ćemo da je skup nul-točaka polinoma $H=H(x,y)$ centralno simetričan u odnosu na točku $S(x_S,y_S)$, ako postoji uređeni par realnih brojeva (x_S,y_S) takav da za svaki uređeni par realnih brojeva (x,y) sa svojstvom $H(x,y)=0$ vrijedi

$$H(2x_S-x,\, 2y_S-y)=0. \tag{13}$$

Zahtjev (13) može se napisati u obliku

$$\begin{aligned} &H(x,y)+4(ax_S^2+2bx_Sy_S+cy_S^2+dx_S+ey_S)\\ &-4x(ax_S+by_S+d)-4y(bx_S+cy_S+e)=0. \end{aligned} \tag{14}$$

Kako je po pretpostavci $H(x,y)=0$, to vidimo da mora biti

$$ax_S^2+2bx_Sy_S+cy_S^2+dx_S+ey_S=0 \tag{15}$$

$$ax_S+by_S+d=0 \tag{16}$$

$$bx_S+cy_S+e=0. \tag{17}$$

Nadalje,

$$\begin{aligned} &ax_S^2+2bx_Sy_S+cy_S^2+dx_S+ey_S\\ &=(ax_S+by_S+d)x_S+(bx_S+cy_S+e)y_S, \end{aligned} \tag{18}$$

što znači da je (15) posljedica relacija (16) i (17). Dakle, koordinate točke S moraju zadovoljavati sustav linearnih jednadžbi

$$\begin{aligned} ax_S+by_S+d&=0\\ bx_S+cy_S+e&=0. \end{aligned} \tag{19}$$

Za pojedini čvrsti μ, rješenje tog sustava postoji ili ne postoji, a ako postoji može biti jedinstveno ili jednoparametarsko. Ako za zadani μ postoji uređeni par realnih brojeva (x_S, y_S) koji je rješenje sustava (19), tada se točka $S(x_S, y_S)$ zove centrom ili središtem konike $H(x,y)=0$. Ako postoji, to središte može, ali ne mora biti jedinstveno.

Eliminiramo li parametar μ iz (19), dobijemo

$$\begin{aligned}&(a_1x_S+b_1y_S+d_1)(b_2x_S+c_2y_S+e_2)\\&=(b_1x_S+c_1y_S+e_1)(a_2x_S+b_2y_S+d_2),\end{aligned} \tag{20}$$

odnosno nakon sređivanja

$$a_Sx_S^2+2b_Sx_Sy_S+c_Sy_S^2+2d_Sx_S+2e_Sy_S+f_S=0, \tag{21}$$

gdje smo označili

$$\begin{aligned}a_S&=a_1b_2-b_1a_2\\2b_S&=a_1c_2-c_1a_2\\c_S&=b_1c_2-c_1b_2\\2d_S&=a_1e_2-b_1d_2+d_1b_2-e_1a_2\\2e_S&=b_1e_2-c_1d_2+d_1c_2-e_1b_2\\f_S&=d_1e_2-e_1d_2.\end{aligned} \tag{22}$$

Na temelju zapisa (21) možemo zaključiti da je skup svih središta pramena konika opet jedna konika, ako je bar jedan od koeficijenata a_S, b_S, c_S različit od nule.

Skup svih središta proizvoljnog pramena konika ne može biti imaginarna konika (imaginarna elipsa ili par imaginarnih pravaca). Naime, ako središte neke krivulje iz pramena postoji, njegove koordinate su rješenje sustava linearnih jednadžbi (19), dakle realni brojevi, jer su takvi svi koeficijenti sustava (19).

5 Krivulja središta pramena konika tipa VI

Ako su zadane četiri točke $P_i(x_i, y_i)$, $i=1,2,3,4$ u ravnini, od kojih ni koje tri nisu kolinearne, te ako je

$$g_{ik}=a_{ik}x+b_{ik}y+c_{ik}=0, \quad i\neq k, \tag{23}$$

jednadžba pravca P_iP_k, tada je jednadžbom

$$g_{12}g_{34}+\mu g_{13}g_{24}=0 \tag{24}$$

predočen pramen konika kojem su točke P_i temeljne (tj. sve konike pramena prolaze točkama P_i) (Cesarec 1957).

Neka su sada zadane dvije točke A i C i neka je t_1 bilo koji pravac koji prolazi točkom A, ali ne sadrži točku C i neka je t_2 bilo koji pravac koji prolazi točkom C, a ne prolazi točkom A. Označimo s g pravac kroz točke A i C. Ako su

$$t_1=0, \quad t_2=0 \quad \text{i} \quad g=0 \tag{25}$$

jednadžbe navedenih pravaca, tada je

$$g^2+\mu t_1t_2=0 \tag{26}$$

jednadžba pramena konika kojem su A i C temeljne točke, a t_1 i t_2 zajedničke tangente svih konika pramena. Pravac t_1 zajednička je tangenta svih konika pramena jer sa svakom konikom ima samo jednu zajedničku točku. Ta zajednička točka A zove se dvostrukom temeljnom točkom pramena. Pravac t_2 također je zajednička tangenta svih konika pramena i točka C dvostruka temeljna točka pramena.

Neka su s pomoću homogenih koordinata zadane točke

$$A=(x_{0A}, x_{1A}, x_{2A}) \quad \text{i} \quad C=(x_{0C}, x_{1C}, x_{2C}). \tag{27}$$

Lako se može vidjeti da se jednadžba pravca g koji prolazi točkama A i C može napisati u obliku

$$g_xx+g_yy+g_z=0, \tag{28}$$

gdje smo označili

$$g_x=\begin{vmatrix}x_{2C}&x_{2A}\\x_{0C}&x_{0A}\end{vmatrix}, \qquad g_y=-\begin{vmatrix}x_{1C}&x_{1A}\\x_{0C}&x_{0A}\end{vmatrix},$$
$$g_z=\begin{vmatrix}x_{1C}&x_{1A}\\x_{2C}&x_{2A}\end{vmatrix}. \tag{29}$$

Pravac t_1 prolazi točkom A, a njegov smjer neka određuje jedna pomoćna točka T_1 s homogenim koordinatama

$$T_1=(x_{0T_1}, x_{1T_1}, x_{2T_1}). \tag{30}$$

Jednadžba pravca t_1 koji prolazi točkama A i T_1 glasi tada

$$t_{1x}x+t_{1y}y+t_{1z}=0, \tag{31}$$

gdje smo označili

$$t_{1x}=\begin{vmatrix}x_{2T_1}&x_{2A}\\x_{0T_1}&x_{0A}\end{vmatrix}, \qquad t_{1y}=-\begin{vmatrix}x_{1T_1}&x_{1A}\\x_{0T_1}&x_{0A}\end{vmatrix},$$
$$t_{1z}=\begin{vmatrix}x_{1T_1}&x_{1A}\\x_{2T_1}&x_{2A}\end{vmatrix}. \tag{32}$$

Pravac t_2 prolazi točkom C, a njegov smjer neka određuje jedna pomoćna točka T_2 s homogenim koordinatama

$$T_2=(x_{0T_2}, x_{1T_2}, x_{2T_2}). \tag{33}$$

Jednadžba pravca t_2 koji prolazi točkama C i T_2 glasi tada

$$t_{2x}x+t_{2y}y+t_{2z}=0, \tag{34}$$

gdje smo označili

$$t_{2x} = \begin{vmatrix} x_{2T_2} & x_{2C} \\ x_{0T_2} & x_{0C} \end{vmatrix}, \qquad t_{2y} = -\begin{vmatrix} x_{1T_2} & x_{1C} \\ x_{0T_2} & x_{0C} \end{vmatrix}, \tag{35}$$

$$t_{2z} = \begin{vmatrix} x_{1T_2} & x_{1C} \\ x_{2T_2} & x_{2C} \end{vmatrix}.$$

S pomoću relacija (28)-(29) lako se može izvesti da je g^2 oblika

$$g^2 = F(x,y) = a_1x^2 + 2b_1xy + c_1y^2 + 2d_1x + 2e_1y + f_1 \tag{36}$$

uz oznake

$$\begin{array}{lll} a_1 = g_x^2 & b_1 = g_xg_y & c_1 = g_y^2 \\ d_1 = g_xg_z & e_1 = g_yg_z & f_1 = g_z^2. \end{array} \tag{37}$$

Sasvim analogno t_1t_2 je oblika

$$\begin{aligned} t_1t_2 &= G(x,y) \\ &= a_2x^2 + 2b_2xy + c_2y^2 + 2d_2x + 2e_2y + f_2 \end{aligned} \tag{38}$$

uz oznake

$$\begin{array}{ll} a_2 = t_{1x}t_{2x} & b_2 = \frac{1}{2}(t_{1x}t_{2y} + t_{1y}t_{2x}) \\ c_2 = t_{1y}t_{2y} & d_2 = \frac{1}{2}(t_{1x}t_{2z} + t_{1z}t_{2x}) \\ e_2 = \frac{1}{2}(t_{1y}t_{2z} + t_{1z}t_{2y}) & f_2 = t_{1z}t_{2z}. \end{array} \tag{39}$$

Ukoliko dvije pomoćne točke T_1 i T_2 padnu zajedno, tada ćemo s $K = T_1 = T_2$ označiti točku koja istrovremeno pripada pravcima t_1 i t_2.

Uvrstimo li u jednadžbu (20) izraze (37) dobit ćemo jednadžbu krivulje središta u obliku

$$\begin{aligned} &(g_xx_S + g_yy_S + g_z)[(g_xb_2 - g_ya_2)x_S \\ &+ (g_xc_2 - g_yb_2)y_S + g_xe_2 - g_yd_2] = 0. \end{aligned} \tag{40}$$

Odatle se odmah vidi da se krivulja središta raspala na pravac g

$$g_xx + g_yy + g_z = 0,$$

i pravac

$$(g_xb_2 - g_ya_2)x + (g_xc_2 - g_yb_2)y + g_xe_2 - g_yd_2 = 0. \tag{41}$$

Pokažimo sada da ovaj posljednji pravac mora prolaziti točkom K. S obzirom da točka K pripada pravcima t_1 i t_2 to njene koordinate zadovoljavaju (31) i (34). Nije teško vidjeti da odgovarajuće linearne kombinacije izraza (31) i (34) daju

$$b_2x + c_2y + e_2 = 0 \quad \text{i} \quad a_2x + b_2y + d_2 = 0. \tag{42}$$

Napišemo li (41) u obliku

$$g_x(b_2x + c_2y + e_2) - g_y(a_2x + b_2y + d_2) = 0, \tag{43}$$

tada je jasno da točka K zadovljava posljednju jednadžbu, što drugim riječima znači da točka K pripada pravcu (41).

Na kraju ćemo još dokazati da pravac (41) prolazi središtem dužine AC, tj. točkom P s koordinatama

$$P\left(\frac{1}{2}(x_A + x_C),\ \frac{1}{2}(y_A + y_C)\right). \tag{44}$$

U tu svrhu dovoljno je uvrstiti koordinate točke P (44) u jednadžbu pravca (41). Međutim, kad se to napravi, ne vidi se baš odmah da je jednadžba zadovoljena. No, ako najprije izrazimo koeficijente a_2, b_2, c_2, d_2 i e_2 prema (39) te iskoristimo činjenice da točka A leži na pravcu t_1 i točka C na pravcu t_2:

$$\begin{aligned} &t_{1x}x_A + t_{1y}y_A + t_{1z} = 0, \\ &t_{2x}x_C + t_{2y}y_C + t_{2z} = 0, \end{aligned} \tag{45}$$

dolazimo do izraza

$$(t_{1y}t_{2x} - t_{1x}t_{2y})[g_x(x_A - x_C) + g_y(y_A - y_C)] = 0 \tag{46}$$

koji je identički jednak nuli zbog toga što točke A i C pripadaju pravcu g:

$$\begin{aligned} &g_xx_A + g_yy_A + g_z = 0, \\ &g_xx_C + g_yy_C + g_z = 0. \end{aligned} \tag{47}$$

6 Krivulja fokusa pramena konika tipa VI

Neka je

$$H = g^2 + \mu t_1t_2 = 0 \tag{48}$$

jednadžba pramena konika tipa VI uz oznake iz prethodnog poglavlja. Izotropna krivulja fokusa pramena konika geometrijsko je mjesto dirališta svih tangenata na pojedine krivulje pramena, uz uvjet da te tangente sadrže i zadanu neizmjerno daleku apsolutnu točku, odnosno da sve tangente imaju jedan te isti smjer. Bez smanjenja općenitosti možemo pretpostaviti da ta neizmjerno daleka apsolutna točka ima homogene koordinate $(0,0,1)$, tj. da se nalazi u smjeru koordinatne osi y. Na taj je način izotropna krivulja fokusa pramena konika određena uvjetom

$$\frac{\partial H}{\partial y} = 0. \tag{49}$$

Na temelju relacija (48) i (49), a uzevši u obzir (28), (31) i (34) može se napisati jednadžba krivulje fokusa u obliku

$$g(2g_yt_1t_2 - t_{1y}gt_2 - t_{2y}gt_1) = 0. \tag{50}$$

Iz posljednje formule slijedi da se za pramenove tipa VI krivulja fokusa raspada na pravac g i koniku. Lako se vidi da pravac g i konika

$$2g_yt_1t_2 - t_{1y}gt_2 - t_{2y}gt_1 = 0 \tag{51}$$

prolaze temeljnim dvostrukim točkama pramena A i C, a konika još i točkom K u kojoj se sijeku zajedničke tangente svih konika pramena.

Jednadžba konike (51) može se transformirati u standardni oblik

$$(g_y a_2 - g_x b_2)x^2 + (g_y b_2 - g_x c_2)xy + (2g_y d_2 - g_x e_2 - g_z b_2)x + (g_y e_2 - g_z c_2)y + (g_y f_2 - g_z e_2) = 0, \tag{52}$$

kojim se možemo poslužiti za njeno grafičko prikazivanje.

7 Primjer

Na temelju formula izvednih u radu (Lapaine 2001) sastavljen je potprogram za računalo koji polazeći od zadanih homogenih koordinata točaka A, C, T_1 i T_2 određuje koeficijente u jednadžbi pripadnog pramena konika. Točke A i C su dvostruke točke, a točke T_1 i T_2 pomoćne točke. Točke A i T_1 definiraju jednu, a točke C i T_2 drugu zajedničku tangentu svih konika pramena. Točke T_1 i T_2 mogu pasti zajedno i tada tu točku označavamo s K.

Nakon što su izračunani koeficijenti u jednadžbi pramena, primjena odgovarajućeg softvera omogućuje grafičko prikazivanje pramena (Lapaine 1997), te pripadne krivulje središta i krivulje fokusa na temelju formula izvednih u ovome radu.

Neka su zadane dvostruke temeljne točke pramena konika $A(1,-1,0)$, $C(1,5,0)$ i pomoćna točka $K(1,0,-1)$.

Račun daje

$g_x = 0, \quad g_y = -6, \quad g_z = 0,$

jednadžba pravca $\quad g \ldots \quad y = 0,$

$t_{1x} = 0, \quad t_{1y} = -1, \quad t_{1z} = -1,$

jednadžba pravca $\quad t_1 \ldots \quad y = -x - 1,$

$t_{2x} = -1, \quad t_{2y} = 5, \quad t_{2z} = 5,$

jednadžba pravca $\quad t_2 \ldots \quad y = \frac{1}{5}x - 1.$

$a_1 = 0, \quad b_1 = 0, \quad c_1 = 36,$

$d_1 = 0 \quad e_1 = 0 \quad f_1 = 0,$

$a_2 = 1, \quad b_2 = -2, \quad c_2 = -5,$

$d_2 = -2 \quad e_2 = -5 \quad f_2 = -5.$

Jednadžba pramena:

$y^2 + \mu(x^2 - 4xy - 5y^2 - 4x - 10y - 5) = 0.$

Krivulja središta:

$m^2 \ldots y(x - 2y - 2) = 0.$

Krivulja fokusa:

$k_f \ldots y(x^2 - 2xy - 4x - 5y - 5) = 0.$

Pramen konika, njegova krivulja središta (crveno) i krivulja fokusa (zeleno) prikazani su na slici 1.

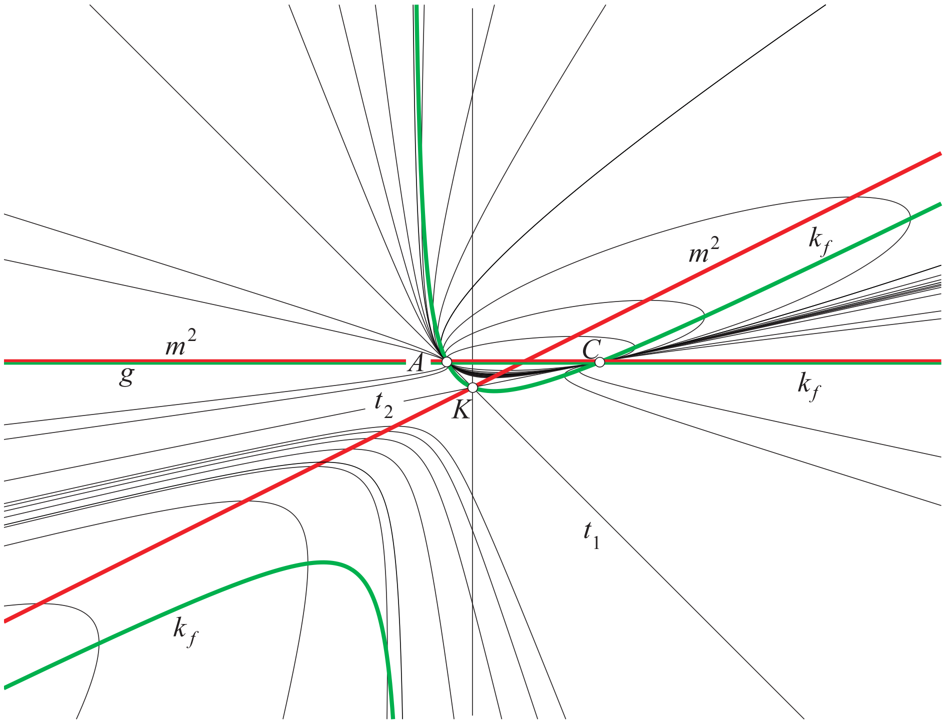

Slika 1. Pramen konika tipa VI

Literatura

CESAREC, R. (1957): Analitička geometrija linearnog i kvadratnog područja, I dio. Školska knjiga, Zagreb.

LAPAINE, M. (1997): Grafički prikaz pramena konika pomoću računala. KoG 2, 43-47.

LAPAINE, M. (1999): Pramen konika zadan pomoću jedne dvostruke i dviju jednostrukih realnih točaka. KoG 4, 27-32.

LAPAINE, M. (2001): Pramen konika zadan pomoću dviju dvostrukih točaka. KoG 5, 25-30.

LAPAINE, M., JOVIČIĆ, D. (1996): Grafički prikazi konika pomoću računala. KoG 1, 19-26.

LAPAINE, Milj., LAPAINE Mir. (1998): Krivulja središta pramena konika. KoG 3, 35-40.

LAPAINE, M., ŠČURIĆ, V. (1994): Curve of all Isotropic Focal Points. 6th International Conference on Engineering Computer Graphics and Descriptive Geometry, Otsuma Women's University, Tokyo, Proceedings, Vol. 2, 338-342.

ŠČURIĆ, V. (1996): Klassifikationstheorie der Kegelschnittbüschel vom Typ VI der Isotropen Ebene. Mathematica Pannonica, 7/1, 47-67.

ŠČURIĆ-ČUDOVAN, V., SACHS, H. (1995): Klassifikationstheorie der Kegelschnittbüschel vom Typ IV der Isotropen Ebene, I. Rad HAZU 470, Matematičke znanosti, sv. 12, 119-137.

ŠČURIĆ-ČUDOVAN, V., SACHS, H. (1997): Klassifikationstheorie der Kegelschnittbüschel vom Typ IV der Isotropen Ebene, II. Rad HAZU 472, Matematičke znanosti, sv. 13, 27-53.

Miljenko Lapaine
Geodetski fakultet Zagreb
10 000 Zagreb, Kačićeva 26
tel.: 45 61 273, faks: 48 28 081
e-mail: mlapaine@geof.hr
http://www.kartografija.hr

Professionelle Arbeit
Angenommen 02. 05. 2002.

VLASTA SZIROVICZA

Die imaginären Elemente bestimmter Kegelschnitte

Krivulja 2. reda zadana imaginarnim elementima

SAŽETAK

U radu je dana konstrukcija nekoliko realnih točaka jedne konike iz pramena konika ako je pramen zadan dvostrukom realnom i parom konjugirano imaginarnih točaka ili parom konjugirano imaginarnih dirališta.

Ključne riječi: imaginarne točke, konika, perspektivna kolineacija

The Conic Given by the Imaginary Elements

ABSTRACT

In this paper the construction of some real points of the conic from the pencil of conics is shown. The pencil of conics is given by a double real point and the pair of imaginary points or by the pair of imaginary touching points.

Key words: conic, imaginary points, perspective collineation

MSC 2000: 51N05

In der Literatur kann man Konstruktionen mit imaginären Elementen nur selten finden. Die folgenden Konstruktionen gehören zu den Themen aus dem Ërdgeschoss der Geometrieünd befassen sich mit den imaginären Grundpunkten eines Kegelschnittbüschels.

Aufgabe 1.

Ein Kegelschnittbüschel ist durch zwei reell zusammenfallende Punkte $F = M$ und ein konjugiert imaginäres Punktepaar D_1 und D_2 an der Geraden q gegeben. Die Punkte D_1 und D_2 sind als Doppelpunkte einer zirkulären Involution mittels Laguerrischen Punkt $Q \notin q$ gegeben (Fig. 1). Die Aufgabe ist ein Paar beliebig reeller Punkte eines Kegelschnittes dieses Büschels zu konstruieren.

Lösungsansatz

Alle Kegelschnitte des Büschels besitzen im Punkt $F = M$ die gemeinsame Tangente f. Mit $F = M$, D_1 und D_2 und einem weiteren Punkt N ist der Kegelschnitt k dieses Büschels eindeutig bestimmt. Dieses Kegelschnittbüschel enthält zwei entartete Kegelschnitte. Eines ist in die Geraden q und f, das andere in konjugiert - imaginäres Geradenpaar FD_1 und FD_2 zerfällt.

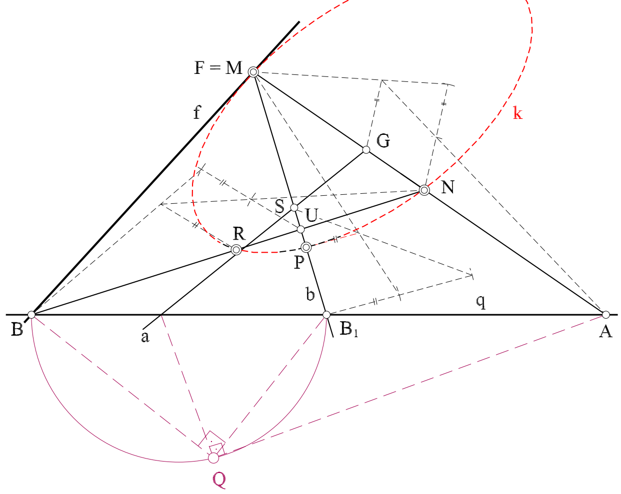

Figur 1.

Stellen wir uns P und p als einen Punkt und seine Polare bezüglich des Kegelschnittes k vor. Die Schnittpunkte einer den Punkt P enthaltenden Geraden t mit k sind mit T_1 und T_2 bezeichnet. Wegen des Polaritätsbegriffes sind diese Punkte in Harmonität mit P und P_1, wobei $P_1 = t \cup p$ entspricht. Es gilt $(T_1 T_2 P P_1) = -1$. Diese Tatsache ermöglicht folgende Konstruktionen.

Konstruktive Lösung

Der Schnittpunkt der Tangente f mit der Geraden q sei mit B bezeichnet. Da jedes Geradenpaar des involutorischen Geradenbüschels sehnkrecht zueinander steht, bekommt man entsprechend dem Punkt B den zugeordneten Punkt $B_1 \in (q)$. Damit wird $b = B_1F$ die Polare des Punktes B bezüglich k.

Nun ist $U = NB \cap b$. Die Gerade NB schneidet den Kegelschnitt k in noch einem Punkt R, wobei $(BUNR) = -1$ gilt. Daraus bekommt man einen zusätzlichen reellen Punkt R des Kegelschnittes k.

Mittels derselben elliptischen Involution an der Geraden q, kann man die Polare a des Punktes $A = FN \cap q$ bekommen, wobei man G mittels der Harmonität $(FNAG) = -1$ konstruiert.

Jetzt wird der Punkt $S = a \cap b$ der Pol der Geraden q in Bezug auf k sein. Er ist der Schnittpunkt von allen Polaren der Punkte von (q). Somit kann man mittels $(B_1SFP) = -1$ den zweiten Schnittpunkt P der Geraden b mit k konstruieren.

Mit diesen fünf reellen Punkten $F = M$, N, R und P von k haben wir die Möglichkeit, weitere Punkte dieses Kegelschnittes mittels Projektivität relativ leicht zu konstruieren [1].

Aufgabe 2.

Es wird ein Kegelschnittberührbüschel mit konjugiert - komplexen Grundpunkten betrachtet [2]. Die Aufgabe ist ein Paar beliebig reeller Punkte eines Kegelschnittes k des Büschels zu konstruieren, wobei k mit einem weiteren Punkt N bestimmt ist.

Lösungsansatz

Sind je zwei der vier Grundpunkte eines Kegelschnittbüschels zusammengefallen, d.h. $A \equiv B$ und $C \equiv D$, es handelt sich um ein Berührbüschel. Alle Kegelschnitte eines solchen Büschels berühren im vorliegenden Fall zwei konjugiert - komplexe Geraden g_1 und g_2 in den an der Geraden q liegenden konjugiert - komplexen Grundpunkten A und C. Diese Punkte sind die Doppelpunkte der elliptischen Involution der konjugierten Punktepaare bezüglich jedes Kegelschnittes des Büschels [1]. Die Punkte A und C in der Fig. 2. kann man als ihre reelle Repräsentanten nennen. Der Zentralpunkt Z der Punktinvolution (q) liegt im Mittelpunkt der Strecke $\overline{AC}$.

Der eigentliche reelle Schnittpunkt Q der imaginären Tangenten g_1 und g_2 ist der gemeinsame Pol der Geraden q bezüglich alle Kegelschnitte des Büschels. An der Geraden ZQ liegt somit ein Durchmesser jedes Kegelschnittes des Büschels.

Mit einem Punkt N ist ein Kegelschnitt k dieses Büschels gegeben. Wir möchten ein paar beliebige Punkte dieses Kegelschnittes, besonders seine Schnittpunkte mit der Polare z des Zentralpunktes Z erreichen. Zu diesem Zweck wird eine perspektive Kollineation gesucht, die den gegebenen Kegelschnitt k in einen Kreis k' abbilden wird. Die Gerade q soll diesen Kreis in derselben elliptischen Involution wie den Kegelschnitt k schneiden, woraus schließt man, dass q die Kollineationsachse ist. An der Geraden ZL wird deutlich ein Durchmesser des gesuchten Kreises liegen (Fig.2).

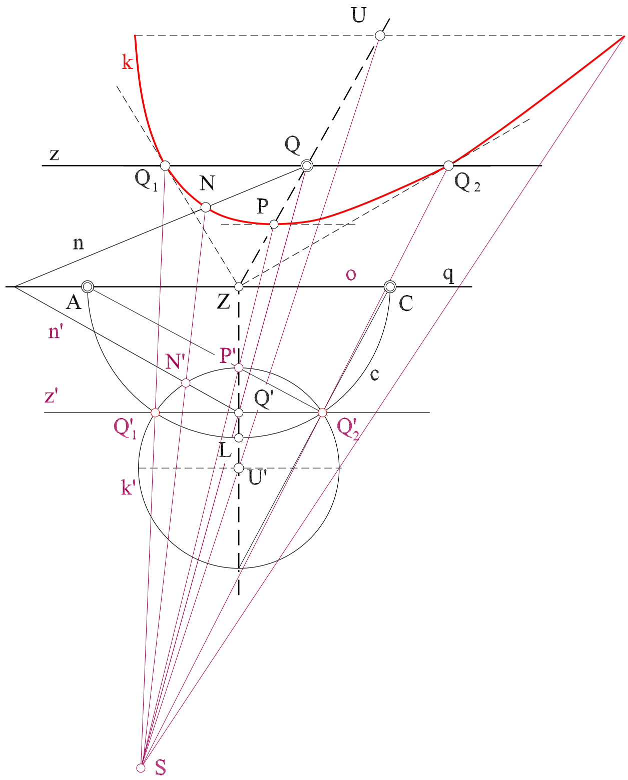

Figur 2.

Konstruktive Lösung

Man kann eine beliebige zu der Kollineationsachse parallele Gerade wählen, die den Kreis c in zwei reelle und verschiedene Punkte schneidet. Diese Gerade z' soll die Polare des Zentralpunktes Z bezüglich des gesuchten Kreises k' sein. Die Schnittpunkte Q'_1 und Q'_2 der Geraden z' mit k' kann man als die Doppelpunkte der hyperbolischen Involution an der Geraden z' bezeichnen [1]. Die Verbindungsgeraden AQ'_2 und CQ'_2 schneiden die Gerade ZL in einem Durchmesser des Kreises k'. Dieser Kreis steht damit ortogonal zum Kreis c. Die Punkte $Q' = z' \cap ZL$ und Q bilden ein zugeordnetes Paar bei der gesuchten perspektiven Kollineation und damit wird ein Kollineationsstrahl bestimmt. Der Geraden $n \equiv QN$ findet man entsprechend die zugeordnete Gerade $n' \equiv Q'N'$, wobei N' am Kreis k' liegt. Der Kollineationsstrahl NN' schneidet QQ' im Zentrum S der perspektiven Kollineation. Entsprechend bekommt man die Schnittpunkte Q_1 und Q_2 der Geraden z mit dem Kegelschnitt k, wie auch alle anderen beliebigen Punkte von k.

Unter der Voraussetzung des fixen Punktes N hängt diese Konstruktion nicht von der Wahl der Geraden z' ab. Für jede Gerade z' wird ein Kreis k' bestimmt, der sich mittels einer perspektiven Kollineation im selben Kegelschnitt des Büschels abbilden lässt.

Für jede Wahl des Punktes N bei fixem Kreis k' bekommt man nach obiger Konstruktion das Zentrum einer anderen Kollineation (S_i, q, Q, Q'_i) und damit einen anderen Kegelschnitt des Berührbüschels.

Literatur

[1] Niče, V., *Uvod u sintetičku geometriju*, Školska knjiga, Zagreb, 1956

[2] Szirovicza, V., *Berührbüschel von Kegelschnitten der isotropen Ebene mit konjugiert-komplexen Grundpunkten*, RAD HAZU **470** (1995), 13-34.

Vlasta Szirovicza
Universität Zagreb
Fakultät für Bauwesen
e-mail: szvlasta@juraj.gradnz.grad.hr

Professional paper
Accepted 20.05.2002

Kamil Maleček
Dagmar Szarková

A Method for Creating Ruled Surfaces and its Modifications

Metoda stvaranja pravčastih ploha i njihovih modifikacija

SAŽETAK

U članku je dana netradicionalna metoda za definiranje pravčastih ploha. Ta metoda omogućuje jednostavnu konstrukciju izvodnica pravčaste plohe prvenstveno pomoću računala, a ne samo u klasičnom smislu. Opisana je metoda za definiranje i konstrukciju poznatih ploha, ali i za modeliranje novih. Uvedeni matematički opis omogućuje stvaranje interaktivnog modeliranja ploha pomoću računala i vrlo brzi dizajn plohe te projekcije njezinih odabranih dijelova. Slike prikazuju računalne grafičke izlaze.

Ključne riječi: pravčaste plohe, razvojne plohe, vitopere plohe

A Method for Creating Ruled Surfaces and its Modifications

ABSTRACT

The paper presents a non-traditional method for defining ruled surfaces. This method enables a simple construction of the ruled surfaces generating lines, not only with the classical means, but first of all with a computer. The method for defining and constructing known surfaces and also modelling of new surfaces is described here. The introduced mathematical description enables creation of the interactive modelling of surfaces by using a computer and very quick surface design and projection of its arbitrary segments. The pictures are presenting the graphical output from a computer.

Key words: developable surface, ruled surface, skew surface

MSC 2000: 65D17, 51N05, 51N20

1 Definition of a ruled surface and construction of generating lines

We will work in the Euclidean space $\mathbf{E}_3$ and in the vector space $V(\mathbf{E}_3)$ with the Cartesian coordinates system $\langle O, x_1, x_2, x_3 \rangle$.

Let these vector functions be set:

$$\begin{aligned} \mathbf{y}_1(x_1) &= (x_1, 0, f(x_1)), \quad x_1 \in I_1, \\ \mathbf{y}_2(x_2) &= (0, x_2, g(x_2)), \quad x_2 \in I_2 . \end{aligned} \qquad (1)$$

Let the real functions f and g in (1) be continuous and differentiable on the intervals I_1 and I_2. These intervals can contain many points for which derivative of the functions f and g are improper. Vector functions (1) describe curves $k_1 \subset x_1x_3$ and $k_2 \subset x_2x_3$. We assume that these curves k_1 and k_2 are not intersected (Fig. 1).

Let the curve m be defined by the vector function (2) in the plane x_1x_2

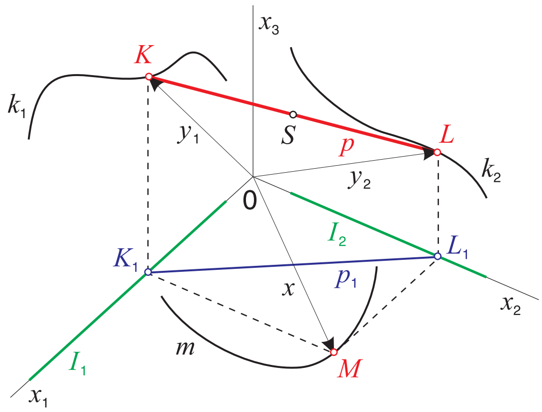

Fig. 1

$$\mathbf{x}(t) = (x(t), y(t), 0), \quad t \in I, \qquad (2)$$

where for any $t \in I$ is $x(t) \in I_1$, $y(t) \in I_2$ and $\dfrac{\mathrm{d}\mathbf{x}(t)}{\mathrm{d}t} = \mathbf{x}'(t)$ is a non-zero vector.

Now, we will construct the generating line p in this way (Fig. 1):

a) We choose a point M on the curve m and mark its orthogonal projections to the axes x_1 and x_2 as K_1 and L_1.

b) Points K and L are points located on curves k_1 and k_2 respectively, while K_1 and L_1 are their orthogonal projections to the plane x_1x_2.

c) The line p joins the points K and L.

The line p is a generating line of the ruled surface φ and with this method we would construct next generating lines of the surface φ.

2 Parametric representation of the ruled surface φ

We obtain the coordinates of the points K and L with the substitution of (2) to (1). Then

$$K = [x(t), 0, F(t)] \quad \text{and} \quad L = [0, y(t), G(t)],$$

where $F(t) = f(x(t))$ and $G(t) = g(y(t))$.
Let the generating line p be defined for example by the centre

$$S = \left[\frac{x(t)}{2}, \frac{y(t)}{2}, \frac{F(t)+G(t)}{2}\right]$$

of the line segment KL and by the direction vector

$$\mathbf{p}(t) = \frac{1}{2}\left(x(t), -y(t), F(t)-G(t)\right). \tag{3}$$

Then the ruled surface φ has the following parametric representation:

$$\begin{aligned} x_1 &= \frac{x(t)}{2}(1+u), \\ x_2 &= \frac{y(t)}{2}(1-u), \\ x_3 &= \frac{F(t)+G(t)}{2} + u\frac{F(t)-G(t)}{2}, \\ & t \in I, \quad u \in R. \end{aligned} \tag{4}$$

Example 1: The surface of an elliptic movement

The vector functions (1) are

$$\begin{aligned} \mathbf{y}_1(x_1) &= (x_1, 0, q_1), \quad x_1 \in R, \\ \mathbf{y}_2(x_2) &= (0, x_2, q_2), \quad x_2 \in R, \end{aligned} \tag{5}$$

where q_1 and q_2 are non-zero constants from R, $q_1 \neq q_2$.

Curves k_1 and k_2 are lines, $k_1 \parallel x_1$ and $k_2 \parallel x_2$. Let the curve m become a circle defined by the vector function

$$\mathbf{x}(t) = (a\cos t, a\sin t, 0), \quad t \in \langle 0, 2\pi \rangle. \tag{6}$$

The surface φ defined in this way has the following parametric representation according to equation (4):

$$\begin{aligned} x_1 &= \frac{a\cos t}{2}(1+u), \\ x_2 &= \frac{a\sin t}{2}(1-u), \\ x_3 &= \frac{q_1+q_2}{2} + u\frac{q_1-q_2}{2}, \\ & t \in \langle 0, 2\pi \rangle, \quad u \in R. \end{aligned} \tag{7}$$

In Fig. 2a the curves k_1, k_2 and m are shown.
In Fig. 2b a surface segment, which is called the surface of an elliptic movement is shown.

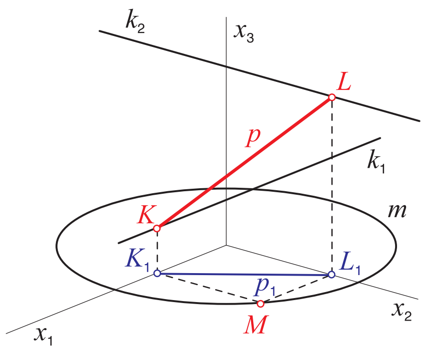

Fig. 2a

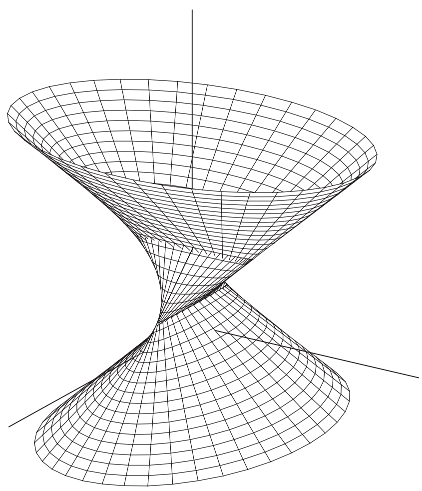

Fig. 2b

3 The section of the surface φ by the plane x_1x_2

If the curve k_3 is the section of the surface φ by the plane x_1x_2, $(x_3 = 0)$, then we get its parametric representation from (4)

$$x_1 = \frac{G(t)x(t)}{G(t)-F(t)},\ x_2 = \frac{-F(t)y(t)}{G(t)-F(t)},\ x_3 = 0,\ t \in I\,. \quad (8)$$

If for any $t \in I$ is

$$G(t) = F(t), \quad (9)$$

then the corresponding generating line $p \parallel x_1x_2$ and its intersection point with the plane x_1x_2 is a point at infinity.

The section of the surface φ of elliptic movement by the plane x_1x_2 (from the example 1 according to (8)) has the following parametric representation

$$x_1 = \frac{aq_2}{q_2-q_1}\cos t, \quad x_2 = \frac{-aq_1}{q_2-q_1}\sin t,$$
$$x_3 = 0, \qquad t \in \langle 0, 2\pi \rangle. \quad (10)$$

This section is the ellipse k_3 with the centre in the origin of the coordinate system, values of the semiaxes are

$$\left|\frac{aq_2}{q_2-q_1}\right| \quad \text{and} \quad \left|\frac{aq_1}{q_2-q_1}\right|.$$

In the case when the equation (9) expresses identity for the interval I all generating lines of the surface φ are parallel to the plane x_1x_2 and the section of the surface by the plane x_1x_2 cannot be described by equations (8).

If we choose the vector functions (1) as

$$\begin{aligned} \mathbf{y}_1(x_1) &= (x_1, 0, f(x_1)), \quad x_1 \in I_1, \\ \mathbf{y}_2(x_2) &= (0, x_2, f(x_2)), \quad x_2 \in I_1, \quad I_1 = I_2 \end{aligned} \quad (11)$$

and the curve m is a line parametrized by the vector function

$$\mathbf{x}(t) = (t, t, 0), \quad t \in R, \quad (12)$$

then $F(t) = G(t) = f(t)$.

The ruled surface φ has the following parametric representation according to (4):

$$\begin{aligned} x_1 &= \frac{t}{2}(1+u), \\ x_2 &= \frac{t}{2}(1-u), \\ x_3 &= f(t), \quad t \in I_1, \quad u \in R \end{aligned} \quad (13)$$

and it is a cylindrical surface. Its generating lines are parallel to the plane x_1x_2. The curves k_1 and k_2 are congruent. Revolving the curve k_1 about the axis x_3 by the angle 90^o we would get the curve k_2.

The section k_3 of the cylindrical surface (13) by the plane x_1x_2 is composed from the surface generating lines. Their number is equal to the number of common points of the curve k_1 and the axis x_1.

Example 2: Circular cylindrical surface

Curves k_1 and k_2 are semicircles with centres $S_1 \in x_1$, $S_2 \in x_2$, with the same radius r and $|OS_1| = |OS_2| = p$. The semicircles are parametrized by the vector functions

$$\begin{aligned} \mathbf{y}_1(x_1) &= \left(x_1, 0, \sqrt{r^2-(x_1-p)^2}\right), \\ & \qquad x_1 \in \langle p-r, p+r \rangle, \\ \mathbf{y}_2(x_2) &= \left(0, x_2, \sqrt{r^2-(x_1-p)^2}\right), \\ & \qquad x_2 \in \langle p-r, p+r \rangle, \quad 0 < p-r\,. \end{aligned}$$

The surface φ is a half of the circular cylindrical surface which has the following parametric representation according to (13)

$$\begin{aligned} x_1 &= \frac{t}{2}(1+u), \\ x_2 &= \frac{t}{2}(1-u), \\ x_3 &= \sqrt{r^2-(t-p)^2}, \\ & \qquad t \in \langle p-r, p+r \rangle, \quad u \in R\,. \end{aligned} \quad (14)$$

Fig. 3a illustrates curves k_1, k_2, m, and the section of the surface by the plane x_1x_2 which is created by lines l_1 and l_2.

In Fig. 3b the segment of the circular cylindrical surface is shown.

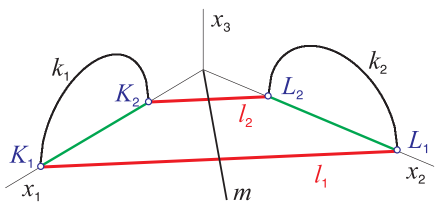

Fig. 3a

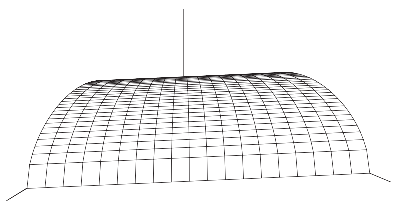

Fig. 3b

4 Developable and skew surfaces φ

The generating line of the surface φ is defined by choice of the parameter $t \in I$. When we substitute the parametric representation (2) of the curve m to the vector functions (1) and differentiate the vector functions (1) according to argument t, then we get:

$$\mathbf{y}_1'(t) = x'(t)\left(1,0,\left[\frac{\mathrm{d}f(x_1)}{\mathrm{d}x_1}\right]_{x_1=x(t)}\right) \quad \text{and}$$
$$\mathbf{y}_2'(t) = y'(t)\left(0,1,\left[\frac{\mathrm{d}g(x_2)}{\mathrm{d}x_2}\right]_{x_2=y(t)}\right).$$

These vector functions for chosen $t \in I$ are defining the direction vectors of the tangent lines of curves k_1 and k_2. To make the generating line of the surface φ torsal, vectors $\mathbf{y}_1'(t)$, $\mathbf{y}_2'(t)$ and (3) must be linearly dependent. From this condition we get equation:

$$x'(t)y'(t)\left(F(t)-x(t)\left[\frac{\mathrm{d}f(x_1)}{\mathrm{d}x_1}\right]_{x_1=x(t)} - \left(G(t)-y(t)\left[\frac{\mathrm{g}(x_2)}{\mathrm{d}x_2}\right]_{x_2=y(t)}\right)\right)=0. \qquad (15)$$

If the equation (15) is identity on the interval I, the surface φ is created by torsal lines only and it is a developable surface. If the equation (15) is not identity, the surface φ is a skew surface on which torsal generating lines can exist.

The equation (15) of the surface of an elliptic movement has the form:

$$a^2(q_1-q_2)\sin t\cos t = 0, \quad t \in \langle 0, 2\pi\rangle.$$

Then the lines for parameters $t = 0,\ \pi/2,\ \pi,\ 3\pi/2$ are torsal lines located in the planes x_1x_3 and x_2x_3.

In the case when the cylindrical surface has the parametric presentation (13) we can simply verify that the equation (15) is an identity and the cylindrical surface will be a developable surface. The intersection points K_1 and L_1 of the line l_1 with the semicircles k_1 and k_2 from the example 2 (Fig. 3a) are examples of points in which derivative of the functions f and g is improper. The tangent lines of the curves k_1 and k_2 in the points K_1 and L_1 are parallel with the axis x_3. Analogously for the line l_2.

5 Continuity between the surfaces φ and skew surfaces

Continuity between the mentioned ruled surfaces φ and skew surfaces, which are defined by three basic curves, is clearly seen on the surface of an elliptic movement. If the section of the surface φ by the plane x_1x_2 is the curve k_3, then it is possible to define the surface φ by basic curves k_1, k_2 and k_3. The generating lines of the surface φ are lines intersecting the basic curves.

6 Envelope of orthographic views of the ruled surface generating lines in the plane x_1x_2

Generating lines of the ruled surface are orthogonally projected to the plane x_1x_2 and parametric representation of these orthographic views can be given by the first two equations in (4) without the parameter u:

$$y(t)x_1 + x(t)x_2 - x(t)y(t) = 0, \quad t \in I. \qquad (16)$$

The equation (16) is the equation of a one-parametric line system and its envelope can be found by differentiating of the equation (16) according to parameter t:

$$y'(t)x_1 + x'(t)x_2 - x'(t)y(t) - x(t)y'(t) = 0. \qquad (17)$$

From the equations (16) and (17) we get:

$$x_1 = \frac{x^2(t)y'(t)}{x(t)y'(t)-x'(t)y(t)},$$
$$x_2 = \frac{-y^2(t)x'(t)}{x(t)y'(t)-x'(t)y(t)},$$
$$x_3 = 0, \qquad t \in I. \qquad (18)$$

If an envelope exists and it is a curve marked as m', then the equations (18) are its parametric representation. The points for which $x(t)y'(t)-x'(t)y(t)=0$ do not have to be necessarily troublesome points. This problem will be not investigated here.

The envelope m' depends only on the curve m, what is evident from the equations (18) and the geometric view, too.

If the curve m is a circle parametrized by the function (6), then according to (18) the envelope m' has the following parametric representation:

$$x_1 = a\cos^3 t,\ x_2 = a\sin^3 t,\ x_3 = 0,\ t \in \langle 0, 2\pi\rangle, \qquad (19)$$

the curve m' is an asteroid (Fig. 4a).

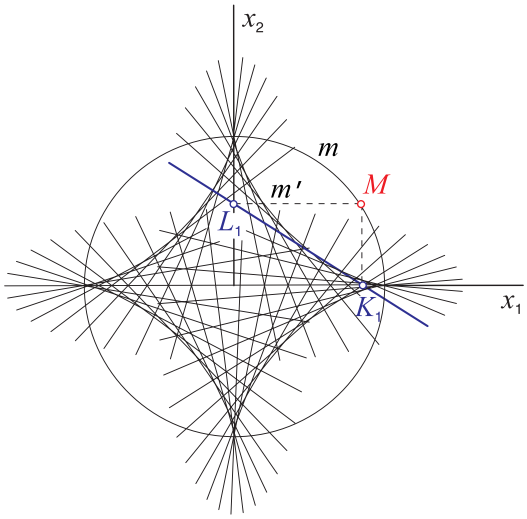

Fig. 4a

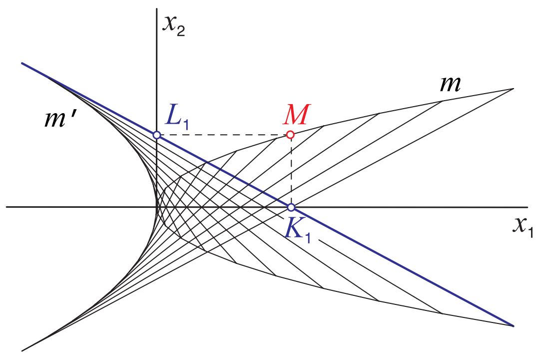

Fig. 4b

Orthographic views of the cylindrical surface generating lines (example 2) in the plane x_1x_2 are examples for the one-parametric system of lines which has not any envelope.

7 Modification of the method for the creation of ruled surfaces

The idea described above allows us to define and create ruled surfaces by a method which we could call dual for defining and creating the surfaces φ. The surface is defined by the curves k_1 and k_2 which are parametrized by the functions (1). Let the curve m' be without singular points in the plane x_1x_2. Tangent lines of the curve m' create a one-parametric system of lines. Let K_1 and L_1 be the intersections of one tangent line (which is the intersecting line with the axes x_1 and x_2 too) of the one-parametric system with the axis x_1 and x_2. We can construct the surface generating line p by means of points K_1 and L_1 with the same method as in the first part (see Fig. 1).

Example 3:

Let the surface φ be defined by curves k_1 and k_2, which are parametrized by the vector functions (5) and the curve $m' \subset x_1x_2$ is a parabola expressed by parametric representation

$$x_1 = -\frac{1}{2p}t^2, \quad x_2 = t, \quad x_3 = 0, \quad t \in R\,.$$

The vector function

$$\mathbf{y}(v) = \left(-\frac{1}{2p}t^2 - \frac{1}{p}tv, t+v, 0\right), \quad v \in R \tag{20}$$

of the parameter v describes the system of tangent lines to the parabola m' for any value of parameter $t \in R$ (Fig. 4b).

The intersections of the tangent lines with the axes x_1 and x_2 are the points K_1 and L_1 with the following coordinates

$$K_1 = \left[\frac{1}{2p}t^2, 0, 0\right] \quad \text{and} \quad L_1 = \left[0, \frac{t}{2}, 0\right]\,. \tag{21}$$

The coordinates of the points K and L are

$$K = \left[\frac{1}{2p}t^2, 0, q_1\right] \quad \text{and} \quad L = \left[0, \frac{t}{2}, q_2\right]\,.$$

The surface parametric representation according to (4) has the following form:

$$\begin{aligned} x_1 &= \frac{t^2}{4p}(1+u), \\ x_2 &= \frac{t}{4}(1-u), \\ x_3 &= \frac{q_1+q_2}{2} + u\frac{q_1-q_2}{2}, \\ & t \in R, \quad u \in R\,. \end{aligned} \tag{22}$$

The set of points M which are projected orthogonally to the points K_1 and L_1 on the axes x_1 and x_2 can be parameterized according to (21) by the function

$$\mathbf{x}(t) = \left(\frac{t^2}{2p}, \frac{t}{2}, 0\right), \quad t \in R\,.$$

The points M are therefore located on the parabola m which is the generatrix of the ruled surface φ constructed by the method described in the first part.

The both modifications of the presented method are illustrated in Fig. 4b showing the construction of the surface φ projected orthogonally to the plane x_1x_2. A similar construction can be seen in Fig. 4a, where the curve m is a circle and the curve m' is an asteroid.

Description of the surface φ construction is shown in Fig. 5a. The segment of the surface is shown in Fig. 5b.

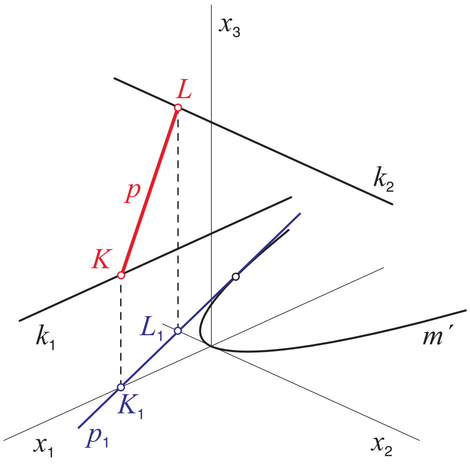

Fig. 5a

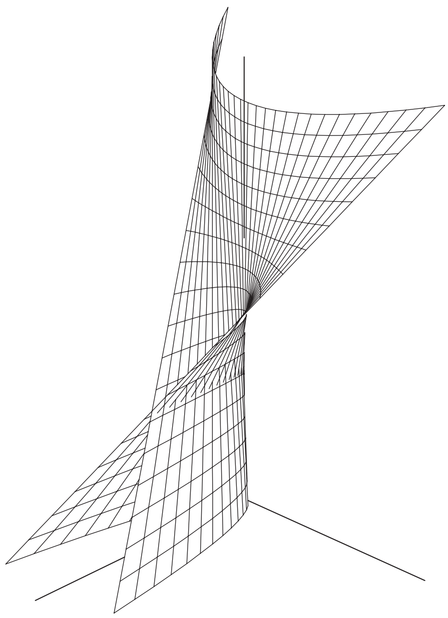

Fig. 5b

The section of the surface φ by the plane x_1x_2 has the following parametric representation according to (8):

$$x_1 = \frac{q_2}{2p(q_2-q_1)}t^2, \quad x_2 = \frac{-q_1}{2(q_2-q_1)}t, \quad x_3 = 0, \quad t \in R\,,$$

the curve k_3 is a parabola.

The equation (15) has the form

$$\frac{1}{2p}t(q_2-q_1) = 0$$

and therefore the surface has only one torsal basic line correspondent to the parameter $t = 0$.

Now we will show some examples of the surfaces φ.

Example 4: Conical surface

The vector functions (1) are

$$\begin{aligned}\mathbf{y}_1(x_1) &= (x_1, 0, q_1), \quad x_1 \in R,\\ \mathbf{y}_2(x_2) &= \left(0, x_2, \frac{1}{2p}x_2^2 + q_2\right), \quad x_2 \in R\,.\end{aligned}$$

The curve k_1 is a line, the curve k_2 is a parabola. Let the curve m be a line parallel to the axis x_2 defined by the vector function

$$\mathbf{x}(t) = (k, t, 0), \quad t \in R, \tag{23}$$

where k is a non-zero constant from R (Fig. 6a).

The surface φ has the following parametric representation according to (4):

$$\begin{aligned}x_1 &= \frac{k}{2}(1+u),\\ x_2 &= \frac{t}{2}(1-u),\\ x_3 &= \frac{2p(q_1+q_2)+t^2}{4p} + u\frac{2p(q_1-q_2)-t^2}{4p},\\ &t \in R, \quad u \in R\,.\end{aligned} \tag{24}$$

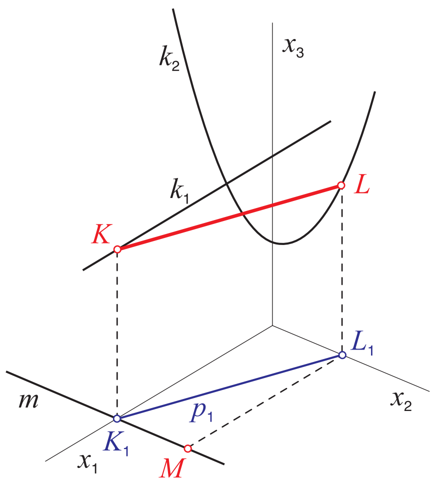

Fig. 6a

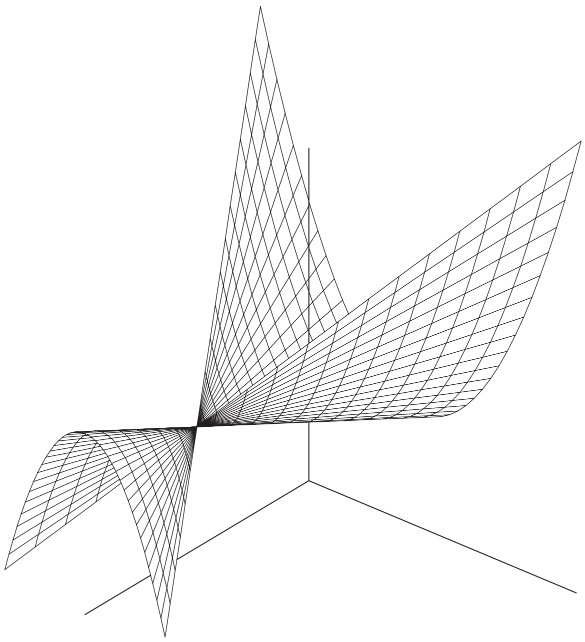

Fig. 6b

It is evident that the surface φ is a conical surface with a vertex in the point K, so this surface is developable. In this case the equation (15) is an identity, because in the vector function (23) is $x'(t) = 0$ for all $t \in R$. The segment of the surface is illustrated in Fig. 6b.

We could construct generating lines by the means of a one-parametric system of lines in the plane x_1x_2, too. In this case, the system of lines would be a pencil of lines with the centre in the point K_1 (without the line m). The line p_1 is one line from the pencil of lines (see Fig. 6a). This is nothing new for us, it is a classical construction of conical surface generating lines.

Example 5: Frezier's cylindroid

The vector functions (1) are

$$\begin{aligned}\mathbf{y}_1(x_1) &= \left(x_1, 0, \sqrt{r^2-(x_1-p)^2}\right), \\ &\qquad x_1 \in \langle p-r, p+r\rangle, \quad 0 < p-r, \\ \mathbf{y}_2(x_2) &= \left(0, x_2, \sqrt{r^2-(x_2-p)^2}+q\right), \\ &\qquad x_2 \in \langle p-r, p+r\rangle,\end{aligned}$$

where q is a non-zero constant from R.

The curves k_1 and k_2 are semicircles as in the example 2 for the cylindrical surface, but the circle k_2 is translated by the translation vector $(0,0,q)$. The curve m is a line defined by the vector function (12), Fig. 7a.

This surface is so called Frezier's cylindroid and its segment is shown in Fig. 7b. The surface is a skew surface which has two torsal generating lines. The equation (15) has the form

$$\begin{aligned}&\sqrt{r^2-(t-p)^2}+\frac{t(t-p)}{\sqrt{r^2-(t-p)^2}} \\ &= \sqrt{r^2-(t-p)^2}+q+\frac{t(t-p)}{\sqrt{r^2-(t-p)^2}}\end{aligned}$$

and this is fulfilled only for the points $t = p \pm r$, in which derivative of the functions f and g is improper. Orthographic views of torsal lines in the plane x_1x_2 are the lines l_1 and l_2 (Fig. 7a).

It is possible to construct cylindroid generating lines analogously using the one-parametric system of lines as at a conical surface. It this case the system of lines is parallel to the line l_1.

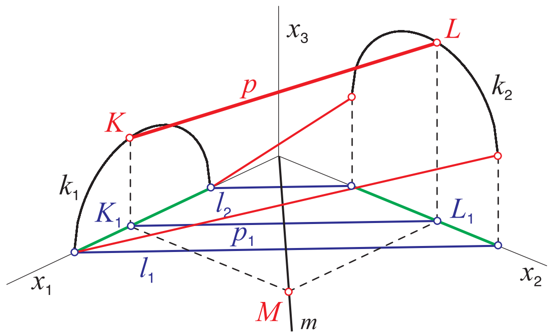

Fig. 7a

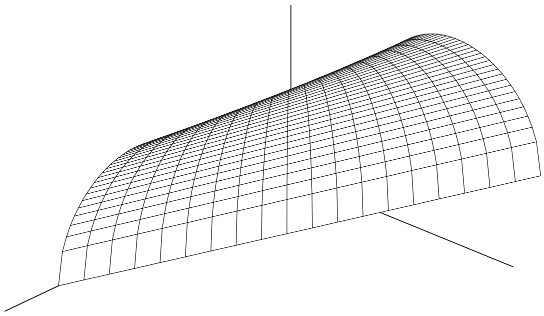

Fig. 7b

At the end of this paper there are illustrated two complicated surfaces (see Figs 8 and 9). The segment of the surface demonstrated in Fig. 8 is defined by curves k_1, k_2 and m, where the curve k_1 is the Witch of Agnési, k_2 is a parabola and the curve m is an epicycloid. In Fig. 9 is a segment of the surface for which the curve k_1 is a parabola, the curve k_2 is Witch of Agnési and the curve m is a circle with its centre in the origin.

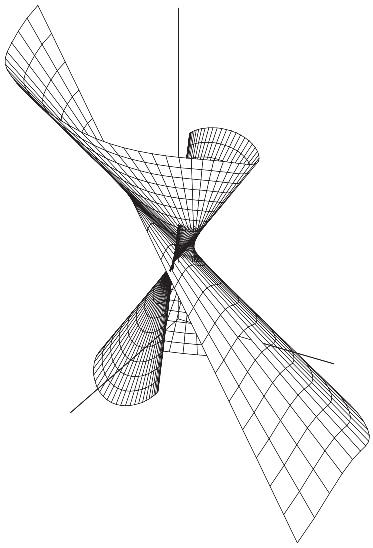

Fig. 8

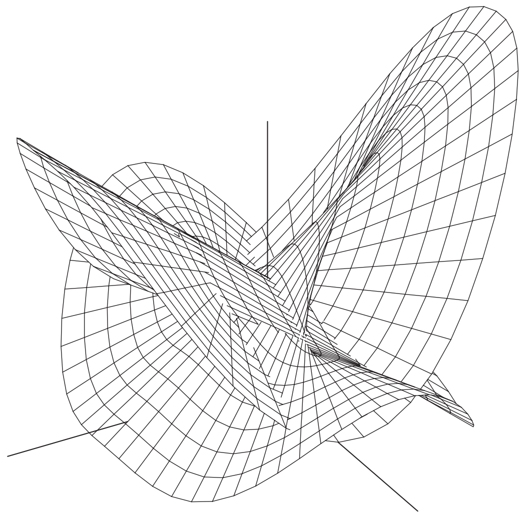

Fig. 9

References

[1] MEDEK, V., ZÁMOŽÍK, J.: *Konštruktívna geometria pre technikov*, Alfa-Bratislava, SNTL-Praha, 1978

[2] BUDINSKÝ B., KEPR. B: *Základy diferenciální geometrie s technickými aplikacemi, SNTL*, Praha 1970

Kamil Maleček
Department of Mathematics
Faculty of Civil Engineering
Czech Technical University
Thákurova 7
166 29 Praha 6, Czech Republic
tel: +420 2 24354384
e-mail: kamil@mat.fsv.cvut.cz

Dagmar Szarková
Department of Mathematics
Faculty of Mechanical Engineering
Slovak University of Technology
Námestie Slobody 17
812 31 Bratislava, Slovakia
tel: +421 2 57296 394
e-mail: szarkova@sjf.stuba.sk

Professional paper
Accepted 29.05.2002

GÖRGYI FÜHRER NAGY

Some Remarks to the Paper "The Goose that Laid the Golden Egg"

Neka zapažanja o članku “Guska koja nese zlatno jaje”

SAŽETAK

Članak [1] potaknuo me da povežem transcedentalne LAMÉove krivulje sa svojim opažnjima o realnim ptičjim jajima [2]. Dijelovi dviju različitih krivulja spajaju se u točkama na osi y. Dobiveni jajoliki oblik izgleda lijepo, ali nas oko vara. U točki spajanja krivulje imaju zajedničku tangentu, ali su polumjeri zakrivljenosti 0 i ∞. Te nezamjetne pojave sažete su u dva teorema.

Ključne riječi: jajolike krivulje, ptičja jaja, zlatni rez

Some Remarks to the Paper "The Goose that Laid the Golden Egg"

ABSTRACT

The paper [1] induced me to combine the transcendental curves of LAMÉ with my observations on real bird-eggs [2]. Two segments of different curves are connected at junctions points located on the y-axis. The obtained egg-like shape looks nice, but the eye is cheating. It turns out that the curvature of these curves at the junction point has some surprising properties. These imperceptible phenomena are summarized in two theorems.

Key words: bird-egs, egg-shaped curves, golden ratio

MSC 2000: 53B99, 92B05

Introduction

It is natural to determine the form of bird-eggs in order to distinguish and describe the eggs of different bird species. It is an old problem for nature scientists named oologists (zoologists studying bird eggs).

Geometers interpret all bird-eggs as bodies with rotational symmetry. Their longitudinal cross section is an egg-curve [2]. As dimensions we usually use the length l, the width denoted by $2b$, and the axial sections denoted by p and $q = l - p$ $(p \geqslant q)$ [3]. These can exactly be measured. To distinguish bird-eggs the oologists use the quotients p/q and $l/2b$, which only by few bird species can be equal to the golden ratio.

In the following we apply the real measured data on Fibonacci-related functions [1] which give egglike shapes.

This type of egglike curve has the advantage that it can easily be modified in order to meet the measurements given by oologists.

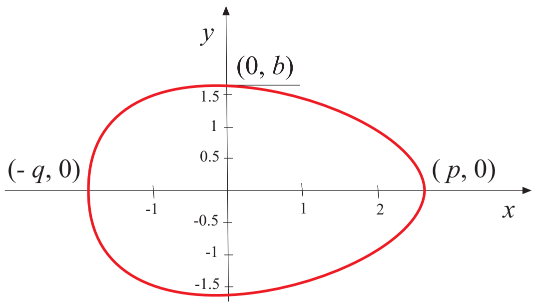

Fig.1 The notation of measured data

1 Basic formulas

In [1] the author used the golden ratio

$$\theta = \frac{\sqrt{5}+1}{2} = 1.618033989$$

for obtaining different shapes of biological forms. Two parts of curves determined by equations

$$\textbf{a)}\ x^{\theta} + y^{\theta} = 1; \quad \textbf{b)}\ x^{\theta^2} + y^{\theta^2} = 1; \quad \textbf{c)}\ x^{\theta} + \left(\frac{y}{\theta}\right)^{\theta} = 1$$

were connected. The junction points of the two segments were located on the y-axis.

Among the presented examples there were also egg-curves, but only of the eggs which have the characteristics $p/q=\theta$, i.e. $l/2b=(1+\theta)/2$.

Now this method will be generalised. For this purpose it is necessary to modify the above equations into

$$\textbf{b1)}\quad \left(\frac{|y|}{b}\right)^{\theta^2}+\left(\frac{|x|}{q}\right)^{\theta^2}=1,$$

$$\textbf{c1)}\quad \left(\frac{|y|}{b}\right)^{\theta}+\left(\frac{|x|}{p}\right)^{\theta}=1.$$

(The curves of this kind are known as transcendent curves of LAMÉ.)

If x is running from $-q$ to 0, the plot of **b**1) presents the blunt end (see Fig.1, left hand side). For $0\leqslant x\leqslant p$ the plot of **c**1) gives the pointed end of the egg-curve. The x-axis is the axis of symmetry. With the data of the peewit egg (*vanellus vanellus*) $b=16.45mm$, $p=26.3mm$, $q=19mm$ we get the "usual" egg-curve given in Fig.1.

If also the left segment obeys formula **c**1), but p is replaced by q and x by $-x$, we get the shape of bird-eggs with two pointed ends in Fig.2a (see "zweispitzige Eier" in [3]). The two segments are corresponding under a perspective affine transformation.

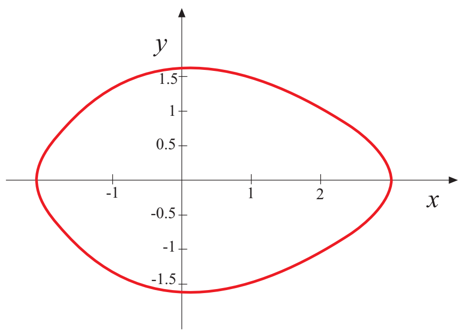

a)

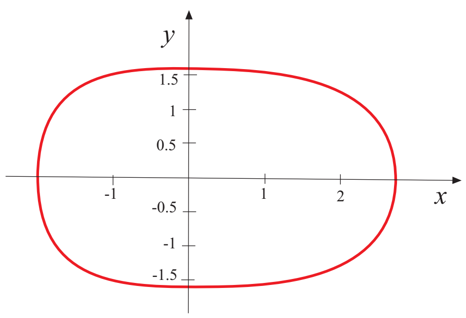

b)

Fig.2 The egg-curve with two pointed ends and two blunt ends

When only the formula **b**1) is used, we get the bird-eggs of the form in Fig.2b ("wurstförmige Eier" in [3]).

Both possibilities can also be used for $p=q$. Contrary to the cases presented in [2], we obtain plots which are not ellipses or circles. Since also the exponent θ can vary, these composed egg-curves offer more possibilities than all the others before.

2 About the curvature in the end points

2.1 The right part

If we observe the formulas of the curves composed in Fig.1 we can also make some conclusions about the variation of the curvature. Let us first observe the right part of the curve:

$$|y|=b\left(1-\left(\frac{x}{p}\right)^{\theta}\right)^{\frac{1}{\theta}}. \tag{1}$$

The first and second derivatives of $y\geqslant 0$ are

$$y'=-\frac{bx^{\theta-1}}{\left(1-\left(\frac{x}{p}\right)^{\theta}\right)^{1-\frac{1}{\theta}}\cdot p^{\theta}} \tag{2}$$

and

$$y''=\frac{-(\theta-1)b}{p^{\theta}}\cdot\left[\frac{x^{2\theta-2}}{\left(1-\left(\frac{x}{p}\right)^{\theta}\right)^{2-\frac{1}{\theta}}\cdot p}+\frac{1}{\left(1-\left(\frac{x}{p}\right)^{\theta}\right)^{1-\frac{1}{\theta}}\cdot x^{1-\frac{1}{\theta}}}\right]. \tag{3}$$

The first derivative vanishes if $x=0$. This gives the maximum point.

The denominator of y'' is equal zero if $x=0$ or $x=p$. It means that the second derivative is undetermined at $x=0$, but $\lim\limits_{x\to 0} y''=-\infty$. In the point $(p,0)$ we have the same situation.

2.2 The left part

The part determined by **b**1) for $-q\leqslant x\leqslant 0$, $y\geqslant 0$ reads:

$$y_1=b\left(1-\left(\frac{-x}{q}\right)^{\theta^2}\right)^{\frac{1}{\theta^2}}. \tag{4}$$

The derivatives are

$$y_1' = \frac{b(-x)^{\theta^2-1}}{\left(1-\left(\frac{-x}{q}\right)^{\theta^2}\right)^{1-\frac{1}{\theta^2}} q^{\theta^2}} \tag{5}$$

and

$$y_1'' = -\frac{\theta b}{q^{\theta^2}}\left[\frac{(-x)^{2\theta}}{\left(1-\left(\frac{-x}{q}\right)^{\theta^2}\right)^{\theta} q^{\theta^2}} + \frac{(-x)^{\theta^2-2}}{\left(1-\left(\frac{-x}{q}\right)^{\theta^2}\right)^{1-\frac{1}{\theta^2}}}\right]. \tag{6}$$

y_1' vanishes if $x=0$, and it is undetermined for $x=-q$. Exactly the same holds for y_1'' but

$$\lim_{x\to -q+0} y_1' = \infty \quad \text{and} \quad \lim_{x\to -q+0} y_1'' = -\infty.$$

2.3 The curvature radius

The formula for the curvature radius (since $y" < 0$ for all $x \in [-q,p]$) is

$$r = -\frac{|1+y'|^{3/2}}{y''} \tag{7}$$

and, on the right hand part of the egg-curve, gives $r=0$ if $x=0$ or $x=p$. It means that at the observed points the curvature $c=1/r$ of the right part tends forwards infinity.

Substitution of y_1' and y_1'' into the definition (7) shows that the curvature radius of the left part at the points $x=0$ and $x=-q$ tends to infinity.

We summarise this surprising facts in

Theorem 1 *In the Fig.1 at the point $(0,b)$ the two curves have the same tangent, but the curvature radii as well as the curvatures are extremely different.*

Theorem 2 *The composed egg-curve given in Fig.1 has at the blunt end $(-q,0)$ the curvature radius $r=\infty$, at the pointed end $(p,0)$ is $r=0$.*

REMARK:

In Fig.1 the curvature radius at the left side appear the minimal value $r\sim 1.58$ in $x\sim -1.6$, and the maximal value of the right side $r\sim 4.2$ in $x\sim 1.1$.

The investigation of the other Fibonacci-related functions listed in [1] is advisable using data appearing in the nature.

References

[1] LEVINE, N.: The Goose that laid the golden Egg, Fibonacci Quarterly, Vol. 22, no.3 (1984), pp. 252-254.

[2] F. NAGY, GY.: Crtanje jajolikih krivulja, KOG, No. 1 (1996), pp. 16-18.

[3] SCHÖNWETTER, M.: Handbuch der Oologie, Vol.41., Akademie-Verlag, Berlin (1985), pp.1-64.

Györgyi F. Nagy
Sopron, POB 132
9401
Hungary
e-mail. fuh@emk.nyme.hu

Professionelle Arbeit
Angenommen am 27.06.2002

GUNTER WEISS
HANS HAVLICEK

Ecken- und Kantenhöhen im Tetraeder

Vršne i bridne visine tetraedra

SAŽETAK

k-visina nekog n-simpleksa siječe njegovu k-stranicu i njoj nasuprotnu stranicu okomito. Tetraedar $\boldsymbol{T}$ ima četiri "vršne visine" $(k=0)$ i tri "bridne visine" $(k=1)$. Visine oba tipa izvodnice su posebnih hiperboloida povezanih s tetraedrom $\boldsymbol{T}$.

Članak obrađuje te hiperboloide na način nacrtne geometrije i daje sintetičke dokaze nekih dobro poznatih svojstava. Pokazuje se, na primjer, da ako se visine jednog tipa sijeku u jednoj točki da se tada i visine drugog tipa sijeku u jednoj točki te da te točke koincidiraju.

Ključne riječi: tetraedar, hiperboloid visina, centralna projekcija

Vertex- and Edge-Altitudes of a Tetrahedron

ABSTRACT

A k-altitude of an n-simplex meets a k-face and its opposite face orthogonally. A tetrahedron $\boldsymbol{T}$ possesses four "vertex-altitudes" $(k=0)$ and three "edge-altitudes" $(k=1)$. The altitudes of each type are generators of special hyperboloids connected with T.

The paper treats these hyperboloids in terms of descriptive geometry and gives synthetic proofs for some well-known properties. It turns out, for example, that if the altitudes of one type intersect in one point, then so do the others, and the points of intersection coincide.

Key words: tetrahedron, hyperboloid of altitudes, central projection

MSC 2000: 51N05, 51N20, 51M04

1 Einführung

Die Anregung von A. Sliepčević aufgreifend, elementargeometrischen Fragestellungen wieder mehr Beachtung zu schenken, (vgl. [21]), wird hier u.a. ein elementares Problem der Raumgeometrie vorgestellt: die Bestimmung und Analyse der Gemeinnormalen windschiefer Kantenpaare eines Tetraeders, also dessen "Kantenhöhen" und der "Eckenhöhen". Ziel ist es einerseits, mit diesem Problemkreis jugendlichen Forschern schon in der Endphase ihres Schulunterrichts ein Trainingsgebiet bereitzustellen. Andererseits werden mittels elementarer darstellend-geometrischer Methoden durchaus auch Zugänge zu den nächsten Etagen der "Höheren Geometrie" eröffnet.

2 Zum Höhenbegriff eines Tetraeders

Aus der ebenen Elementargeometrie ist geläufig, dass die Höhen eines Dreiecks kopunktal sind, (kurz, jedes ebene Dreieck besitzt ein Orthozentrum O). Ebenso sind die Mittelsenkrechten der Dreiecksseiten und die Schwerlinien kopunktal (mit den Schnittpunkten C bzw. G). Genau für gleichseitige Dreiecke fallen diese drei Punkte zusammen, sodass diese Dreiecke eine Sonderrolle spielen. Für alle anderen Dreiecke sind O, C und G verschieden und kollinear mit der sogenannten Euler-Geraden e. Eine erste, dimensionsmäßige Verallgemeinerung des Begriffs "Dreieck" ist der des "Tetraeders" bzw. "n-Simplexes". Ein Tetraeder $\boldsymbol{T}$ besitzt 4 Ecken $A_0,\ldots,A_3$, 6 Kanten $a_{ij}=A_iA_j$, die als drei windschiefe Paare auftreten, sowie 4 Facettendreiecke $\alpha_l=A_iA_jA_k$.

Ein einen n-dimensionalen (euklidischen) Raum aufspannender n-Simplex $\boldsymbol{S}^{(n)}$ besitzt dementsprechend $(n+1)$ Ecken und $\binom{n+1}{k+1}$ k-dimensionale Facetten.

***Definition*:**

Unter einer Höhengeraden (kurz: "Höhe") $h_{j_1},\ldots,h_{j_k}$ von $\boldsymbol{S}^{(n)}$ wollen wir das "Gemeinlot" des Facettenraumes $\alpha_{j_1},\ldots,\alpha_{j_k}$ und dessen komplementärer Facette verstehen.

Demnach besitzt ein Dreieck nur eine Art von Höhen, ein Tetraeder hingegen zwei Arten, von denen den "Eckenhöhen" h_j seit G. MONGE weitreichende Untersuchungen gewidmet wurden, (siehe [4], [6], [10], [15], [20]).

Weniger Beachtung fanden die "Kantenhöhen" h_{ij} von $\boldsymbol{T}$.

Im Folgenden sollen beide Arten von Tetraederhöhen mit darstellend-geometrischen Mitteln behandelt werden.

3 Die Eckenhöhen eines Tetraeders

Bekanntlich gilt (vgl. etwa [10]) der

***Satz* 1 :**

Für jedes Tetraeder $\boldsymbol{T}$ mit zwei bzw. genau einem bzw. keinem Paar orthogonaler Gegenkanten schneiden die vier Höhengeraden einander in genau einem Punkt O bzw. zweimal 2 Höhengeraden in verschiedenen Punkten O_1, O_2 bzw. gehören sie einem Regulus auf einem gleichseitigen Hyperboloid Ψ an.

Bemerkung 1: Für Tetraeder $\boldsymbol{T}$ mit zwei Paaren orthogonaler Gegenkanten ist auch das dritte Kantenpaar orthogonal. Solche Tetraeder heißen “orthozentrisch” mit O als Höhenschnittpunkt.

Bemerkung 2: Der Mittelpunkt M des Regulus Ψ bzw. der Strecke $[O_1,O_2]$ bzw. der Punkt O liegt zur Umsphärenmitte C bezüglich des Eckenschwerpunktes G spiegelbildlich. Die Trägergerade e von C, G und M heißt EULER-Gerade von $\boldsymbol{T}$. Der Punkt M heißt der MONGE-Punkt von T; er verallgemeinert also den Höhenschnittpunkt eines Dreiecks.

Bemerkung 3: Ein (bekannter) konstruktiv-geometrischer Beweis für die im allgemeinen Fall reguloide Lage der vier Höhengeraden h_i benützt einen Normalriss von $\boldsymbol{T}$ auf eine Facettenebene, etwa auf α_4, siehe Figur 1.

Dann ist h_4 projizierend, $(A_4' = h_4')$, und h_1', h_2', h_3' fallen in die mit dem Dreieckshöhenschnittpunkt M_4 kopunktalen Höhengeraden des Dreiecks $(A_1A_2A_3)$. (Der (nichtprojizierende) Normalriss einer Ebenennormalen ist nämlich stets normal zu den Hauptgeraden dieser Ebene, ein Sachverhalt, der als “Satz vom Normalriss eines rechten Winkels” bekannt ist.) Damit existiert eine zu h_4 parallele Treffgerade n_4 an h_1, h_2, h_3; ihr Normalriss fällt in den Höhenschnittpunkt M_4 von $(A_1A_2A_3)$. In der projektiven Erweiterung des Anschauungsraumes ist n_4 mithin eine Treffgerade aller vier Tetraederhöhen h_i. Zu jeder der vier Facetten von $\boldsymbol{T}$ existiert also eine zu dieser normale Treffgerade n_i der Höhen h_i. Da vier nicht-reguloide, windschiefe Geraden höchstens zwei Treffgeraden besitzen können [1], folgt damit, dass die Höhen reguloid liegen und deshalb einer einzigen Quadrik Ψ angehören. Aus der Existenz paralleler Erzeugenden auf Ψ folgt unmittelbar, dass Ψ eine Mittelpunktquadrik sein muss und kein Paraboloid sein kann. Diese Überlegungen lassen allerdings offen, dass Ψ ein gleichseitiges Hyperboloid ist, also eine einparametrige Schar von Tripeln paarweise orthogonaler Erzeugenden besitzt.

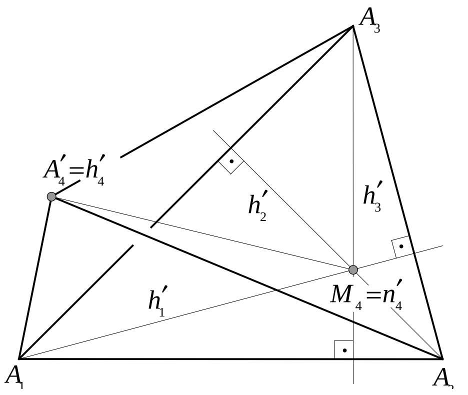

Figur 1: Normalriss eines Tetraeders $\boldsymbol{T}$ auf eine Facettenebene α_4.

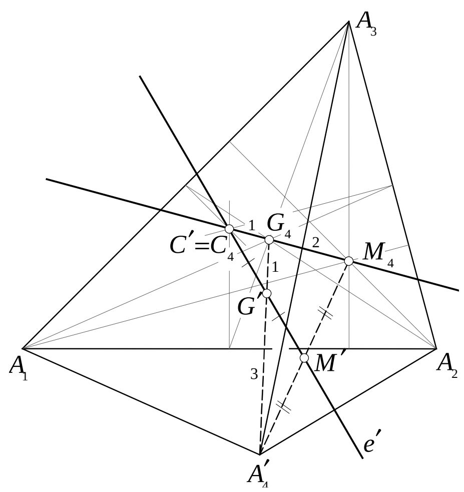

Figur 2: Die EULER-Geraden e, e_4 eines Tetraeders $\boldsymbol{T}$ und seines Facettendreiecks $(A_1A_2A_3)$.

Bemerkung 4: Da parallele Erzeugenden einer Ringquadrik spiegelbildlich zum Mittelpunkt M liegen, erscheint der Normalriss M' dieses Mittelpunktes als der Mittelpunkt der Strecke $[A_4', m_4]$, vgl. Figur 2. Der Riss C' der Umkugelmitte C von $\boldsymbol{T}$ koinzidiert mit der Umkreismitte C_4 des Basisdreiecks und ist ein gemeinsamer Punkt des Euler-Geradenbildes $e' = C'M'$ von $\boldsymbol{T}$ und der Eulergeraden $e_4 := C_4M_4$ des Basisdreiecks $(A_1A_2A_3)$. Liegt A_4' nicht auf e_4, dann sind e' und e_4 verschieden. Der Schwerpunkt G_4 von $(A_1A_2A_3)$ ist dann vom Normalriss G' des Schwerpunktes von $\boldsymbol{T}$ ebenfalls verschieden.

Insgesamt bilden die sechs Punkte M', M_4, G', G_4, A_4' und C' die Ecken eines vollständigen Vierseits und auf dessen Seiten “merkwürdige Teilverhältnisse”. Im Einzelnen gilt:

[1] Drei der vier windschiefen Geraden bestimmen genau einen Treffgeradenregulus, also eine Ringquadrik Φ. Eine Treffgerade aller vier Geraden gehört diesem Treffgeradenregulus an und geht durch einen Schnittpunkt von Φ mit der vierten gegebenen Geraden.

$$\mathrm{TV}(C',M',G') = -1, \qquad \mathrm{TV}(A'_4,M_4,M') = -1,$$
$$\mathrm{TV}(M_4,C',G_4) = -2, \qquad \mathrm{TV}(A'_4,G_4,G') = -3.$$

Dieser Sachverhalt legt die Untersuchung von Punkt-Konfigurationen nahe, deren Geraden ausschließlich Punktetripel mit ganzrationalem Teilverhältnis enthalten.

Bemerkung 5: Die Spurkurve k_4 der Trägerquadrik Ψ des Höhenregulus in der Ebene α_4 enthält die Punkte (A_1,A_2,A_3,A'_4) und k_4 ist wie jeder durch die Ecken eines Dreiecks und dessen Höhenschnittpunkt gehende Kegelschnitt eine *gleichseitige* Hyperbel, Figur 3. (Das durch die Punkte (A_1,A_2,A_3) und M_4 bestimmte Kegelschnittbüschel induziert nämlich auf der Ferngeraden seiner Ebene genau die von einer Rechtwinkel-Involution induzierte "absolute Involution" als DESARGUES-Involution.)

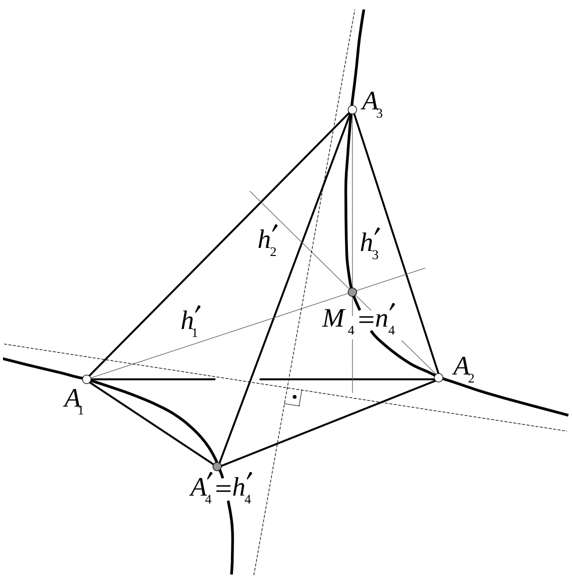

Figur 3: Die Spurkurve k_4 des Höhenregulus in der Facettenebene α_4 ist eine gleichseitige Hyperbel.

Auf Ψ existieren somit zu den Asymptoten von k_4 parallele Erzeugenden, die gemeinsam mit der Erzeugenden h_4 ein Tripel paarweise orthogonaler Erzeugenden bilden. Da alle Facettenebenen gleichberechtigt sind, liegen auf Ψ vier solche Tripel paarweise orthogonaler Erzeugenden.

Für den synthetischen Nachweis, dass damit eine einparametrige stetige Schar solcher Erzeugendentripel existiert, ist es zweckmäßig, den Anschauungsraum durch die Fernebene ω projektiv abzuschließen und den Fernkegelschnitt k_ω von Ψ zu untersuchen, Figur 4.

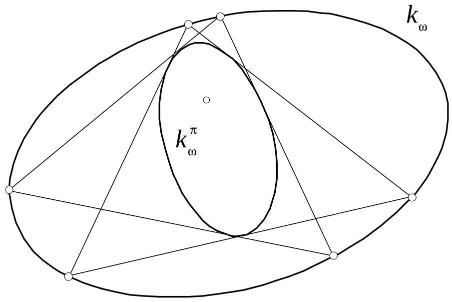

Figur 4: Der Fernkegelschnitt k_ω von Ψ und sein absolut-polarer Bildkegelschnitt k^π_ω als Kegelschnittpaar in 'PONCELETscher Schließungslage' für ein- und umbeschriebene Dreiecke.

Die Orthogonalitätsstruktur des Anschauungsraumes induziert in ω eine elliptische Polarität π, die sogenannte "absolute Polarität". (Im Zentralriss aus einem Augpunkt A auf eine Ebene α erscheint diese absolute Polarität π bekanntlich als "Antipolarität" π^c des Distanzkreises von A.) Demgemäß bilden die Fernpunkte der in Rede stehenden Erzeugendentripel Poldreiecke in π. Wie jede Polarität sind π und k_ω bereits durch zwei solche Dreiecke bestimmt. Die Seiten dieser Dreiecke sind Tangenten eines zu k_ω absolut polaren Kegelschnittes k^π_ω, sodass das Paar (k_ω,k^π_ω) gemäß einem *poristischen Problem* von PONCELET eine stetige Schar von k^π_ω um- und k_ω einbeschriebenen, Dreiecken besitzt, die nun sämtlich auch Poldreiecke in π sind. Somit ist Ψ ein Hyperboloid mit einer stetigen Schar von Tripeln paarweise orthogonaler Erzeugenden, also ein gleichseitiges Hyperboloid. (Der Asymptotenkegel eines solchen Hyperboloides besitzt ebenfalls eine solche Schar orthogonaler Dreibeine, vgl. [19], [10].)

Bemerkung 6: Der zum Höhenregulus ergänzende Regulus enthält neben den schon betrachteten Normalen n_i durch die Höhenschnittpunkte der Facettendreiecke von $\mathbb{T}$ noch weitere einfach zu konstruierende Erzeugenden: die durch die Ecken A_i legbaren Treffgeraden t_i der Höhen h_i.

Im Zentralriss aus A_4 auf (A_1,A_2,A_3) erscheint Ψ als ein Punktepaar, bestehend aus dem Punkt A'_4 und dem Schnittpunkt T_4 der Zentralrisse $h^c_i := A_iH^c_{iu}$ der Höhen h_1, h_2, h_3, vgl. Figur 5. Dabei repräsentiert $T_4 = T^c_{4u}$ den als "elliptischen Höhenschnittpunkt" von $(H^c_{1u},H^c_{2u},H^c_{3u})$ deutbaren Zentralriss der Erzeugenden t_4 durch den Augpunkt A_4. Die Erzeugende t_i entsteht als Schnitt der Verbindungsebenen $A_i \vee h_4$ und $A_i \vee h_j$. Das Spur-Fluchtspurpaar ersterer fällt in die Gerade $A_iA'_4$ das Spur-Fluchtspurpaar der zweiten besteht aus der Geraden A_iA_j und der zu ihr parallelen durch H^c_{ju}, siehe Figur 5. Damit fällt der Spurpunkt T_i von t_i in A_i und der Fluchtpunkt in den Schnittpunkt T^c_{ju} der genannten Fluchtspuren.

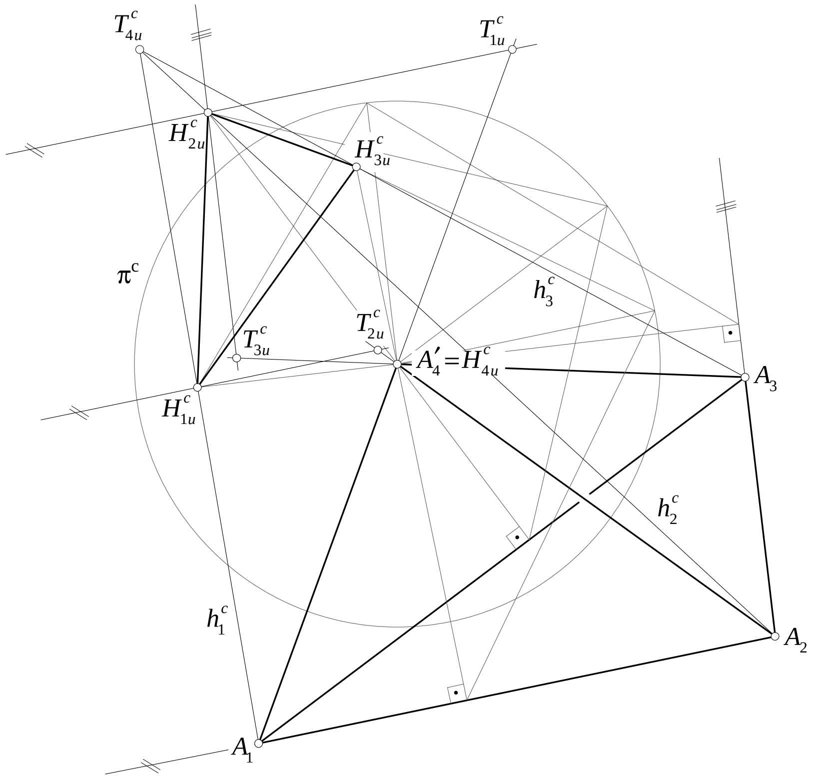

Figur 5: Zentralprojektion des Tetraeders $\mathbb{T}$ aus der Ecke A_4 auf (A_1,A_2,A_3) von $\boldsymbol{T}$. Der Fluchtpunkt von h_4 fällt in A'_4 die übrigen Höhenfluchtpunkte H^c_{ju} sind die Antipole der Seiten des Basisdreiecks (A_1,A_2,A_3) von $\boldsymbol{T}$. Die Dreiecke (A_1,A_2,A_3) und $(H^c_{1\mathrm{u}},H^c_{2u},H^c_{3u})$ sind perspektiv; das Perspektivitätszentrum ist der (projizierende) Zentralriss der durch A_4 gehenden Erzeugenden des ergänzenden Regulus zum Höhenregulus.

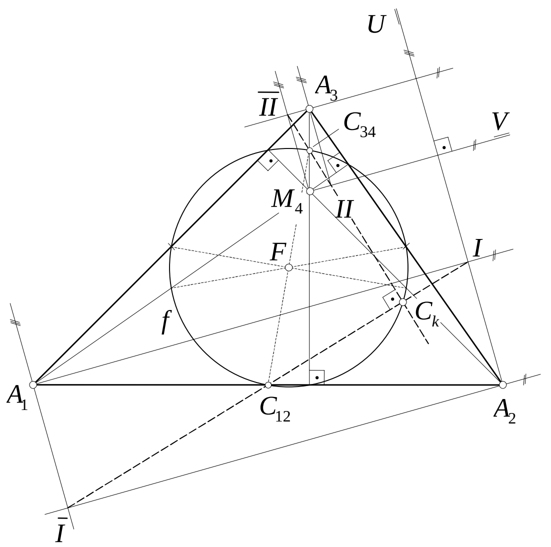

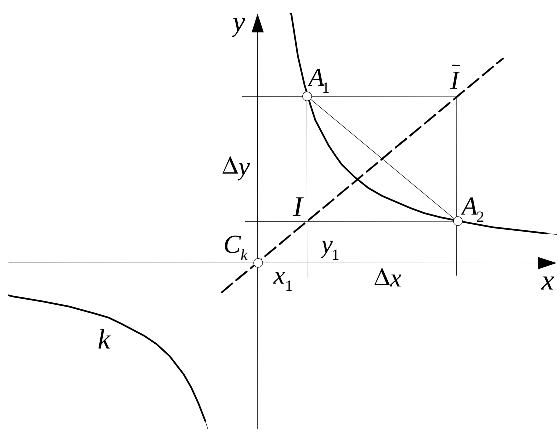

Figur 6a: Der Mittelpunkt jeder gleichseitigen Hyperbel durch ein Dreieck und dessen Höhenschnittpunkt liegt auf dem Feuerbach-Kreis dieses Punktsystems.

Figur 6b: Das zu einer Sehne einer Hyperbel k gehörige asymptotenparallele Parallelogramm besitzt eine durch den Mittelpunkt von k gehende Diagonale.

Bemerkung 7: Die Spurkurve k_4 der Trägerquadrik Ψ des Höhenregulus ist nach Bemerkung 5 eine gleichseitige Hyperbel durch das Viereck (A_1,A_2,A_3,M_4) und den Punkt A'_4 vgl. Figur 3. Man beachte dabei den

***Hilfssatz*:**

Die Mittelpunkte aller Kegelschnitte durch ein Dreieck und dessen Höhenschnittpunkt liegen auf dem FEUERBACH-Kreis des Dreiecks.

Da in einem Punktsystem bestehend aus einem Dreieck und dessen Höhenschnittpunkt jeder Punkt Höhenschnittpunkt des Rest-Dreiecks ist, und jedes dieser Dreiecke ein und denselben FEUERBACH-Kreis f besitzt, sprechen wir im Folgenden vom FEUERBACH-Kreis des Punktesystems.
Zum Beweis von Hilfssatz 1 projiziert man die vier Grundpunkte des Büschels aus Fernpunkten U und V orthogonaler Richtungen. Dabei repräsentieren U und V die Asymptotenfernpunkte einer speziellen gleichseitigen Hyperbel k durch diese Grundpunkte, vgl. Figur 6a und Figur 6b.
Zu einer Sehne $[A_1,A_2]$ gehörige Projektionsstrahlen geben Anlass zu einem Rechteck, vgl. Figur 6b, dessen zweite Diagonale ein Durchmesser von k ist. (Mit den Bezeichnungen aus Figur 6b folgt dies unmittelbar aus $x_1(y_1+\Delta y)=(x_1+\Delta x)y_1=\text{const.}$).

Für orthogonale Sehnen sind die entstehenden Rechtecke ähnlich und um $\pi/2$ gegeneinander verdreht. Deren "zweite" Diagonalen sind daher rechtwinklig und gehen durch die Sehnenmittelpunkte. Der Thaleskreis über der Sehnenmittenstrecke $[C_{12},C_{34}]$ ist aber genau der FEUERBACH-Kreis zu dem aus den vier Sehnenendpunkten bestehenden Punktsystem (vgl. hierzu auch [12]). Der Schwerpunkt dieses Punktsystems fällt übrigens in den Mittelpunkt F des FEUERBACH-Kreises. □

4 Die Kantenhöhen eines Tetraeders

Im Gegensatz zu den vier Eckenhöhen von $\mathbb{T}$, die liniengeometrisch abhängig sind und zu weiteren mit $\mathbb{T}$ verknüpften Gebilden in besonderen Relationen stehen, (siehe [4], u.a.), scheinen die Gemeinnormalen der drei Gegenkantenpaare eines Tetraeders, also die Kantenhöhen h_{i4} nur wenige nennenswerten Eigenschaften zu besitzen.

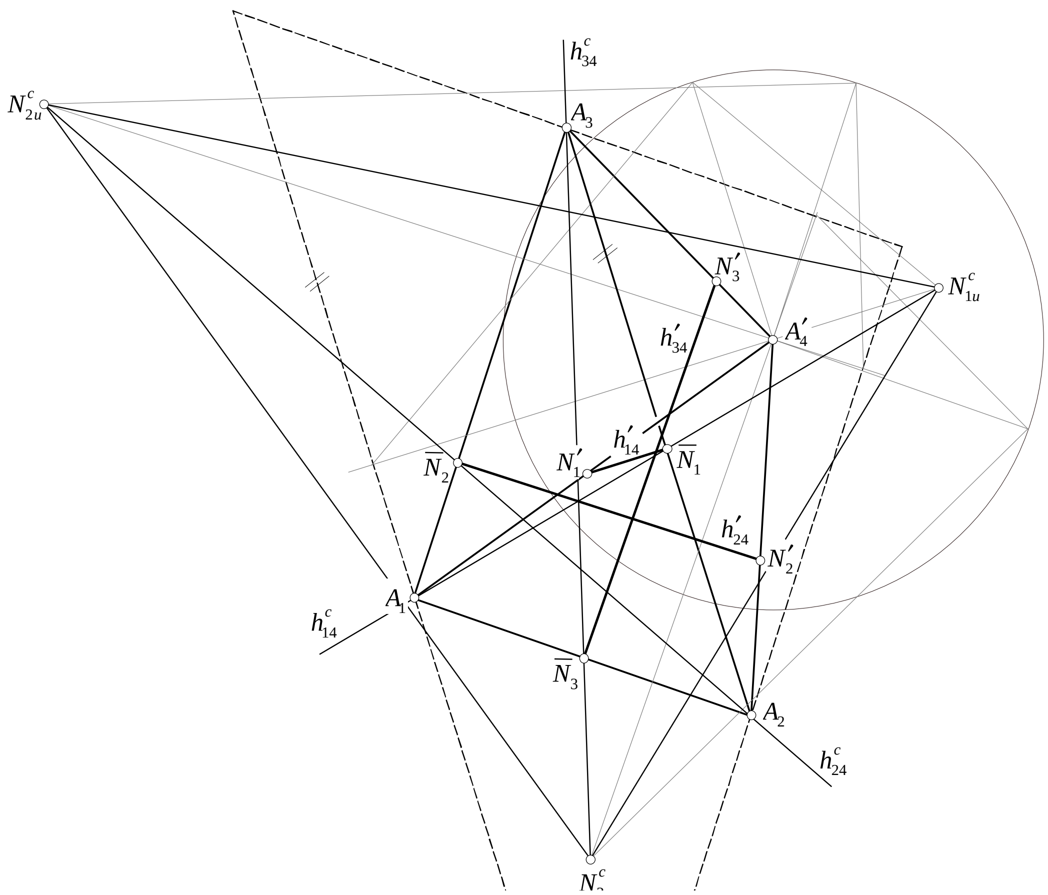

Figur 7: Konstruktion der Zentral- und Grundrisse der Kantenhöhen eines Tetraeders.

Für die konstruktive Behandlung erweist sich ebenfalls die oben verwendete Zentralprojektion aus der Tetraedeecke A_4 auf die Ebene α_4 der übrigen drei Ecken als zweckmäßig.

Die Spur der Richtebene ρ_i des Kantenpaares (A_iA_4, A_jA_k) verläuft durch A_i parallel zur Kante A_jA_k und fällt mit der Fluchtspur von ρ_i zusammen. Demnach ist das Fluchtpunktedreieck $(N^c_{1u}, N^c_{2u}, N^c_{3u})$ der drei Kantenhöhen h_{i4} jenes Dreieck, welches bezüglich der Antipolarität π^c des Distanzkreises von A_4 antipolar zu dem Basisdreieck von $\boldsymbol{T}$ seitenparallel umschriebenen Dreiseits ist, Figur 7. Folglich fallen die Zentralrisse h^c_{i4} der Kantenhöhen in die Verbindungsgeraden $A_iN^c_{iu}$, welche die Kante A_jA_k im Höhenfußpunkt $\overline{N}_i$ schneidet. Der Grundriss von h_{i4} ist dann parallel zu $A'_4N^c_{iu}$ und schneidet den Grundriss der Gegenkante A_4A_i im Normalriss des Höhenfußpunktes N_i.

Bemerkung 8: Offenbar bilden die Zentralrisse der Kantenhöhen im allgemeinen Fall ein Dreieck (vgl. Figur 7), andernfalls müssten die Dreiecke $(N^c_{1u}, N^c_{2u}, N^c_{3u})$ und $(A_1A_2A_3)$ perspektiv sein. Also sind die Kantenhöhen nicht für jedes Tetraeder $\boldsymbol{T}$ kopunktal und spannen einen Regulus Φ auf. Zur Konstruktion des Mittelpunktes N von Φ gehen wir wie in Bemerkung 3 vor: Wir konstruieren die zu einer Kantenhöhe h_{i4} parallele Treffgerade u_i aller Kantenhöhen als Schnittgerade der Verbindungsebenen eines Höhenfernpunktes mit den beiden übrigen Höhen, vgl. Figur 8. Die Spurkurve k von Φ enthält die drei Spurpunkte $\overline{N}_i$ der Kantenhöhen sowie die Spurpunkte U_i der zu ihnen parallelen Treffgeraden u_i und ist damit bestimmt. Das Zentralbild k^c_u der Fernkurve k_u von Φ besitzt mit k die selben Fernpunkte und ist durch diese und durch die Fluchtpunkte N^c_{iu} der Kantenhöhen festgelegt.

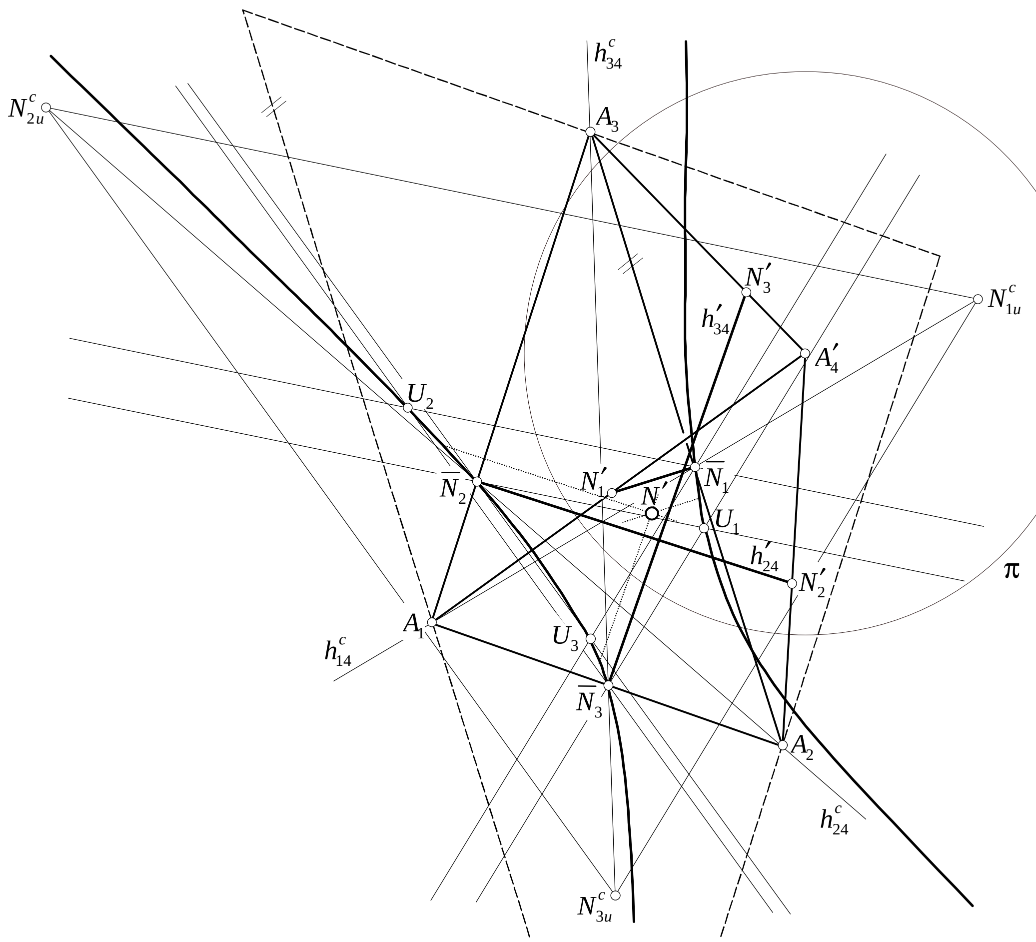

Figur 8: Konstruktion des Mittelpunktes N des Kantenhöhenregulus Ψ unter Benützung des Zentral- und Grundrisses der Kantenhöhen und der zu diesen parallelen Treffgeraden u_i aus dem ergänzenden Regulus.

Bemerkung 9: Auch für die Kantenhöhen ist die Diskussion sinnvoll, unter welchen Bedingungen der von den drei Kantenhöhen gebildete Regulus Φ ausartet oder eine Sonderform bildet.
Wir untersuchen im Folgenden den Fall schneidender Kantenhöhen.

Projiziert man ein Tetraeder $\boldsymbol{T}$ orthogonal auf eine Richtebene ρ zweier Kantenhöhen h_{24}, h_{34}, so muss $\boldsymbol{T}$ wegen des 'Satzes vom Normalriss eines rechten Winkels' als (vollständiges) Parallelogramm $\boldsymbol{T}^n = (A_1^n, \ldots, A_4^n)$ erscheinen. Die Kantenhöhenbilder h_{24}^n, h_{34}^n sind gewisse Normalen der parallelen Seitenpaare von $\boldsymbol{T}^n$; wir bezeichnen ihre auf den Tetraederkanten liegenden Fußpunkte mit 2, $\overline{2}$ bzw. 3, $\overline{3}$. Dann gilt, vgl. Figur 9.

Bedingung: Die Verbindung der Fußpunkte 2, $\overline{3}$ auf den von A_2 ausgehenden Kanten A_1A_2, A_2A_4 trifft die Kante A_1A_4 in einem Punkt und dieser gehört der Verbindungsgeraden der anderen Fußpunkte 2, $\overline{3}$ genau dann an, wenn h_{24} und h_{34} einander schneiden.

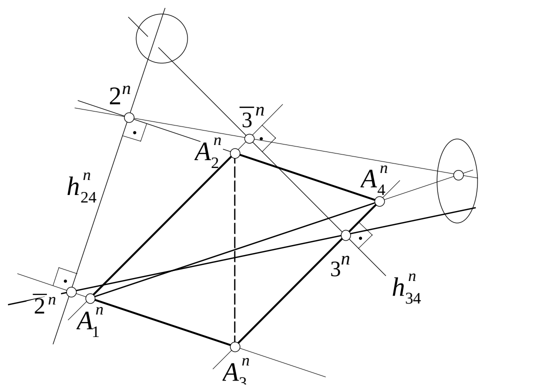

Figur 9: Normalprojektion eines Tetraeders auf eine Richtebene zweier schneidenden Kantenhöhen.

Zur Realisierung dieser Bedingung fassen wir in Figur 10 das Kantenbild $A_1^nA_4^n$ als Perspektivitätsachse q zweier Parallelbüschel der Richtbene ρ auf, deren Richtungen s und t normal zu h_{24}^n bzw. zu h_{34}^n sind. Dann liegt $Q := 2^n\overline{3}^n \vee 3^n\overline{2}^n$ genau dann auf q, wenn für die Büschelgeraden s_Q bzw. t_Q gilt

$$\mathrm{TV}(s_2, s_{\overline{2}}, s_Q) = \mathrm{TV}(t_3, t_{\overline{3}}, t_Q). \qquad \oplus$$

Diese Bedingung $\oplus$ kennzeichnet aber auch, dass die Dreiecke $(Q2^n\overline{2}^n)$ und $(Q3^n\overline{3}^n)$ ähnlich sind: Sie besitzen in Q gleiche Winkel und der Höhenfußpunkt auf der Q jeweils gegenüberliegenden Seite $(2^n, \overline{2}^n)$ bzw. $(3^n, \overline{3}^n)$ bildet mit deren Endpunkten gleiches Teilverhältnis, vgl. Figur 10. Daher stimmen auch die Winkel $\angle \overline{2}^n3^n\overline{3}^n$ und $\angle \overline{2}^n2^n\overline{3}^n$ überein und $\oplus$ ist gleichbedeutend damit, dass $(2^n, \overline{2}^n, 3^n, \overline{3}^n)$ ein Kreisviereck ist. Ist die Bedingung $\oplus$ erfüllt und legen wir die Richtebene ρ durch den Punkt 2, so fallen 2, $\overline{2}$, 3, $\overline{3}$ mit ihren Normalprojektionen zusammen. Somit gilt:

***Satz* 2 :**

Ein Tetraeder $\boldsymbol{T}$ besitzt genau dann zwei schneidende Kantenhöhen, wenn ihre Fußpunkte im Normalriss auf die Richtebene dieser Höhen ein Kreisviereck bilden. (Diese Fußpunkte bilden dann dieses Kreisviereck.)

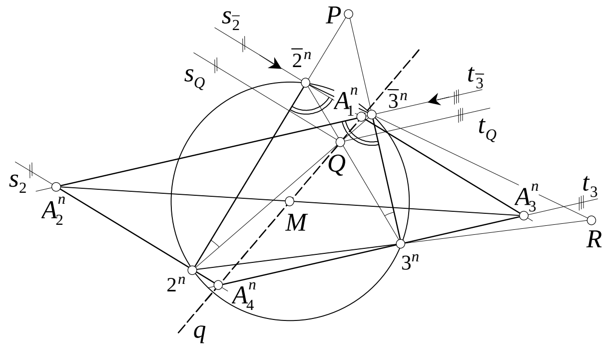

Figur 10: Normalprojektion eines Tetraeders auf eine Richtebene zweier schneidender Kantenhöhen.

Es interessiert die Lage der dritten Kantenhöhe im Fall eines schneidenden Kantenhöhenpaares.
Gibt man gemäß Satz 2 die Normalrisse zweier Kantenhöhen h_{24}, h_{34} auf deren Richtebene r durch den Punkt 2 zulässig vor, so sind die Normalrisse A_i^n der Tetraederecken A_i bestimmt. Gibt man dann noch den (orientierten) Distanzkreis [2] A_i^z eines der Punkte A_i vor, so sind die (orientierten) Distanzkreise A_j^z der übrigen Ecken A_j mitbestimmt: z.B. sind A_4^z und A_3^z zentrisch ähnlich, wobei das Ähnlichkeitszentrum ein Diagonalpunkt R des Fußpunktsvierecks der Höhen h_{24}, h_{34} ist. Für die Zykelpaare A_2^z, A_4^z bzw. A_3^z, A_4^z sind 2 bzw. 3 die Ähnlichkeitszentren, vgl. Figur 11. Damit kann die Tetraederkante A_2A_3 durch parallel verschoben werden. Ihr Spurpunkt $\tilde{R}$ und der Spurpunkt Q von A_4A_1 spannen die Fluchtspur n_u^c der Richtebene des dritten Kantenpaares von $\boldsymbol{T}$ auf, wenn man wieder A_4 als Augpunkt einer Zentralprojektion auf ρ auffasst. Der Antipol dieser Fluchtspur bezüglich A_4^z ist somit der Fluchtpunkt N_{1u}^c der gesuchten Höhe h_{14} die wiederum als Treffgerade aus N_{1u} an A_1A_4 und A_2A_3 bestimmt wird, vgl. Figur 11:
Die Spur e und die Fluchtspur e_u^c der projizierenden Ebene $N_{1u} \vee (A_4A_1)$ fallen in die Gerade QN_{1u}^c; die Ebene $N_{1u} \vee (A_2A_3)$ hat die Fluchtspur $f_u^c = \tilde{R}N_{1u}$ und die dazu parallele Spur f durch R, sodass sich der Spurpunkt N_1 von h_{14} im Schnitt von e und f findet. Variiert die Distanz von A_4,

[2] Wir benutzen also zusätzlich zum Normalriss auf die Richtebene ρ noch eine *"Zyklographie"* genannte Abbildung der Raumpunkte auf ihre orientierten Distanzkreise. Entsprechend heißt das zyklographische Bild eines Raumpunktes dessen *"Bildzykel"* und als Abbildungszeiger verwenden wir.

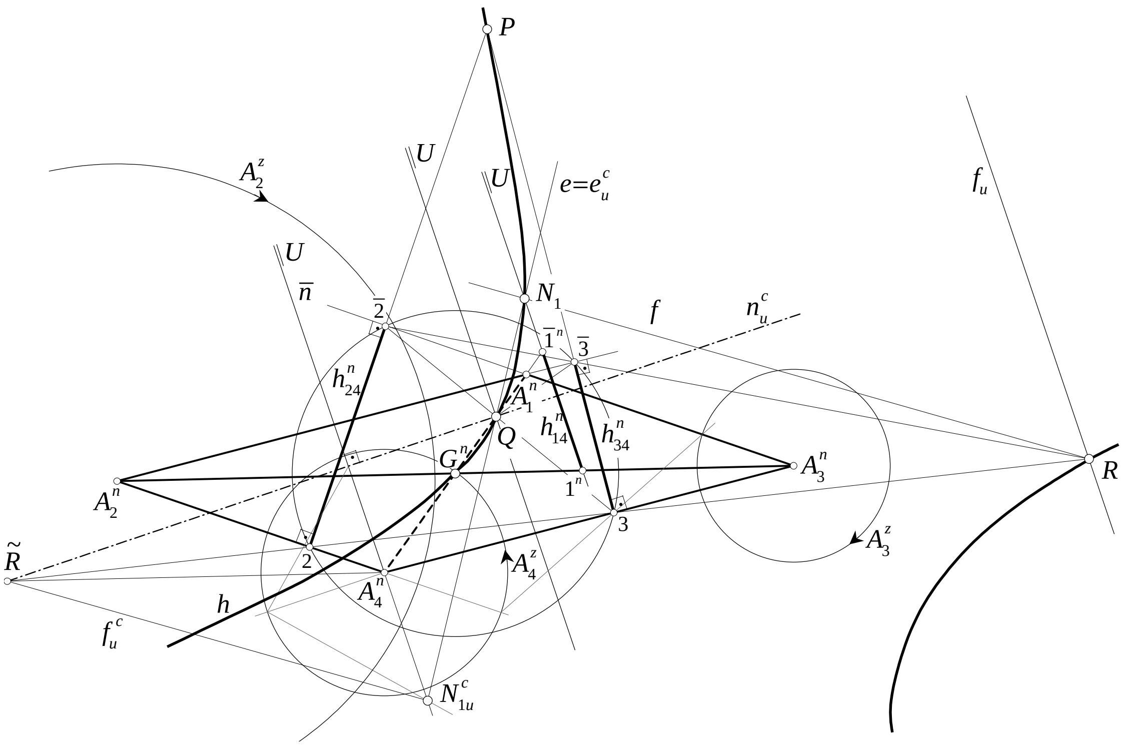

Figur 11: Konstruktion möglicher Tetraeder zu gegebenem Paar schneidender Kantenhöhen. Die dritte Höhe hat ihren Spurpunkt auf einer gleichseitigen Hyperbel durch die Diagonalpunkte des Fußpunktvierecks der schneidenden Höhen und den Mittelpunkt des Umkreises dieses Fußpunktvierecks.

so variiert der Spurpunkt N_1 der Höhe h_{14} als Erzeugnis projektiv gekoppelter Büschel um Q und um $\tilde{R}$ auf einem Kegelschnitt. Dieser enthält die Diagonalpunkte des Fußpunktsvierecks $(2,\overline{2},3,\overline{3})$ und den Mittelpunkt von dessen Umkreis. Letzterer ist Höhenschnittpunkt des Diagonaldreiecks; (vgl. hierzu auch [23, "Schmetterlingssatz"]), also ist der in Rede stehende Kegelschnitt eine *gleichseitige Hyperbel h*.

Da der Fluchtpunkt N^c_{1u} der Kantenhöhe h_{14} auf der zu n^c_u normalen Geraden $\overline{n}$ durch A^n_4 und mit dem zugehörigen Spurpunkt projektiv gekoppelt variiert, wobei der gemeinsame Fernpunkt U von $\overline{n}$ und der Hyperbel h dabei selbstentsprechend ist, durchläuft h_1 ein *Paraboloid*.

Zusammenfassend gilt also

***Satz* 3 :**

Es gibt zu vorgegebenem Paar von Kantenhöhen, deren Endpunkte ein Kreisviereck bilden, eine stetige Schar von Lösungstetraedern, die durch orthogonale perspektive Affinität auseinander hervorgehen. Die dritte Kantenhöhe variiert dabei auf einem Paraboloid, welches von der Ebene der beiden gegebenen Höhen nach einer gleichseitigen Hyperbel geschnitten wird.

Bemerkung 10: Wir schließen nun eine Kennzeichnung derjenigen Tetraeder $\boldsymbol{T}$ an, deren drei Kantenhöhen einander in einem gemeinsamen Punkt schneiden.

Aus der Schnittbedingung für je zwei Kantenhöhen gemäß Satz 2 folgt, dass sämtliche Höhenfußpunkte einer einzigen Kugel angehören müssen:

- Die Höhenfußpunkte liegen nie sämtlich komplanar, andernfalls die drei Kantenhöhen eine Richtebene ρ besizen müssten, wobei sich die Gegenkantenpaare von $\boldsymbol{T}$ bei Normalprojektion auf ρ in drei Paare paralleler Geraden projizieren. Ein vollständiges Viereck kann aber höchstens 2 Paare paralleler Gegenseiten haben.[3]
- Die Umkreise der vier Höhenfußpunkte von h_{14}, h_{24} und von h_{14}, h_{34} haben genau die Höhenfußpunkte 1, $\overline{1}$ von h_{14} gemeinsam, liegen also sämtlich auf einer Kugel.
- Im Normalriss auf die Ebene $\rho_j = h_{i4} \vee h_{k4}$ fällt der Mittelpunkt $\overline{N}$ dieser Kugel in den Mittelpunkt G^n des jeweiligen Tetraeder-Normalrisses, also stimmt $\overline{N}$ mit dem Schwerpunkt G von $\boldsymbol{T}$ überein.

Diese im Augenblick konstruktive nicht verwertbare Eigenschaft ergänzen wir durch eine weitere mit folgender, die Figur 11 weitgehend wiederholenden Konstruktion in Figur 12: Wählen wir den Spurpunkt N_1 von h_{14} im

[3] In affinen Nicht-FANO-Ebenen ist diese Aussage falsch.

Schnittpunkt P der beiden anderen Höhen, so ergibt sich N^c_{1u} als Schnitt von $\overline{n}$ mit $e = e^c_u = Q \vee P$.
Nun ist durch N^c_{1u} und n^c_u als Paar Antipol/Antipolare der Distanzkreis $A^z_4 =: \pi$ von A_4 bestimmt und es erweist sich $(Q, \tilde{R}, N^c_{1u})$ als Antipoldreieck von π^c. Die Kanten A_1A_4 und A_2A_3 mit den bezüglich π konjugierten Fluchtpunkten Q bzw. $\tilde{R}$ sind daher orthogonal!
Aus analogen Überlegungen für die Richtebenen $\rho_1 = h_{24} \vee h_{34}$ und $\rho_2 = h_{34} \vee h_{14}$ folgt unmittelbar, dass auch die anderen beiden Kantenpaare Fluchtpunkte $2 = A^c_{24u}, A^c_{13u}$ bzw. $3 = A^c_{34u}, A^c_{12u}$ besitzen, die bezüglich π^c konjugiert sind. Somit besitzt $\boldsymbol{T}$ drei Paare orthogonaler Gegenkanten und ist damit (bezüglich der Eckenhöhen) orthozentrisch. Umgekehrt besitzt jedes orthozentrische Tetraeder auch kopunktale Kantenhöhen, wobei deren Schnittpunkt und der Schnittpunkt der Eckenhöhen zusammenfällt. Zusammenfassend gilt

***Satz* 4 :**

Ein Tetraeder $\boldsymbol{T}$ besitzt genau dann drei kopunktale Kantenhöhen, (es heißt dann "kantenhöhen-orthozentrisch"), wenn es "eckenhöhen-orthozentrisch" ist, also drei Paare orthogonaler Gegenkanten besitzt. Für ein solches Tetraeder $\boldsymbol{T}$ fallen der Schnittpunkt der Kantenhöhen und derjenige der Eckenhöhen zusammen, was die Bezeichnung "orthozentrisch" für $\boldsymbol{T}$ rechtfertigt. Die Kantenhöhenfußpunkte gehören sämtlich einer im Schwerpunkt von $\boldsymbol{T}$ zentrierten Kugel an.

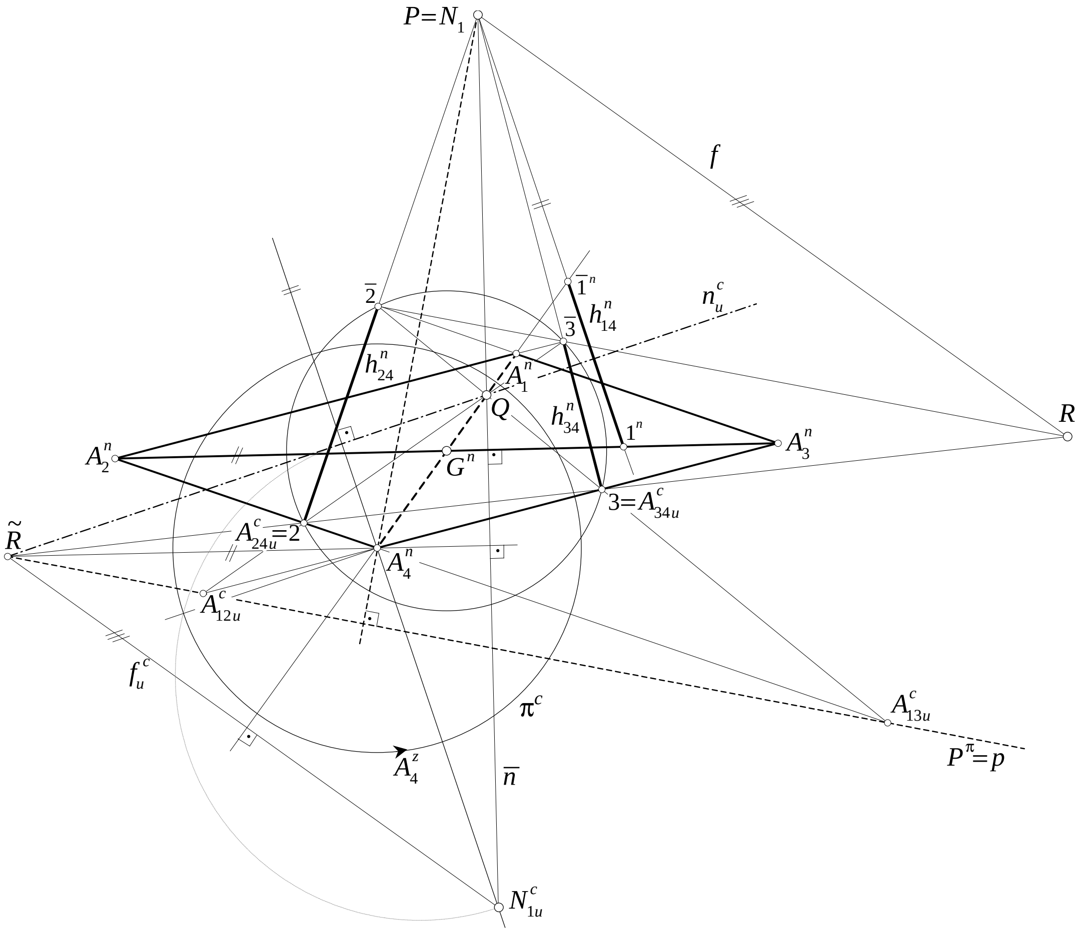

Figur 12: Konstruktion eines Tetraeders mit kopunktalen Kantenhöhen.

Literatur

[1] COUDERC, P.; BALLICCIONI, A.: *Premier Livre du Tètraèdre*, Gauthier-Villars, Paris, 1935.

[2] COURT, N. A.: *On the theory of the tetrahedron*, Bull. Am. Math. Soc., **48** (1942), 583-589.

[3] COURT, N. A.: *The biratio of the altitudes of a tetrahedron*, Duke Math. J., **13** (1946), 383-386.

[4] COURT, N. A.: *The tetrahedron and its altitudes*, Scripta Math., **14** (1948), 85-97.

[5] COURT, N. A.: *The semi-orthocentric tetrahedron*, Am. Math. Mon., **60** (1953), 306-310.

[6] COURT, N. A.: *Modern Pure Solid Geometry*, Chelsea, 2nd edition, New York, 1964.

[7] GERBER, L.: *The altitudes of a simplex are associated*, Math. Mag., **46** (1973), 155-157.

[8] FRITSCH, R.: *“Höhenschnittpunkte” für n- Simplizes*, Elemente Math., **31** (1976), 1-8.

[9] GRUENBERG, K. W.; WEIR, A. J.: *Linear Geometry*, Springer, New York - Heidelberg - Berlin, 1977.

[10] HAVLICEK, H.; WEISS, G.: *The Altitudes of a Tetrahedron and Traceless Quadric Forms* (eingereicht).

[11] KOMERELL, K.: *Vorlesungen über Analytische Geometrie des Raumes*, Koehler Amelang, Leipzig, 1953.

[12] LAPINE, M; LAPINE, M.: *Krivulja središta pramena konika*, KoG **3** (1998), 35-40.

[13] MANDAN, S. R.: *Altitudes of a simplex in n-space*, J. Aust. Math. Soc., **2** (1962), 403-424.

[14] MANDAN, S. R.: *Uni- and demi-orthocentric simplexes*. II, J. Indian Math. Soc., n. Ser., **26** (1962), 5-11.

[15] MANDAN, S. R.: *Altitudes of a general n-simplex*, J. Aust. Math. Soc., **5** (1965), 409-415.

[16] MICULITA, M.: *On a property of the anticentre of a tetrahedron*, Gaz. Mat., Bucur., **93** (1988), 100-102.

[17] ROSENFELD, B.A.; JAGLOM, I.M.: *Mehrdimensionale Räume*, In Alexandroff, P. S. and Markuschwitsch, A. I. and Chintschin, A. J. (ed.): Enzyklopädie der Elementarmathematik, Bd. V, VEB Dt. Verlag d. Wissenschaften, Berlin, 1969.

[18] SATYANARAYANA, K.: *The tetrahedron the feet of whose altitudes are coplanar*, Math. Stud., **50** (1982), 275-281.

[19] SEMPLE, J.G.; KNEEBONE, G.T.: *Algebraic Projective Geometry*, Oxford University Press, Oxford, 1998 (Reprint).

[20] SCHRÖTER, H.: *Theorie der Oberflächen zweiter Ordnung und der Raumkurven dritter Ordnung als Erzeugnisse projektivistischer Gebilde*, B.G. Teubner, Leipzig, 1880.

[21] SLIEPČEVIĆ, A.: *Aus dem Erdgeschoß der höheren Geometrie*, KoG **5** (2000/01), 73.

[22] SLIEPČEVIĆ, A.: *Eine Anwendung der perspektiven Kollineation*, KoG **5** (2000/01), 51-55.

[23] SLIEPČEVIĆ, A.: *A geneneralisation of the butterfly theorem* (im Druck).

[24] THIEME, H.: *Zur Geometrie des Tetraeders*, Z. Math. Phys., **27** (1882), 56-61.

[25] WUNDERLICH, W.: *Ebene Kinematik*, B.I. Hochschultaschenbücher 447, 1970.

[26] ZACHARIAS, M.: *Elementargeometrie und elementare nicht-euklidische Geometrie in synthetischer Behandlung*, In Meyer, W.Fr. and Mohrmann, H.: Enzyklopädie der Mathematischen Wissenschaften III 1.2, B.G. Teubner, Leipzig, 1914-1931.

Gunter Weiss
Institute of Geometry
Dresden University of Technology
D-01062 Dresden
tel.: +49-351-463 37516, fax: +49-351-463 36027
e-mail: weiss@math.tu-dresden.de
URL: http://www.math.tu-dresden.de/ weiss/index.html

Hans Havlicek
Institute of Geometry
Vienna University of Technology
Wiedner Hauptstraße 8-10/1133, A-1040 Wien
tel: +43-1-588 01 11330 fax: +43-1-588 01 11399
e-mail: havlicek@geometrie.tuwien.ac.at
URL: http://www.geometrie.tuwien.ac.at/havlicek/

MILJENKO LAPAINE

O problemu istoznačnica u matematičkoj terminologiji

Sve šira primjena geodezije u raznim oblicima ljudske djelatnosti, kao i utjecaj općeg razvitka znanosti i tehnike na geodeziju, znatno su proširili opseg jezika kojim se danas geodeti služe. Već se duže vrijeme osjeća u našoj geodetskoj djelatnosti, i to u znanstvenom, nastavnom i stručnom radu, nedostatak rječnika u kojima bi bilo zabilježeno stručno nazivlje kakvo se danas upotrebljava.

Na hrvatskom jeziku objavljen je 1977. god. *Višejezični kartografski rječnik* što su ga priredili nastavnici Zavoda za kartografiju Geodetskog fakulteta. Taj rječnik može poslužiti kao osnovni izvor za područje kartografije. Osim toga 1980. god. objavljen je *Višejezični geodetski rečnik* u izdanju tadašnjeg Saveza geodetskih inženjera i geometara Jugoslavije. Međutim, taj nas rječnik ni u terminološkom, ni u jezičnom pogledu ne zadovoljava.

Stoga je Državnoj geodetskoj upravi 1995. godine predložen projekt izrade geodetskog rječnika. Ideja je prihvaćena i od tada se jezična građa prikuplja i obrađuje. Bilo je predviđeno da će rad na projektu trajati tri godine, no to je razdoblje udvostručeno. Voditelj projekta je prof. dr. sc. Nedjeljko Frančula, a suradnici su aktivni i umirovljeni nastavnici te pojedini poslijediplomanti Geodetskog fakulteta Sveučilišta u Zagrebu.

Geodetski rječnik koji se pomalo dovršava obuhvaća termine iz sljedećih područja (navedenih abecednim redoslijedom): fizika, fizikalna geodezija, fotogrametrija i daljinska istraživanja, geodetski instrumenti, informatika, inženjerska geodezija, kartografija, katastar i zemljišna knjiga, matematika, metrologija, praktična geodezija, viša geodezija i ostalo.

Pojedini termin obavezno obuhvaća definiciju i podatke o području kojem pripada i o autoru, tj. osobi koja je taj termin obradila. U neobaveznom dijelu mogu doći istoznačnice, upute na srodne termine, engleski, francuski i njemački ekvivalent i upotrijebljena literatura. Ilustrirajmo to na dva primjera iz matematičkog dijela rječnika:

binom

Također: dvočlani izraz; dvočlan
Algebarski izraz koji se sastoji od dva člana; npr. $2x+5y$ ili $2-(a+b)$.
Vidi: monom, trinom, polinom
Područje: matematika
En. binomial
Fr. binôme
Nj. Binom
Lit. Gusić: Matematički rječnik
Autor: Lapaine

promjer

Također: dijametar
Promjer kružnice je dužina koja spaja dvije točke kružnice i prolazi središtem kružnice. Ujedno je i duljina te dužine. Analogno se definiraju promjeri kruga, sfere i kugle. Promjer se može definirati i za općenitije skupove.
Vidi: tetiva, polumjer
En. diameter, diametre
Fr. diamètre
Nj. Durchmesser, Diameter
Lit. Gusić: Matematički rječnik
Autor: Lapaine

Pri izradi matematičkog dijela geodetskog rječnika pojavio se problem obrade istoznačnica ili sinonima. Prirodno se postavilo pitanje treba li uvijek dati prednost hrvatskoj riječi pred stranom ili posuđenicom. Ima li možda neki drugi ključ kojim bi se riješio uočeni problem? Odgovor na to pitanje potražen je na sastanku Hrvatskoga društva za konstruktivnu geometriju i kompjutorsku grafiku, održanom 26. veljače 2001. Nakon kraćeg usmenog objašnjenja, dvadeset nastavnika matematičkih kolegija, uglavnom s hrvatskih tehničkih fakulteta, zamoljeno je za sudjelovanje u anketi koju donosim u nastavku u izvornom obliku:

Molim od predloženih parova izabrati onaj koji je po Vašem mišljenju kod nas uobičajeniji i označiti ga znakom $\surd$. Ukoliko se po Vašem mišljenju ne radi o sinonimima, molim staviti znak $\neq$.

baza	osnovica
bisektrisa	simetrala kuta
centar	središte
čunjosječnica	konika
djelitelj	divizor
direktrisa	ravnalica
faktor	djelitelj
fokus	žarište
generatrisa	izvodnica
granična vrijednost	limes
homogenost	jednorodnost
interpolacija	umetanje
iteracija	ponavljanje
koeficijent	faktor
medijan	težišnica
modul	apsolutna vrijednost
nesumjerljiv	inkomenzurabilan
paralelnost	usporednost
paralelogram	romboid
poligon	mnogokut
polumjer	radijus
prirast	priraštaj
promjer	dijametar
segment	odsječak
simetrala	os simetrije
produkt	umnožak
spirala	zavojnica
stožac	konus
valjak	cilindar

Anketa je anonimna, ali ako želite slobodno se potpišite. Cilj ankete je utvrđivanje prioritetnih naziva u hrvatskoj matematičkoj terminologiji. Rezultati ankete upotrijebit će se pri izradi geodetskog rječnika.

Zahvaljujem na uloženom trudu!

Svi prisutni odazvali su se pozivu. Rezultati ankete prikazani su i zorno na slici 1. Točke koje u koordinatnoj ravnini određuju parovi istoznačnica označene su kvadratićima. Koordinate svake točke predstavljaju broj izbora jedne, odnosno druge inačice pojedinog termina. Sa slike se ne vidi o kojim je istoznačnicma riječ, ali se svakako lijepo vidi da nema nekog općeg zakona ili čarobne formule koja bi dala globalno rješenje na postavljeno pitanje. Koso postavljeni pravci su pomoćni pravci koji će nam pomoći u donošenju zaključaka. Najprije uočimo značenje srednjeg pravca. Kad bi točka pripadala tome pravcu, to bi značilo da je broj ispitanika za obje inačice međusobno jednak. Što je točka bliža tome pravcu, to znači da se broj ispitanika koji su se odlučili za jednu ili drugu inačicu manje razlikuje. I obratno, što je točka udaljenija od srednjeg pravca, to znači da se broj ispitanika koji su se odlučili za jednu inačicu, jače razlikuje od broja onih koji su izabrali drugu inačicu. Nacrtana elipsa izdvaja ”sumnjive” istoznačnice, tj. one parove za koje je velik dio ispitanika ustvrdio da nisu istoznačnice.

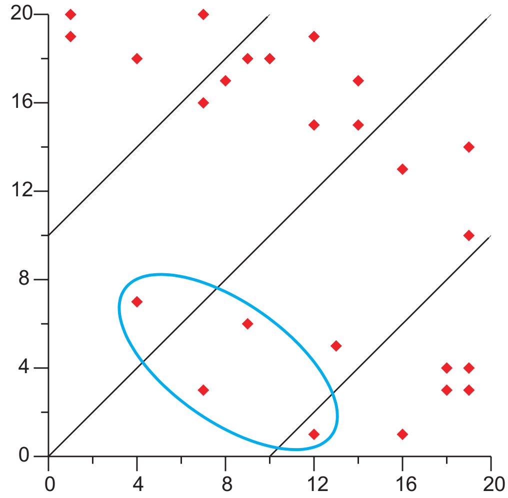

Slika 1. Grafički prikaz rezultata ankete

Na primjer, točka s koordinatama (1, 20), predstavlja par (generatrisa, izvodnica), a znači da je samo jedan ispitanik odabrao inačicu *generatrisa*, a dvadeset ispitnika inačicu *izvodnica*.

Točke koje su na slici 1 u gornjem lijevom uglu ili u donjem desnom uglu predstavljaju termine kod kojih su ispitanici dali veliku prednost jednoj od dvije ponuđene inačice.

Točke koje su na slici 1 bliže srednjem pravcu predstavljaju termine kod kojih su ispitanici dali izvjesnu prednost jednoj od dvije ponuđene inačice.

Za pojedine ispitanike nisu istoznačnice: bisektrisa i simetrala kuta, faktor i djelitelj, homogenost i jednorodnost, koeficijent i faktor, poligon i mnogokut, segment i odsječak, paralelogram i romboid, simetrala i os simetrije. U tablici 3 prikazani su oni takvi parovi za koje veći broj ispitanika smatra da to nisu istoznačnice. Pogledajmo pobliže svaki od tih parova.

Tablica 1. Parovi istoznačnica kod kojih se jedna upotrebljava prilično rijetko, a druga vrlo često

Upotrebljava se prilično rijetko	*Upotrebljava se prilično često*
bisektrisa	simetrala kuta
centar	središte
čunjosječnica	konika
divizor	djelitelj
generatrisa	izvodnica
jednorodnost	homogenost
umetanje	interpolacija
medijan	težišnica
inkomenzurabilan	nesumjerljiv
priraštaj	prirast
konus	stožac
cilindar	valjak

Tablica 2. Obje se istoznačnice upotrebljavaju često, a ispitanici su dali izvjesnu prednost terminu u lijevom stupcu

osnovica	baza
ravnalica	direktrisa
žarište	fokus
limes	granična vrijednost
apsolutna vrijednost	modul
paralelnost	usporednost
mnogokut	poligon
polumjer	radijus
promjer	dijametar
odsječak	segment
produkt	umnožak
zavojnica	spirala

Tablica 3. "Sumnjive" istoznačnice

		Broj ispitanika za koje navedeni parovi nisu istoznačnice
faktor	djelitelj	10
koeficijent	faktor	8
paralelogram	romboid	15
simetrala	os simetrije	10

Faktor i djelitelj

Deset ispitanika smatralo je da to nisu istoznačnice, četiri daje prednost terminu *faktor*, a sedam terminu *djelitelj*. U drugom razredu osnovne škole uči se množenje i da se pritom u izrazu $ab = c$, a naziva množenikom, b množiteljem, a c umnoškom. Nekada smo učili da se množenje još naziva multiplikacijom, a multiplikandom, b multiplikatorom, a c produktom. Množenik i množitelj, odnosno multiplikand i multiplikator zajednički se nazivaju faktorima. S druge strane, u drugom razredu osnovne škole također se uči dijeljenje i da se pritom u izrazu $a : b = c$, a naziva djeljenikom, b djeliteljem, a c količnikom. Nekada smo učili da se dijeljenje još naziva divizijom, a dividendom, b divizorom, a c kvocijentom (Krajnović, 1999/2000).

Uzevši u obzir navedeno, u prvi se čas čini da termini *faktor* i *djelitelj* ne mogu biti istoznačnice jer se pojavljuju pri različitim računskim operacijama - faktor pri množenju, a djelitelj pri dijeljenju. Međutim, ako npr. pogledamo u Višu algebru Đ. Kurepe (1965) vidjet ćemo da se tvrdnje "k je kratnik od m", "k je djeljivo s m" ili "k je kongruentno 0 modulo m", mogu izreći i ovako: "m je faktor od k", "m je mjera od k" ili "m je djelilac od k".

U Matematičkom rječniku (Gusić, 1995) stoji: FAKTOR - djelitelj, čimbenik. Na primjer, prirodni brojevi 1, 2, 3, 4, 6 i 12 su faktori (djelitelji) broja 12. Broj 12 nije pravi faktor, a ostali jesu. Polinom $g(x) = x - 1$ jest faktor polinoma $f(x) = x^3 - x^2 + x - 1$. Naime, $x^3 - x^2 + x - 1 = (x-1)(x^2+1)$.

U The Pan Dictionary of Mathematics (Gibson, 1990) stoji: **factor** (divisor) A number by which another number is divided. See also common factor.

U jednom drugom matematičkom rječniku (Clapham, 1990): **factor** See divides

divides Let a and b be integers. Then a **divides** b (which may be written as $a|b$) if there is an integer c such that $ac = b$. It is said that a is a **divisor** or **factor** of b, that b is **divisible** by a, and that b is a **multiple** of a.

Na temelju izloženoga, mogli bismo zaključiti da se termini faktor i djelitelj ipak mogu smatrati istoznačnicama.

Koeficijent i faktor

Osam ispitanika smatralo je da to nisu istoznačnice, 12 je dalo prednost terminu *koeficijent*, a samo jedan *faktoru*. U Matematičkom rječniku (Gusić, 1995) piše:

KOEFICIJENT - pojam koji se rabi u raznim okolnostima u matematici.
1. koeficijent polinoma ili algebarske jednadžbe je broj koji množi neki od monoma. Tako je u jednadžbi $x^2-3x+5=0$, broj 5 nulti (slobodni), -3 prvi, a 1 drugi (vodeći) koeficijent.
2. koeficijent smjera pravca s jednadžbom $y=kx+l$ jest broj k.
3. koeficijent sličnosti dvaju sličnih trokuta je kvocijent duljina odgovarajućih stranica. Analogno se definira koeficijent sličnosti dvaju sličnih geometrijskih likova ili tijela.

Dakle, mogli bismo zaključiti da koeficijent može biti faktor (kao što je to npr. u slučajevima 1. i 2.), ali i ne mora biti (slučaj 3.). Međutim, iako je -3 faktor u produktu $-3x$, ne kaže se da je -3 faktor polinoma $P(x)=x^2-3x+5$ ili faktor jednadžbe $x^2-3x+5=0$, nego se kaže da je -3 koeficijent polinoma, odnosno koeficijent u jednadžbi (primjer 1.). Isto tako, iako je k faktor u produktu kx, ne kaže se da je k faktor jednadžbe $y=kx+l$, nego njezin koeficijent što stoji uz x (primjer 2.).

Paralelogram i romboid

Petnaest ispitanika smatralo je da to nisu istoznačnice, sedam daje prednost terminu paralelogram, a tri terminu romboid. Pogledajmo zbog čega čak 75% ispitanika ne prihvaća paralelogram i romboid za sinonime. U Matematičkom rječniku (Gusić, 1995) čitamo:

PARALELOGRAM (usporednik) - četverokut kojemu su suprotne stranice paralelne. Ekvivalentno: paralelogram je četverokut kojemu se dijagonale prepolavljaju. Također, paralelogram je četverokut kojemu su suprotne stranice jednake. Paralelogram kojemu su nutarnji kutevi pravi jest pravokutnik, a paralelogram koji ima jednake stranice jest romb; ako je ispunjeno i jedno i drugo, paralelogram je kvadrat.

Pojam romboid naći ćemo u jednom drugom matematičkom rječniku (Manturov i dr., 1969): ROMBOID - vidi Deltoid.

DELTOID - konveksni čeverougao $ABCD$ koji ima jednu osu simetrije (dijagonala BD na slici). Deltoid se naziva i romboidom.

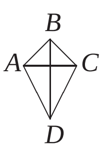

U Hrvatskom općem leksikonu (Kovačec, 1996) čitamo: **romboid** (grč.), paralelogram s nasuprotnim stranicama jednake duljine i kutovima različitima od pravog, od kojih su nasuprotni jednaki.

U Rječniku stranih riječi (Anić, Goldstein 1999): **romboid** kosi četverokut jednakih nasuprotnih strana.

U vrlo opsežnom američkom rječniku (Flexner, 1993) stoji slika i sljedeći tekst: **rhomboid** an oblique-angled parallelogram with only opposite sides equal

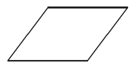

Ako pogledamo definiciju paralelograma naći ćemo sljedeću sliku i tekst:

parallelogram quadrilateral having both pairs of opposite sides parallel to each other

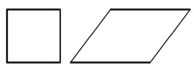

U The Pan Dictionary of Mathematics (Gibson, 1990) stoji: **rhomboid** A parallelogram that is neither a rhombus nor a rectangle. See parallelogram.

parallelogram A plane figure with four straight sides, and with opposite sides parallel and of equal length. The opposite angles of a parallelogram are also equal. In the special case in which the angles are all right angles the parallelogram is a rectangle; when all the sides are equal it is a rhombus.

Iz navedenoga je očito da dok je pojam paralelograma manje-više jasan, postoje različita poimanja pojma romboid. Za neke je to sinonim za paralelogram, za druge je specijalni slučaj paralelograma, a za treće deltoid, tj. četverkout koji općenito nije paralelogram.

Simetrala i os simetrije

Deset ispitanika smatralo je da to nisu istoznačnice, devet daje prednost terminu simetrala, a šest terminu os simetrije.

U Matematičkom rječniku (Gusić, 1995) piše: SIMETRALA (raspolovnica, sumjernica) 1. simetrala podskupa ravnine jest pravac s obzirom na koji je taj podskup

osno simetričan (os simetrije). Tako se govori o simetrali dužine (pravcu koji je okomit na dužinu i prolazi njezinim polovištem), simetrali I. i III. kvadranta (pravcu s jednadžbom $y = x$), simetrali dvaju pravaca koji se sijeku u točki. Neki podskupovi ravnine nemaju simetrale, dok je svaki pravac koji prolazi središtem kruga, simetrala kruga. Taj se naziv katkad upotrebljava u nešto drugačijem značenju. Tako je:
a) simetrala kuta jest zraka s početkom u vrhu kuta kojoj je bar još jedna (dakle sve) točka jednako udaljena od krakova kuta.
b) simetrala kuta trokuta jest simetrala tog kuta, ali i dužina određena vrhom kuta i točkom u kojoj simetrala kuta siječe suprotnu stranicu trokuta, a i duljina te dužine.
2. simetrala podskupa prostora jest ravnina s obzirom na koju je taj podskup simetričan (ravnina simetrije). Tako se govori o simetrali dužine (ravnini koja je okomita na dužinu i prolazi polovištem dužine), simetrali dviju ravnina kojima je presjek pravac, itd.

Dakle, možemo na kraju zaključiti da je *simetrala* općenitiji pojam od *osi simetrije*.

Zaključak

Na temelju provedene ankete i njezine obrade može se donijeti nekoliko zaključaka. Prvi je da na hrvatskom jeziku nemamo sveobuhvatnijeg matematičkog rječnika. Drugi je da za veći broj matematičkih pojmova postoji dvojnost u nazivima. Anketa je pokazala da tu dvojnost nije moguće riješiti na jednostavan način, tj. da ne postoji neko jasno pravilo za odabir. Jedanput se prednost daje hrvatskoj riječi, a drugi put posuđenici. Treći je zaključak da postoje matematički pojmovi za čije nazive među matematičarima, a pogotovo među autorima raznih rječnika (koji obično nisu matematičari) postoji izvjesna nesigurnost i kolebljivost. Možda bi jedan od zadataka Hrvatskoga društva za konstruktivnu geometriju i kompjutorsku grafiku mogao biti izrada rječnika pojmova iz područja kojima se društvo bavi.

Literatura

Anić, V., Goldstein, I. (1999): Rječnik stranih riječi, Novi Liber, Zagreb.

Flexner, S. B. (ed., 1993): Random House Unabridged Dictionary, Radnom House, New York.

Gibson, E. (ed., 1990): The Pan Dictionary of Mathematics, Pan Books, London.

Gusić, I. (1995): Matematički rječnik, Element, Zagreb.

Kovačec, A. (urednik, 1996): Hrvatski opći leksikon, Leksikografski zavod ”Miroslav Krleža”, Zagreb.

Krajnović, M. (1999/2000): Rječnik matematičkih naziva, Matematičko-fizički list, izvanredni broj.

Kurepa, Đ. (1965): Viša algebra, Knjiga I, Školska knjiga, Zagreb.

Manturov, O. V., Solncev, J. K., Sorkin, J. I., Fedin, N. G. (1969): Rečnik matematičkih termina sa tumačenjima, Naučna knjiga, Beograd.

ANA SLIEPČEVIĆ

Koliko poznajemo perspektivnu kolineaciju?

U prošlom broju KoG-a u članku "Eine Anwendung der perspektive Kollineation" na nekoliko je primjera pokazana velika primjenjivost perspektivne kolineacije u rješavanju zadataka vezanih uz krivulje drugoga stupnja konstruktivnom metodom. Neka sljedeći zadatak bude samo još jedan u nizu zadataka toga tipa.

Zadatak

S pet točaka A, B, C, D, E zadana je hiperbola. Odredite joj središte, osi i asimptote.

Analiza rješenja:

Prema položaju zadanih točaka evidentno je zadana hiperbola. Osnovni nam je cilj konstruirati joj asimptote, jer tada će joj osi biti simetrale kuteva među asimptotama, a u njihovom će sjecištu biti središte hiperbole. Analizirat ćemo ovdje dvije mogućnosti rješenja, te jedno od njih i konstruirati.

Prvi način

Ako dobro vladamo projektivitetima, pa ako znamo nadopunjavati kolokalne [1, str. 23], pa i beskonačno daleke projektivne nizove, zadatak možemo riješiti na sljedeći način.

Spojimo li dvije od zadanih pet točaka, npr. točke A i B s preostale tri točke hiperbole, dobivamo dva projektivna pramena pravaca (A) i (B), koji proizvode zadanu hiperbolu. Beskonačno daleki pravac siječe ova dva pramena u dva kolokalna projektivna niza točaka [1, str. 23], a njihove će dvostruke točke biti beskonačno daleke točke hiperbole. U tim se točkama onda mogu konstruirati tangente, dakle asimptote, uz pomoć npr. Pascalova teorema [1, str. 38].

Drugi način

Ukoliko ne prijateljujemo s projektivitetima, ali zato poznajemo sve tajne perspektivne kolineacije u ravnini, zadatak se može i ovako riješiti.

Treba odrediti elemente (os, središte i par pridruženih točaka) jedne od beskonačno mnogo mogućih perspektivnih kolineacija u ravnini, koje će zadanu hiperbolu preslikati u kružnicu, pri čemu će se beskonačno daleke točke hiperbole preslikati u sjecišta te kružnice s nedoglednim pravcem te perspektivne kolineacije. Tangente kružnice u tim sjecištima bit će kolinearne slike asimptota, pa je same asimptote iz te činjenice lako moguće konstruirati. Uz pretpostavku da je ova druga mogućnost rješenja većini prihvatljivija, opisat ćemo odgovarajući konstruktivni postupak.

Konstruktivno rješenje:

Po analogiji rješavanja zadataka u prethodnom broju KoG-a [[2]] potrebno je po volji odabrane četiri zadane točke, npr. A, B, C, D preslikati u vrhove pravokutnika. Tom pravokutniku opisana kružnica mora biti kolinearna slika hiperbole, a na njoj mora ležati i kolinearna slika točke E.

Da bi se četverokut $ABCD$ preslikao u paralelogram $A'B'C'D'$, moraju sjecišta N_1, N_2 njegovih nasuprotnih stranica ležati na izbježnom pravcu i te perspektivne kolineacije, a da bi to bio pravokutnik, moraju mu susjedne stranice biti medusobno okomite. Slijedi da je spojnica N_1N_2

izbježni pravac perspektivne kolineacije kojoj se središte S mora nalaziti na Talesovoj kružnici s promjerom $\overline{N_1N_2}$.

Da bi se kolinearna slika E' točke E nalazila na spomenutoj kružnici, moraju se spojnice EA i ED preslikati u međusobno okomite tetive nad promjerom $\overline{AD}$ kružnice. Slijedi da se sjecišta $M_1 = EA \cap i$, $M_2 = ED \cap i$, moraju preslikati u beskonačno daleke točke međusobno okomitih smjerova. Središte perspektivne kolineacije stoga mora ležati i na Talesovoj kružnici s promjerom $\overline{M_1M_2}$. Time je središte S tražene perspektivne kolineacije određeno u sjecištu spomenutih dviju Talesovih kružnica.

Os kolineacije o postavimo po volji paralelno s izbježnim pravcem. Točku A' pridruženu točki A odredimo kao sjecište zrake $\overline{SA}$ perspektivne kolineacije s pravcem koji je paralelan s $\overline{SN_2}$ i prolazi sjecištem $o \cap \overline{AB}$.

Sada smo u mogućnosti konstruirati kružnicu h' koja je pri ovako odabranoj perspektivnoj kolineaciji slika zadane hiperbole h.

Odredimo li nedogledni pravac n' ove kolineacije, njegova će sjecišta A_1', A_2' s kružnicom h' biti slike beskonačno dalekih točaka hiperbole, a tangente kružnice u tim točkama bit će slike asimptota, pa je zadatak riješen.

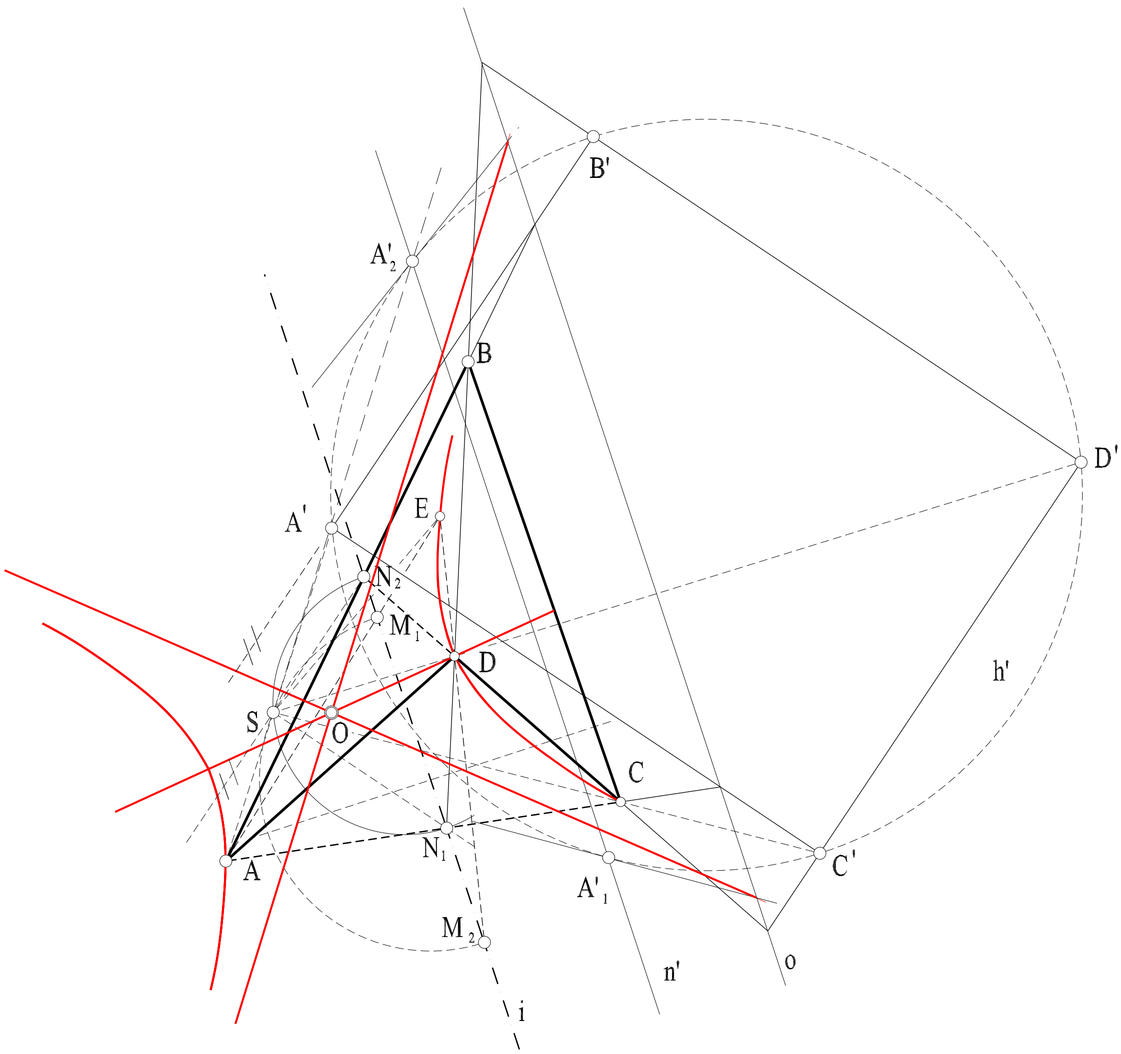

Literatura

[1] Niče, V., *Uvod u sintetičku geometriju*, Školska knjiga, Zagreb, 1956

[2] Sliepčević, A., *Eine Anwendung der perspektive Kollineation*, KoG 5-2000/01, 51-55.

LIDIJA PLETENAC

Hipar - aproksimacija minimalne plohe

Minimalne plohe

U graditeljstvu i arhitekkturi, posebno na području najnovijih laganih konstrukcija, minimalne plohe su od izuzetnog značaja zbog svojih osobina. Naprezanja konstrukcija na takvoj plohi u ravnotežnom stanju jednolika su i uvijek u dirnoj ravnini plohe. No, te idealne oblike konstrukcije teško je postići zbog anizotropnosti materijala. Nekad se namjerno odustaje od minimalne plohe da bi se zadovoljilo neke druge uvjete.

Minimalne plohe dobiju se minimalizacijom površine za dane rubne uvjete. Karakterizira ih srednja zakrivljenost jednaka nuli u svakoj točki. One zadovoljavaju Lagrangeove diferencijalne jednadžbe:

$$(1+f_y^2)f_{xx}+2f_xf_yf_{xy}+(1+f_x^2)f_{yy}=0. \tag{1}$$

Minimalne plohe su beskonačne, vitopere (što garantira geometrijsku krutost konstrukcije) i lokalno sedlastog oblika. Ima ih beskonačno mnogo, klasificirane su i mogu se parametrizirati. Osim sustava Mathematica i Maple, za vizualizaciju složenih minimalnih ploha računalom postoji grafički sustav Mesh (http://www.msri.org/publications/sgp/jim/software/mesh/mainc.html) koji aproksimira sve familije ovih ploha. Dakle, prikladna aproksimacija olakšava vizualizaciju.

Minimalnost ili približna minimalnost plohe može biti potrebna iz konstruktivnih, funkcionalnih ili estetskih razloga. Minimalnost plohe omogućava uštedu materijala za pokrov, oblaganje pa i minimalnu oplatu konstrukcije (npr. betonske konstrukcije nad nekim paviljonom, graničnim prijelazom ili željezničkim peronom).

Kod ploha u arhitekturi, koje imaju relativno male visinske razlike, prve derivacije daju male iznose ($f_x \approx 0, f_y \approx 0$) pa ne utječu bitno na Lagrangeovu jednadžbu. Ako se zanemare ti članovi, Lagrangeova jednadžba aproksimira se Laplaceovom:

$$f_{xx}+f_{yy}=0. \tag{2}$$

Kod ploha koje moraju imati relativno velike visinske razlik ti članovi nisu zanemarivi.

Hipar- najčešća ploha

Hiperbolički paraboloid (hipar) poznat je svim studentima građevine i arhitekture kao beskonačna kvadrika negativne Gaussove zakrivljenosti s dva sustava izvodnica (i ravnalica) i dvije direkcijske ravnine. To je ujedno i klizna ploha koja nastaje translacijom parabole po paraboli. Hipar[1] je poslije ravnine možda najzastupljenija ploha u arhitekturi. Njime se lako natkrivaju tlocrti različitih oblika, od neke zatvorene krivulje do nepravilnog četverokuta, deltoida, paralelograma ili trokuta. To može biti i drvena konstrukcija s mimoilaznim nosačima ili čak zid promjenjivog nagiba.

U nekim radovima konačni dio hipara spominje se i tretira kao minimalna ploha (http://www.hoberman.com/fold/Hypar/hypar.htm). U matematičkim klasifikacijama minimalnih ploha hipara nema. Tu su ravnina, katenoid i helikoid[2], Enneperova, Scherkova[3] ploha i mnoge druge. Ipak, hipar u nekim uvjetima može poslužiti kao dobra i jednostavna aproksimacija minimalne plohe.

Poznato je da neopterećeno horizontalno uže poprima oblik lančanice zbog vlastite težine. Kad se optereti kontinuiranim opterećenjem lančanica prelazi u parabolu. Ako je neka lagana viseća konstrukcija sastavljena od takvih nosača, u dva međusobno okomita smjera, oni ne mogu zadržati oblik lančanice. Ti nosači stalno djeluju jedni na druge (vise jedni na drugima) i bez opterećenja vanjskim silama. Pod djelovanjem tih jednakih i pravilno raspoređenih sila međudjelovanja točke lančanice prelaze u točke parabole. Nastaje prostorna poligonska mreža upisana u hipar.

Smješten simetrično u odnosu na ishodište hipar ima jednadžbu:

$$z=f(x,y)=\frac{x^2}{a^2}-\frac{y^2}{b^2}. \tag{3}$$

Kad su direkcijske ravnine vertikalne i međusobno okomite hipar lako natkrije pravokutni tlocrt. Za razliku od

[1]Naziv ”hypar” uveo je arhitekt Heinrich Engel u knjizi ”Structure Systems” 1967 (strana 215.)
[2]Katenoid i helikoid pronašao je još 1776 Meusnier.
[3]Konstruirane su pomoću računala.

drugih materijala, tkani materijali za lagane konstrukcije ne preuzimaju posmična naprezanja tj. deformiraju se pa tako kvadrat na tkanini prelazi u romb.

Ako je $a=b$, tada su horizontalni presjeci plohe istostrane hiperbole, a jednadžba (3) može se pisati u obliku:

$$f(x,y)=c(x^2-y^2), \tag{4}$$

gdje je $c=1/a^2$ konstanta to manja što je dimenzija poluosi a plohe veća.

Hipar kome se horizontalne izvodnice poklapaju s osima x i y (uz relativno male poluosi $a=b=1$) ima jednadžbu:

$$z=f(x,y)=xy. \tag{5}$$

Provjera aproksimacije

Za hipar (3) s poluosima a i b parcijalne derivacije

$$f_x=\frac{2x}{a^2}, \quad f_y=-\frac{2y}{b^2},$$

$$f_{xy}=f_{yx}=0, \quad f_{xx}=\frac{2}{a^2}, \quad f_{yy}=-\frac{2}{b^2} \tag{6}$$

mogu poprimiti male vrijednosti (za $a,b\gg 1$), ali pokazuju da hipar nije minimalna ploha jer jednadžba (1) nije zadovoljena. Naime,

$$\left(1+\frac{4y^2}{b^4}\right)\frac{2}{a^2}-\left(1+\frac{4x^2}{a^4}\right)\frac{2}{b^2}\neq 0. \tag{7}$$

Za istostrani hipar parcijalne derivacije funkcije (4) su

$$f_x=2cx, \quad f_y=-2cy,$$

$$f_{xy}=f_{yx}=0, \quad f_{xx}=2c, \quad f_{yy}=-2c, \tag{8}$$

pa Lagrangeova jednadžba (1) poprima oblik

$$8c^3(y^2-x^2)=0. \tag{9}$$

To je ispunjeno samo za točke u ravninama $y=x$. Kako je $c\ll 1$, za ostale točke taj izraz teži k nuli to brže što je c manji. Ovo nije minimalna ploha, ali se u okolini ishodišta i za velike vrijednosti poluosi a ponaša se slično minimalnoj.

Međutim, takav hipar ($a=b$) očito zadovoljava Laplaceovu jednadžbu (2) pa ga smatramo dobrom aproksimacijom minimalne plohe.

Funkcija (5) ima parcijalne derivacije

$$f_x=y, \quad f_y=x,$$

$$f_{xy}=f_{yx}=1, \quad f_{xx}=0, \quad f_{yy}=0, \tag{10}$$

što ne zadovoljava Lagrangeovu jednadžbu ($2xy=0$) osim u ishodištu, ali zadovoljava Laplaceovu.

Zaključak

Hipar nije minimalna ploha, ali konačni dio hipara ponaša se kao minimalna ploha - aproksimira je. U graditeljskoj praksi plitki hipar je "praktički" minimalna ploha, posebno dio oko ishodišta kod istostranog hipara. U slučaju visokog hipara na nekim njegovim djelovima *odustajemo* od približno minimalne plohe. Koliko je to u pojedinom slučaju poželjno odlučuje projektant.

Vijesti i izvješća

Godišnja skupština HDKGIKG-a

U dvorani P2 Građevinskog fakulteta u Zagrebu održana je 25.rujna 2001. godine godišnja skupština HDKGIKG-a. Sastanak je tekao prema uobičajenom dnevnom redu: prvo izvještaji predsjednice, tajnice, Izdavačkog savjeta i Nadzornog odbora, a zatim plan rada Društva za slijedeću godinu.

Predsjednica Društva Ana Sliepčević izvjestila je o radu u proteklom razdoblju. Ministarstvu znanosti i tehnologije RH podneseni su zahtjevi za dodjelu sredstava za održavanje znanstvenog skupa, za podupiranje udruge i izdavanje časopisa KoG. Održani su sastanci Društva i to u veljači i lipnju 2001. Na sastanku u veljači, uz dva održana predavanja, raspravljalo se o kadrovskoj problematici, a o lipanjskom druženju pod nazivom Dan HDKGIKG-a može se čitati u 5. broju KOG-a. Predsjednica je zatim izvjestila o dopisu Ukrajinskog društva za geometriju i grafiku u kojem pozivaju da napišemo članak o hrvatskim geometričarima za knjigu ”Who is who in Geometry and Graphics”. Na kraju je predsjednica istaknula da imamo i nekoliko novih mladih članica Društva.

Tajnica Društva Ivanka Babić izvjestila je o financijskom stanju. Istaknula je da je Ministarstvo znanosti i tehnologije dodijelilo sredstva za podupiranje udruge i djelomično za izdavanje časopisa KoG. Uplaćena je međunarodna članarina za Zentrallblatt. Sredstava ima dovoljno za sve troškove vezane uz tisak časopisa KoG i ostale tekuće izdatke.

Za Izdavački savjet izvjestila je Sonja Gorjanc. Istaknula je da je časopis KoG izašao kao dvobroj, a novost je što je tisak digitalan. Kako je već ranije najavila Sonja Gorjanc je ponovila da zbog opsežnosti posla ne može više biti glavna urednica časopisa i predložila je Jelenu Beban-Brkić. Prihvaćen je prijedlog da urednice časopisa KoG budu Sonja Gorjanc i Jelena Beban-Brkić. Vlasta Szirovicza je povukla svoje članstvo u Izdavačkom savjetu te predložila na svoje mjesto Nikoletu Sudetu. Prijedlog je prihvaćen.

Nadzorni odbor nije imao primjedbi. Sva izvješća su prihvaćena.

Na kraju sastanka usvojen je plan rada Društva za slijedeću godinu. Plan uključuje: organizaciju i održavanje skupova u veljači, lipnju i znanstveno-stručnog kolokvija u rujnu 2002. godine, izdavanje novog broja časopisa KoG, sudjelovanje članica i članova Društva na međunarodnim skupovima, suradnju sa kolegama iz inozemstva, konzultantima i recenzentima na znanstvenim temama.

Ivanka Babić

7. znanstveno-stručni kolokvij HDKGIKG-a

Zagreb, 24-25. rujna 2001.

U Zagrebu je 24. i 25. rujna 2001. održan 7. znanstveno - stručni kolokvij Hrvatskog društva za konstruktivnu geometriju i kompjutorsku grafiku. Sponzori skupa bili su Građevinski fakultet u Zagrebu i poduzeće za grafičke usluge SAND d.o.o. iz Zagreba. Uz dvadeset i dvoje domaćih sudionika, skupu je prisustvovao i gost iz Ljubljane dipl. ing. Domen Kušar. Održana su sljedeća znanstvena i stručna predavanja:

J. Beban-Brkić, N. Sudeta:
Mathematica u nastavi

S. Gorjanc:
Mathematica u nastavi geometrije na tehničkim fakultetima

K. Jurasić:
Grafovi ravninskih i prostornih krivulja zadanih prirodnom jednadžbom prikazani pomoću programa *Mathematica*

L. Pletenac:
Necirkularne cisoidne krivulje i plohe

A. Sliepčević:
Svi leptirovi teoremi

V. Szirovicza:
Inverzija u hiperboličkoj ravnini

M. Lapaine:
O problemu istoznačnica u matematici

Z. Čerin:
Lucasove kružnice

Tematski sastanak HDKGIKG-a

Zagreb, 25. veljače 2002.

U vijećnici AGG fakulteta u Zagrebu održan je 25. veljače 2002. tematski sastanak HDKGIKG-a. Osim članova Društva sastanku su prisustvovali i gosti prof. dr.sc. Mirko Polonijo s PMF-a te prof. dr. sc. Branko Kučinić s Građevinskog fakulteta u Zagrebu.

Prvi dio sastanka posvećen je stogodišnjici rođenja Vilka Ničea. Spomenuli smo ga se kao velikog znanstvenika i još većeg čovjeka o čemu su nam svjedočile Vlasta Ščurić i Ana Sliepčević. Svoje uspomene i razmišljanja o njemu podijelili su s ostalima Ksenija Horvatić-Baldasar, Branko Kučinić, Sonja Gorjanc, Zdravka Božikov te na kraju Mirko Polonijo.

Prva tema razgovora bili su udžbenici iz geometrije. Izviješćeno je o radu nastavnica Građevinskog fakulteta u Zagrebu na udžbeniku prilagođenom vježbama iz Nacrtne geometrije na veleučilištu. Izdavač udžbenika biti će HDKGIKG.

Nastavnice Građevinskog fakulteta u Zagrebu, Babić, Gorjanc, Sliepčević i Szirovicza, prijavile su MZT-u znanstveni projekt koji je i prihvaćen. Na projekt je, od 01.03.2002., kao znanstvena novakinja primljena Dora Predrijevac.

Zdravka Božikov obavijestila nas je o otvaranju studija arhitekture u Splitu povodom čega je sastavila plan nastave iz kolegija Metode projiciranja. Nadalje, radi na pripremi udžbenika iz Primijenjene geometrije prilagođenom predavanjima na Građevinskom fakultetu u Splitu.

Uslijedila su izvješća, o financijskom stanju izvjestila je tajnica Društva Ivanka Babić, a o situaciji u časopisu KoG Sonja Gorjanc.

Ema Jurkin i Marija Šimić

DAN HDKGIKG-A

ZAGREB, 1. SRPNJA 2002.

Naše uobičajeno lipanjsko druženje, koje se ove godine trebalo održati 24. lipnja, odgodili smo za 1. srpanj radi državnog praznika. Osim razgovora o raznim problemima u vezi s visokoškolskom nastavom geometrijskih predmeta, čuli smo nekoliko zanimljivih izlaganja.

Jelena Beban-Brkić u kratkim je crtama opisala područje djelovanja Studentskog informacijskog obrazovnog centra SIC. To je savjetodavni centar o mogućnostima visokog obrazovanja u Hrvatskoj i inozemstvu u kojem se mogu polagati razredbeni ispiti za američke fakultete. J.Beban Brkić pokazala je jedan takav test iz matematike.

Sonja Gorjanc upoznala nas je s pozivom MZT-a za prijavu projekta primjene informacijske tehnologije za 2002. godinu. Informacije se mogu dobiti na adresi **www.mzt.hr/djelatnosti/informatika/projekti**.

M.Lapaine je predstavio knjigu "Ugledni znanstvenici u svijetu" urednika Janka Heraka te dao pregled geometrijskih sadržaja u srednjoškolskim udžbenicima geografije uz demonstraciju na jednom od devet(!) udžbenika za prvi razred.

Na kraju sastanka predsjednica Društva Ana Sliepčević izvjestila nas je da će u rujnu ove godine biti realiziran tečaj AutoCAD-a te nas obradovala obaviješću da će se VIII Znanstveno-stručni kolokvij HDKGIKG-a 23. i 24. rujna održati u Begovom Razdolju.

Dora Predrijevac

10. INTERNACIONALNA KONFERENCIJA O GEOMETRIJI I GRAFICI

KIJEV, 28. 7. - 2. 8. 2002.

U organizaciji Međunarodnog društva za geometriju i grafiku (International Society of Geometry and Graphics - ISGG - **www.isgg.tu-dresden.de**) i Ukrajinskog društva za primjenjenu geometriju (Ukrainian Association of Applied Geometry) u Kijevu (Ukrajina) je od 28. srpnja do 2. kolovoza 2002. održana *10. međunarodna konferencija o geometriji i grafici* (10th International Conference on Geometry and Graphics - **www.geometry.kiev.ua**).

O prethodnim konferencijama u organizaciji ISGG-a, njihovoj ulozi i svrsi te o sudjelovanju članova našega Društva u njihovom radu može se čitati u 1. i 3. broju KoG-a.

11. konferencija za geometriju i grafiku održat će se 2004. u NR Kini, na *Tehničkom sveučilištu Guandong*.

Za Kijev kažu da je najstariji slavenski grad, nazivaju ga i "majkom ruskih gradova", ima gotovo tri miliona stanovnika, 30 kazališta, 5 sveučilišta,... Smješten je na brežuljcima uz obale velikog Dnjepra, bogat zelenilom te lijepom i zanimljivom arhitekturom. Stanovnici su srdačni i blagi, a komunikacija ukrajinski-hrvatski funkcionira. Tri članice našega Društva (Jelena Beban-Brkić, Sonja Gorjanc i Nikoleta Sudeta) provele su ugodan ljetni tjedan u tom dalekom gradu te sudjelovale u radu Konferencije koja okuplja nastavnike geometrije sa tehničkih fakulteta širom svijeta.

Konferencija je započela pozdravnim govorima *M. Z. Zgurovskog* (Rektor Ukrajinskog nacionalnog univerziteta) i *G. Weissa* (predsjednik ISGG-a) te pozivnim predavanjima:

V. Ye. Mykhailenko (Ukrajina):
Achievements of the Ukrainien School of Applied Geometry

G. S. Ivanov (Rusija):
The History and Perspectives of Development of Applied Geometry in Russia

K. Suzuki (Japan):
The Activites of Japan Society for Graphic Science - Research and Education.

Rad je nastavljen u tematskim sekcijama: *Teorijska grafika*, *Primjenjena geometrija*, *Grafička edukacija i kompjuterska tehnologija*, a posebnu su grupaciju činili *Posteri*.

U dvije knjige Zbornika radova, koje svatko zainteresiran može dobiti na uvid, objavljeno je 135 članaka.

Članice našeg Društva održale su četiri zapažena predavanja:

J. Beban - Brkić:
Isometric Invariants of Quadrics in Double Isotropic Space

S. Gorjanc:
Quartics with Multiple Line in E^3

S. Gorjanc:
Some Examples of Using MATHEMATICA in Teaching Geometry

N. Sudeta, J. Beban - Brkić:
New Geometric Package at Software MATHEMATICA.

Nikoleta Sudeta i Sonja Gorjanc

11th SEFI

European Seminar on Mathematics in Engineering Education

Göteborg, 9.-12. 6. 2002.

Ponovo smo se sastali u jednoj skandinavskoj zemlji. U Švedskoj, u Göteborgu, vrlo lijepo uređenom gradu, prometno dobro organiziranom i prepunom zelenila, od 9. do 12. lipnja 2002. godine održan je *Jedanaesti SEFI europski seminar o matematici u inžinjerskoj naobrazbi* (11th SEFI European Seminar on Mathematics in Engineering Education). SEFI-Europsko društvo za inžinjersku naobrazbu (European Society for Engineering Education) osnovano je 1973. godine. Svrha je društva širiti informacije o obrazovanju inžinjera, pospiješiti komunikaciju i razmjenu iskustava među nastavnicima, istraživačima i studentima, razvijati suradnju među institucijama koje se bave naobrazbom inžinjera, promoviranje suradnje na nivou industrija - obrazovne ustanove te pridonositi razvoju i poboljšanju istoga u postojećem socijalnom, kulturnom i gospodarskom okviru (vidi **http://www.ntb.ch/SEFI/** i **http://learn.lboro.ac.uk/mwg/**).

Matematička radna grupa u sklopu SEFI udruženja (Mathematics Working Group of SEFI) osnovana je 1982. godine i od tada, približno svake druge godine, organizira seminare o matematici. Ovaj put domaćini su bili kolege sa *Chalmers University of Technology* u Göteborgu, jedne od dvije najveće takve obrazovne ustanove u Švedskoj, s 8800 upisanih studenata u širokom rasponu obrazovnih programa (vidi **http://www.chalmers.se**). Svi su referati održani na *Department of Mathematical and Computing Sciences*, uz poneku nedostatnu tehničku podršku. Rad Seminara odvijao se u jednoj sekciji, a prisustvovalo je pedesetak matematičara i inžinjera iz gotovo svih europskih zemalja. Osnovne teme ovogodišnjeg seminara bile su:

- Obrazovanje ”na daljinu” (Distance Education)

- Kontinuirana matematička izobrazba (Lifelong Learning of Mathematics)

- Ocjenjivanje kompjuterski podržanog učenja matematike (Evaluation of Computer Aided Learning of Mathematics)

- Kompjuterski podržano ocjenjivanje (Computer Aided Assessment)

- Nastava matematike & Bolonjska Deklaracija

U radu Seminara sudjelovala sam referatom napisanim u koautorstvu s doc. dr. sc. *Goranom Novaković*, pod naslovom *The Way of Solving Some Geodetic Tasks*. Sažeci izlaganja su tiskani u knjizi Abstractsa, dok se knjiga Proceedingsa uskoro očekuje na web-u.

Sljedeći Seminar će se održati u Austriji, u Beču 2004. godine.

Jelena Beban-Brkić

Kako nabaviti KoG?

KoG je najjednostavnije nabaviti u uredništvu časopisa:

Nikoleta Sudeta (nsudeta@arhitekt.hr)
Arhitektonski fakultet, Kačićeva 26, 10 000 Zagreb
Tel: 01 4561 219 , Fax: 01 4828 079

Za Hrvatsku je cijena primjerka 145 KN + 10 KN za poštarinu.

Nakon uplate za:
HDKGIKG (za KoG), Kačićeva 26, 10000 Zagreb
žiro račun broj 2360000-1101517436
poslati ćemo časopis na Vašu adresu.

Ako Vas zanima tematika časopisa i rad našega društva, preporučamo Vam da postanete članom HDKGIKG (godišnja članarina iznosi 100 KN). Za članove društva časopis je besplatan.

How to get KoG?

The easiest way to get your copy of KoG is by contacting the editor's office:
Nikoleta Sudeta (nsudeta@arhitekt.hr)
Faculty of Architecture, Kačićeva 26, 10 000 Zagreb, Croatia
Tel: (+385 1) 4561 219, Fax: (+385 1) 4828 079

The price of the issue is €20 + mailing expenses €5 for European countries and €10 for other parts of the world.

The amount is payable to:
Account name: Hrvatsko društvo za konstruktivnu geometriju i kompjutorsku grafiku, Kačićeva 26, 10000 Zagreb, Croatia
Account No.: 2421809001
Bank Name: Zagrebačka banka
Swift-Code: ZABA HR 2X

Znanstveno–stručno–informativni časopis Hrvatskog društva za konstruktivnu geometriju i kompjutorsku grafiku

Osnivač i izdavač
Hrvatsko društvo za konstruktivnu geometriju i kompjutorsku grafiku

Izdavački savjet
Sonja Gorjanc, Miljenko Lapaine, Nikoleta Sudeta

Uredništvo
Miroslav Ambruš-Kiš, Jelena Beban-Brkić, Krešimir Fresl, Sonja Gorjanc, Miljenko Lapaine, Lidija Pletenac

Urednice
Sonja Gorjanc, Jelena Beban-Brkić

Grafičko oblikovanje
Miroslav Ambruš-Kiš

Grafička priprema
Sonja Gorjanc

Ovitak
Sven Gorjanc-Fabić
Strukture, fotografije

Tisak
SAND d.o.o., Zagreb

Adresa uredništva
Građevinski fakultet
Avenija V. Holjevca 15
10 010 Zagreb
tel.: 66 70 509
faks : 66 00 642
e-mail:
sgorjanc@grad.hr
jbeban@geof.hr

KoG na Internetu
www.hdgg.hr/kog

Naklada
250 primjeraka

Izlazi jednom na godinu

Ovaj broj časopisa financiralo je Ministarstvo znanosti Republike Hrvatske.

PDF format 5. i 6. broja KoG-a može se slobodno podići na adresi **www.hdgg.hr/kog**.

PDF format of KoG No.5 and No.6 can be downloaded free at **www.hdgg.hr/kog**.

Scientific and Professional Information Journal of Croatian Society for Constructive Geometry nad Computer Graphics

Founder and Publisher
Croatian Society for Constructive Geometry nad Computer Graphics

Board of Trustees
Sonja Gorjanc, Miljenko Lapaine, Nikoleta Sudeta

Editorial Board
Miroslav Ambruš-Kiš, Jelena Beban-Brkić, Krešimir Fresl, Sonja Gorjanc, Miljenko Lapaine, Lidija Pletenac

Editors
Sonja Gorjanc, Jelena Beban-Brkić

Design
Miroslav Ambruš-Kiš

Layout
Sonja Gorjanc

Cover Illustration
Sven Gorjanc-Fabić
Structures, photographs

Print
SAND d.o.o., Zagreb

Editorial Address
Faculty of Civil Engineering
Av. V. Holjevca 15
10 010 Zagreb, Croatia
tel.: (385 1)66 70 509
faks : (385 1) 66 00 642
e-mail:
sgorjanc@grad.hr
jbeban@geof.hr

KoG on Internet
www.hdgg.hr/kog

Edition
250

Published annually

This issue has been financially supported by Ministry of Science of Republic Croatia.

ISSN 1331-1611
9 771331 161005